METHODS FOR ESTABLISHING THE EFFICIENCY OF THE PHOTOCATALYTIC DESTRUCTION OF HUMIC SUBSTANCES IN DRINKING WATER

Valeska Cloete

Thesis presented in partial fulfillment of the requirements
for the degree of Master of Natural Sciences (Chemistry)
at the University of Stellenbosch

Promotors: Prof. W.J. Engelbrecht
Dr. G.F.S. Wessels

Stellenbosch
December 1999

DECLARATION

I, the undersigned, hereby declare that the work contained in this thesis is my own original work and that I have not previously in its entirety or in part submitted it at any university for a degree.

METHODS FOR ESTABLISHING THE EFFICIENCY OF THE PHOTOCATALYTIC DESTRUCTION OF HUMIC SUBSTANCES IN DRINKING WATER

ABSTRACT

For decades the production of potable water, from surface and ground waters, was based mainly on the process of coagulation and flocculation for the removal of natural organic matter (NOM). The incomplete removal of NOM from these waters has however resulted in the formation of potentially harmful disinfection by-products in treated water. This problem, together with increased quantities of pollution in raw and surface waters, has necessitated research in alternative methods to be used in conjunction with existing methods for water purification.

A water treatment process, which has received much attention in recent times, is heterogeneous photocatalysis. A semiconductor photocatalyst is required for the production of highly reactive hydroxyl radicals in aqueous medium for the photocatalytic oxidation of the relevant organic pollutants. A novel photocatalytic reactor (developed at the University of Stellenbosch) was employed to investigate the efficiency of heterogeneous photocatalysis for the production of potable water. TiO_2 was used as semiconductor catalyst in the investigation. Various factors were optimised by means of statistical experimental design for the optimal destruction of NOM in the raw water.

Monitoring the NOM destruction efficiency by the photocatalytic process proved to be difficult. Three analytical methods for monitoring were investigated.

Firstly, the widely accepted method of reduction of UV (at 254 nm) as a measure of NOM removal, as applied in the flocculation process, was investigated. The photocatalytic process, however, reduces NOM to smaller molecular species before complete removal by oxidation. These smaller molecules do not absorb at 254 nm and therefore cannot be detected by this method.

Secondly, the reduction of the total organic carbon content as determined by a low temperature total carbon analyser, was investigated. The smaller molecules produced by the photocatalytic process before complete removal, are still registered as total organic carbon content, and therefore presents a wrong picture.

Finally, a protocol was developed whereby the trihalomethane formation potential (THMFP) of photocatalytically treated water could be monitored. This procedure was based on simulating the chlorination process, followed by the extraction of the formed trihalomethanes by means of the technique of solid phase microextraction (SPME) and the consequent quantitative analysis of these compounds by means of a gas chromatograph coupled to a mass spectrometer. This proved to be a superior method in comparison with the other methods.

METODES VIR DIE BEPALING VAN DIE EFFEKTIWITEIT VAN DIE FOTOKATALITIESE VERNIETIGING VAN HUMUSSURE IN DRINKWATER

UITTREKSEL

Drinkwater was die afgelope paar dekades hoofsaaklik geproduseer deur 'n proses wat bestaan uit 'n kombinasie van koagulasie- en flokkulasie-prosesse vir die verwydering van natuurlike organiese materiaal (NOM) teenwoordig in grond- en oppervlakwater. As gevolg van onvolledige verwydering van NOM uit die waterbronne, het potensiële skadelike ontsmettingsneweprodukte gevorm in die behandelde water. Hierdie probleem, tesame met die toenemende hoeveelheid besoedeling in rou- en oppervlakwaters, het navorsing genoodsaak om alternatiewe prosesse, vir die suiwering van water in oorleg met bestaande metodes, te ondersoek.

'n Proses wat die afgelope ruk baie aandag geniet het, is gebaseer op heterogene fotokatalise. 'n Halfgeleier fotokatalisator is nodig vir die generering van hoogs aktiewe hidroksielradikale in waterige medium wat fotokatalitiese oksidasie van die gegewe organiese besoedelingstowwe tot gevolg het. 'n Nuwe fotokatalitiese reaktor (ontwikkel aan die Universiteit van Stellenbosch) is gebruik om ondersoek in te stel na die effektiwiteit van heterogene fotokatalise vir die verskaffing van drinkwater. TiO_2, is gebruik as halfgeleier katalisator tydens hierdie ondersoek. Verskeie faktore is met behulp van statistiese eksperimentele ontwerp geoptimiseer om optimale toestande vir die vernietiging van NOM uit rou water vas te stel.

Die effektiwiteit van die vernieting van NOM, deur middel van die fotokatalitiese proses, was moeilik om te monitor. Drie verskillende metodes is vir die monitering ondersoek.

Eerstens is die algemeen aanvaarde metode, waar die afname in UV absorpsie (by 254 nm) 'n maatstaf is vir die NOM verwydering, soos toegepas in die flokkulasie proses, ondersoek. Die fotokatalitiese proses reduseer egter eers die NOM tot kleiner molekulêre spesies voor die finale vernietiging deur oksidasie. Hierdie kleiner molekule absorbeer nie lig by 254 nm nie en kan dus nie deur hierdie metode waargeneem word nie.

Tweedens is die afname in totale organiese koolstof inhoud bepaal deur 'n lae temperatuur totale organiese koolstof inhoud analiseerder. Die kleiner molekule wat deur die fotokatalitiese

proses geproduseer is voor die totale verwydering daarvan, word wel geregistreer as deel van die totale organiese koolstof inhoud en skep dus 'n verkeerde indruk.

Laastens is 'n protokol, vir die bepaling van die trihalometaan formasie potensiaal (THMFP) van die fotokatalities behandelde water, ontwikkel. Hierdie metode is gebaseer op die simulasie van die chlorineringsproses, gevolg deur die ekstraksie van die trihalometaanverbindings deur middel van die tegniek van soliede fase mikroekstraksie (SFME) en die daarmee gepaardgaande kwantitatiewe analise van die verbindings deur middel van 'n gaschromatograaf gekoppel aan 'n massaspektrometer. Hierdie metode is by verre beter in vergelyking met die ander metodes.

ACKNOWLEDGEMENTS

I would hereby like to thank the following persons and institutions for their support.

Prof. W.J. Engelbrecht
Dr. G.F.S. Wessels
Mr. D. de Villiers
Mr. I. Goldie
Ms. S.R. Paarman
Mr. L. van Niekerk
Water Research Commission
Cape Metropolitan Council

TABLE OF CONTENTS

CHAPTER 6: Experimental Investigation of Photocatalytic Degradation

ABBREVIATIONS

ANOVA	Analysis of Variance
AOPs	Advanced Oxidation Processes
BDOC	Biodegradable Organic Carbon
BET Isotherm	Brunauer Emmet Teller Isotherm
BTHMFP	Basic Trihalomethane Formation Potential
cb	Conduction Band
CCD	Central Composite Design
DBPs	Destruction By-products
DOC	Dissolved Organic Carbon
e^-_{cb}	Conduction Band Electron
FA	Fulvic Acids
FAC	Fibrous Activated Carbon
GAC	Granular Activated Carbon
GC	Gas Chromatograph
GC/MS	Gas Chromatograph coupled to Mass Spectrometer
h^+_{vb}	Valence Band Hole
HA	Humic Acids
HU	Humin
LLE	Liquid-Liquid Extraction
MAC	Maximum Acceptable Concentration
MTHMFP	Maximum Trihalomethane Formation Potential
NOM	Natural Organic Matter
OED	Optimal Experimental Design

PAC	Powdered Activated Carbon
PAHs	Poli-Aromatic Hydrocarbons
PCBs	Polychlorobiphenyls
PDMS	Polydimethylsiloxane
RDP	Reconstruction and Development Program
SDSTHMC	Simulated Distribution System Trihalomethane Concentration
SFE	Supercritical Fluid Extraction
SPE	Solid Phase Extraction
SPME	Solid Phase Microextraction
THMs	Trihalomethanes
THMFP	Trihalomethane Formation Potential
TIC	Total Ion Count
TOC	Total Organic Carbon
TTHMs	Total Trihalomethanes
USEPA	United States Environmental Protection Agency
UV	Ultra Violet
UTHMFP	Ultimate Trihalomethane Formation Potential
vb	Valence Band
VOCs	Volatile Organic Compounds
VUV	Vacuum Ultra Violet
WHO	World Health Organization
WRC	Water Research Commission

CHAPTER 1

1.1 INTRODUCTION

The rapid deterioration of our living environment has become a matter of concern in recent times. Overpopulation has placed great demands on our planet. With an estimated population of over 8 billion people by the year 2010, prospects of relief for our environment seem unlikely (Kruger, 1992).

Our water resources have been exposed to the harsh effects of rapid industrialisation and development. Industry, mining, farming and households are the main contributors to pollution of natural water resources, resulting in nitrates, fluorides, phosphates, harmful pesticides, detergents and numerous toxic materials being released into rivers, lakes, water storage dams and the ocean. These contaminants pose a direct threat to mankind since crops, cattle, drinking water, etc. are affected by it. Apart from staggering effects of water pollution, growing populations are placing great demands on industry, with the consequent release of large quantities of poisonous gases (e.g. oxides of carbon, nitrogen and sulfur) into the atmosphere. These gases contribute to the water pollution e.g. when acid rain is produced.

The pollutants in water of anthropogenic origin can be categorised as follows:

- Organic wastes: this include human and animal waste, and numerous organic compounds used in industry, mining and agriculture
- Inorganic materials: these mainly originate from industry and include toxic metals, nitrates, phosphates and acids

Apart from the pollutants mentioned above, there are some organic materials of natural origin e.g. humic substances. Although well-established water purification processes do exist, they are often not effective in the presence of pollutants in solution. Metals such as Cd, Fe and Mn form stable complexes with humic and other organic substances, thereby rendering the standard flocculation processes ineffective (Galvin, 1996). Although certain metal ions are essential for humans, eg. Ca, Cu and Fe, many have detrimental effects. Some metal ions, such as Be, Pb, Hg etc. pose possible carcinogenic risks, while others have a damaging effect on the nervous or

cardio-vascular system (Sb, Cd, Li), respiratory tract (Al, Mn) and organs (Galvin, 1996; Casarett, 1975).

Apart from the possible carcinogenic nature of certain organic compounds, their disinfection by-products, which form after chlorination of water in water treatment plants, often exhibit similar tendencies and are, therefore, toxic to humans. Complete removal of organic material of anthropogenic and natural origin from water, before chlorination is, therefore, essential.

Recent years have also seen a growing awareness of the depletion of our planet's water resources. South Africa, with its diverse rainfall regions, has limited natural water resources to support its growing population (Van der Merwe, 1995; Laburn, 1995). Compared to the rest of the world, the RSA receives less than 60% of the world average rainfall per annum. Because of high evaporation losses of water stored in dams, the focus is now moving toward ground water supplies, which, as industrialisation increases, will become more polluted. Water consumption in the country varies from 600L per capita per day in the affluent urban areas, to less than 10L per capita per day in the rural areas. The lack of basic services, such as potable water supply and sanitation, to the greater part of the population of the country, is receiving much attention by the government. With the Reconstruction and Development Program (RDP), these problems are now being addressed. Projects to improve these conditions have already been implemented, and many more will ensue. This, together with the reality of a rapid growing population, is placing an even greater demand on the dwindling water supply of South Africa.

To be able to address both the water pollution scenario, as well as the dwindling water supplies world wide, the development of alternative water purification processes must receive serious consideration. The possibility of utilising other water resources, eg. waste waters and polluted ground waters, must therefore be carefully examined. Methods, such as photocatalytic oxidation, which can address both aspects of water purification, will prove to be very important in the future.

1.2 PROJECT OBJECTIVES

The objective of this study was to develop and establish a water purification process, which could serve as an alternative to conventional processes of coagulation and flocculation currently being used to supply potable water. The process must be capable of purifying ground waters containing natural organic material and organic pollutants, thereby broadening the scope of water sources to be used for drinking water purposes.

The initial study objective was to determine whether NOM in raw water could be destroyed by means of a novel large laboratory scale photocatalytic reactor, designed and built in the Department of Chemistry at the University of Stellenbosch.

The second initial objective was to optimise the NOM destruction process occurring in the specific reactor design.

A further objective was added during the investigation, namely to develop a method to effectively monitor the destruction of NOM by the photocatalytic process.

REFERENCES

Casarett L.J., Doull J. (Editors) (1975) Toxicology: The Basic Science of Poisons. MacMillan Publishing Co. Inc.

Galvin R.M. (1996) Occurrence of metals in waters: An overview. *Water SA* **22** No.1 p.7-18

Kruger H. (1992) Chemistry and our endangered environment. *SPECTRUM* **30** No.4 p.59-62

Laburn R.J. (1995) Water Supply in South Africa. *J.Water SRT – Aqua* **44** No.4 p.161-165

Van der Merwe S.W. (1995) An Overview of Water Supply Management in South Africa. *J.Water SRT – Aqua* **44** No.4 p.151-160

CHAPTER 2

Natural Organic Matter and Water Treatment Processes for the Production of Potable Water

2.1 RAW WATER

Surface and ground waters contain a complex variety of natural organic matter (NOM) characteristic to the natural vegetation of the environment for each specific catchment area. The NOM present in waters exhibit a significant effect on water treatment processes, the application of different disinfectants and the stability of the water. The water quality of potable water in terms of the disinfection by-products (DBPs), the biological regrowth in the distribution systems, colour, taste and odours are directly influenced by the NOM present in the water (Owen, 1995). For efficient water purification it is, therefore, of great importance that the NOM is sufficiently characterised where it occurs.

2.2 NATURAL ORGANIC MATTER

Both insoluble and soluble organic matter contribute to the NOM in raw water. NOM in water constitutes of the following compounds (Kunin, 1986):

Insoluble Organic Matter	**Soluble Organic Matter**
Debris of vegetable and animal origin	Humic Matter
Microorganisms	Fatty acids
Oily matter	Nitrogenous matter (proteins, peptides, amino acids)
Humic matter	Saccharides
	Dissolved organic gases (such as methane)
	Soluble extracts of vegetable and animal matter
	Synthetic organic compounds

An alternative classification of NOM in raw water is based on the humic character of the organic matter. NOM are consequently devided into a humic or hydrophobic category and a non-humic or hydrophilic category. Each category is further subdivided (Owen, 1995).

Humic Matter	**Non-Humic Matter**
Humic Acids	Hydrophyllic Acids
Fulvic Acids	Proteins
	Amino Acids
	Carbohydrates

Most of the non-humic compounds are readily attacked by microorganisms and, therefore, have a short life span in soils and sediments. In the past, the non-humic section has been thought to present less of a drinking water quality problem. Research has, however, indicated that the non-humic section (Owen, 1995) could contribute a significant percentage of the potential DBPs. The non-humic section is further responsible for a greater percentage of the biodegradable organic carbon (BDOC), which is of great concern for bacterial regrowth in distribution systems.

2.3 HUMIC SUBSTANCES

For many decades researchers have tried to determine the exact origin and composition of humic substances. Many papers have been published on this matter, but a great deal still remains to be interpreted. Humic substances are believed to originate from the chemical and biological degradation of plant and animal materials and from the synthesizing activities of microorganisms. Contrary to the non-humic materials, humic substances are stable for longer periods. They exhibit no strong physical and chemical characteristics, e.g. no definite IR spectrum or a sharp melting point, which are normally associated with well-defined organic compounds. They can be defined as anionic, predominantly aromatic, polyelectrolytes, containing mainly carboxylic and phenolic groups. Their molecular weights vary from a few hundred to several thousand mass units (Schnitzer, 1987, p.2). The yellow-brown colour of surface waters can be attributed to the dark colour of the humic substances. This is confirmed by a UV spectrum (Figure 2.1) of raw water containing humic substances, where the absorption of the shorter wavelengths results in transmitted light with a wavelength longer than 500nm, which is responsible for its yellow-brown colour.

Humic substances consist of three main fractions (Schnitzer, 1987, p.2):

- **fulvic acids** (FA) are the lowest molecular weight fraction; it is soluble over the whole pH range; and it is the most susceptible to microbiological degradation

- **humic acids** (HA) have an intermediate molecular weight and are soluble only in alkaline solution
- **humin** (HU) is the highest molecular weight fraction; it is insoluble over the whole pH range; and it is the least susceptible to microbiological degradation

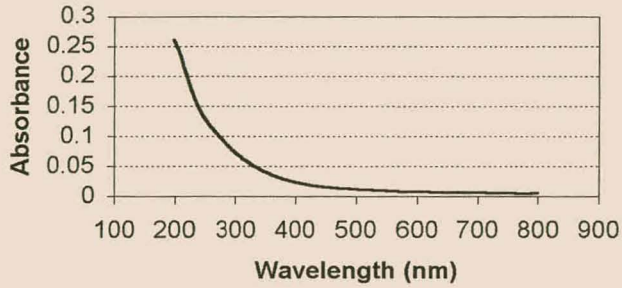

Figure 2.1: UV absorbance spectrum of raw water containing humic substances

2.3.1 The Characterisation of HA and FA

HA and FA differ from each other by possessing a unique elementary and functional group composition. This has an important influence on the physical and chemical behaviour of the different humic substances. Table 2.1 summarises some differences between HA and FA.

Characterisation of the functional groups of HA and FA is very important when different treatment processes are considered for e.g. surface water. The difference in functional group composition of the humic substances results in great differences in response to water treatment, e.g.

- FA have a higher combined carboxylic and phenolic acidity and therefore a higher charge density than HA, resulting in FA being more difficult to coagulate by charge neutralisation (Owen, 1995).

- Molecules with lower charge density can easily be removed by means of activated carbon adsorption. By lowering the pH of the water, the charge density of the FA can be lowered, thereby allowing for removal of both FA and HA (Owen, 1995).

- The solubility of HA and FA are influenced by the presence of different functional groups (Owen, 1995).

Table 2.1: Summary of some differences between HA and FA (Gieseking, 1975, p.50)

Elementary Composition		
Element	Humic Acid (%)	Fulvic Acid (%)
Carbon	56.72	50.92
Hydrogen	5.21	3.34
Nitrogen	2.37	0.74
Sulfur	0.35	0.26
Oxygen (by difference)	35.35	44.74
Oxygen-containing functional groups (m-equivalent per gram of dry ash-free material)		
Group	Humic Acids (%)	Fulvic Acids (%)
Total acidity	5.7	12.4
Carboxyl	1.5	9.1
Total hydroxyl	6.9	6.9
Phenolic hydroxyl	4.2	3.3
Alcoholic hydroxyl	2.7	3.6
Carbonyl	0.9	3.1
Molecular weight	1,684	669

Scanning electron micrographs of precipitates from water solutions, after complete solvent evaporation, at various pH's reveal further information concerning the characteristics of the surfaces of HA and FA - and thus coagulation behaviour - as a function of the pH (Chen, 1976). Hydrogen bonding, Van der Waals' interactions and the interactions between the π-electron systems of adjacent molecules cause a drastic change in surface character with varying pH levels. At low pH the strong intermolecular forces cause the FA to have a fibrous multi-layered structure. An increase in pH causes a decrease in these forces with a consequent change in the surface character to a sheet-like structure. These structural changes result from ionisation of carboxylic, phenolic and hydroxyl functional groups. The resultant electrostatic forces between the functional groups cause the structural change of the FA surface (Figure 2.2(a)).

Similar phenomena can be observed for HA. The pH range over which the surface character can be monitored is however much smaller due to the limiting pH range of solubility for HA (Figure 2.2(b)).

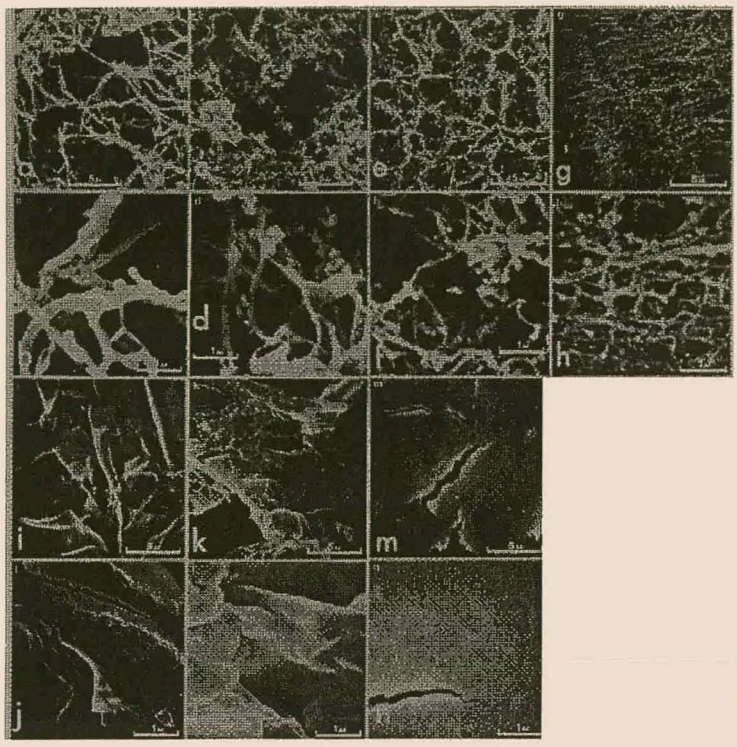

Figure 2.2(a): Scanning electron micrographs of FA at various pH's (From left to right: a (pH 2); c (pH 4); e (pH 6); g (pH 7); b (pH 2); d (pH.4); f (pH 6); h (pH 7); l (pH 8); k (pH 9); m (pH 10); j (pH 8); l (pH 9); n (pH 10)) (Chen, 1976)

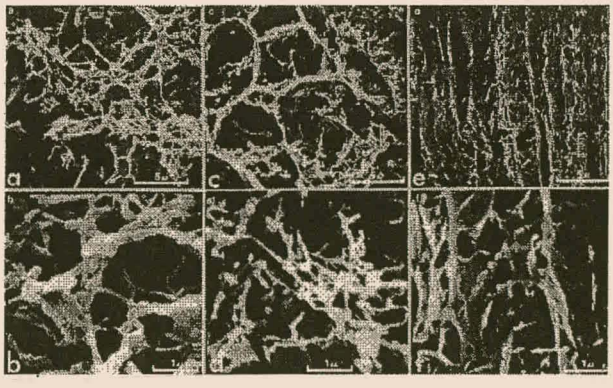

Figure 2.2(b): Scanning electron micrographs of HA at various pH's (From left to right: a (pH 6); c (pH 8); e (pH 10); b (pH 6); d (pH 8); f (pH 10) (Chen, 1976)

2.3.2 Acid-Base Equilibria of Humic Substances

The weak polyelectrolyte character of humic and fulvic acids, contributes to buffering capabilities in soil and aqueous environments. By constructing pK distribution curves at specific ionic strengths for the humic substances, it was shown that it was possible to monitor the deprotonation of the humic substances with an increase in the pH (Fukushima, Tanaka et al., 1995). The behaviour of the humic substances at different pH values can therefore easily be predicted according to the state in which the functional groups are found.

2.3.3 Complexation Ability of Humic Substances

Since humic substances contain elements with lone pair electrons (e.g. nitrogen and oxygen), they are inclined to act as ligands in the formation of complexes with heavy metal ions (Fukushima, Nakayasu et al., 1995). FA and HA possess various binding sites for complexation, eg. -COOH, -COOH- (phenolic) and -OH (phenolic) functional groups. The binding capabilities of heavy metal ions are therefore correlated to the functional group distribution of the humic substances (Warwick, 1994). Useful information concerning the complexation ability of humic substances with heavy metal ions can therefore be deduced from the acid-base equilibria (Fukushima, Tanaka et al., 1995).

Conditional binding constants of various metal-HA complexes have been reported. The conditional binding constants in terms of logK' can be summarised as follows (Schnitzer, 1970):

$$Fe^{3+}\ (7.5) > Al^{3+}\ (5.1) > Cu^{2+}\ (4.6) > Ni^{2+}\ (4.4) > Co^{2+}\ (4.2) > Pb^{2+} = Ca^{2+}\ (3.5) > Zn^{2+}\ (3.1) > Mn^{2+}\ (2.8) > Mg^{2+}\ (2.6)$$

A possible explanation for the insolubility of HU over the entire pH range is that it bonds firmly to inorganic soil and sediment constituents.

This behaviour of humic substances toward metal ions in water immediately provides another analytical method whereby coloured waters could be characterised, namely polarography. By monitoring the complexation of humic substances with metal ions such as Fe^{3+}, Cu^{2+} and Zn^{2+} at various pH levels, humic substances can be characterised.

The occurrence of metals in water originates mainly from natural resources, e.g. from minerals such as barite and limestone, or natural volcanic emissions. In recent times, discharges from factories, mining effluents and other industries have however dramatically increased the amount of metals in our water sources. Complexation of humic substances with metals and/or clays have resulted in resistance against microbiological degradation. A further complication is the reduction in the effectiveness of the flocculation process.

The presence of multivalent ions, such as ferric ions, in the raw water could also enhance complexation between humic substances and clay colloids (Kunin, 1986).

2.3.4 Adsorption Properties of Humic Substances

Kopinke et al. (1995) has performed a series of experiments to investigate the sorption of organic pollutants onto the surface of humic matter. Log K values for several poli-aromatic hydrocarbons (PAHs) as well as polychlorobiphenyls (PCBs) were determined for the sorption onto FA and HA. The results imply strong adsorption. With increasing industrial pollution of surface waters, this characteristic could cause several problems for standard water purification methods.

The hydrophobic properties of the aromatic rings and aliphatic chains contained within humic substances adsorb strongly onto the surface of mercury with a zero charge. The charged functional groups are oriented toward the aqueous medium. This phenomenon could facilitate the analysis of humic substances by means of voltammetry.

2.3.5 Spectroscopic Properties of Humic Substances

The basic humic acid structure, consisting of long conjugated aromatic polymer chains, allows for efficient UV absorption. All humic samples exhibit a featureless increase in UV absorbances with shorter wavelength (See Figure 2.1). By the absorption of UV light, humic substances are activated indirectly from a singlet state to a triplet state. This allows humic substances to photoinduce the transformation of non-absorbing organic compounds. Different chromophores are responsible for the photoreactivity at different wavelengths (Aguer, 1996). Chin and co-workers have indicated that the molar absorptivity (ε) of humic substances at specific wavelengths may reveal important clues concerning the aromaticity,

the source of the humic substances, as well as the extent of humification. They specifically looked at 280nm where the $\pi \rightarrow \pi^*$ electron transitions occur for phenolic substances, aniline derivatives, benzoic acids, polyenes and polycyclic aromatic hydrocarbons. Many of these compounds are either precursors or components of humic substances. ε (280nm) is therefore a useful parameter whereby humic substances can be characterised.

These characteristics could be utilised to develop a further method for the characterisation of coloured waters. This is achieved by the addition of a compound, which is UV inactive, to the coloured water, such that the humic substances induce fluorescence in this compound. The resultant fluorescence spectrum could then be recorded and used in the characterisation of the coloured water.

Another idea for water purification flows from the knowledge of the excited electronic states of humic substances that can be reached as a result of initial activation by radiation. The triplet states of the humic substances might have sufficient energy to activate dissolved oxygen in the ($X\ ^3\Sigma^-_g$) ground electronic state to the first ($^1\Delta_g$) activated electronic state through intermolecular collisions. The singlet oxygen being a powerful oxidant can initiate the oxidation of organic pollutants as well as humic substances.

2.3.6 Analysis of Humic Substances

The chemical and physical composition of humic substances can be determined by a series of experiments. Firstly, the humic substances can be extracted and separated by employing the knowledge of solubility of the various fractions. See Figure 2.3 for a summary on this procedure. Each fraction can further be categorised according to their molecular weight by the process of ultrafiltration.

Many non-degradative methods for the determination of the physical properties exist, e.g. (Schnitzer, Khan, 1987, p.10):

- Ultraviolet and visible light absorption
- Infra-red analysis
- X-ray diffraction

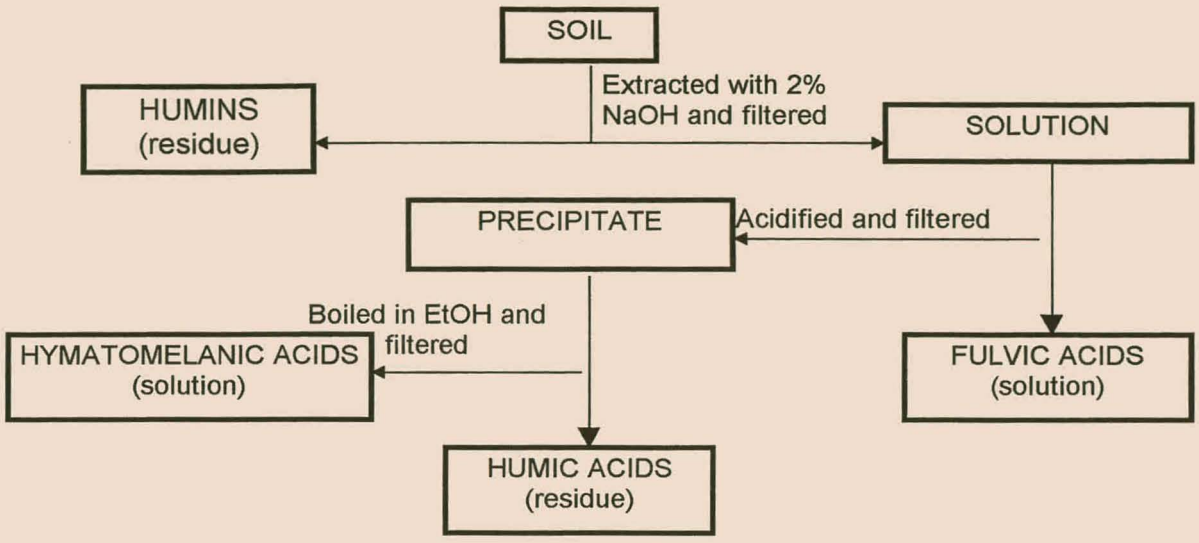

Figure 2.3: Summary of the determination of different fractions of a soil sample (Gieseking, 1975, p.6).

2.4 CONVENTIONAL WATER PURIFICATION METHODS AS RELATED TO NOM

Early civilisations invariably developed around regions with abundant water supplies. Little was known about the quality of water and the relation between water quality and disease. Early water purification was exclusively for cosmetic purposes. Apart from the improvement of appearance or taste, no other standards for water purification were recorded. By the eighteenth century, filtration of water as a means of removal of particles from water, to clarify it, was established. The first, municipal, water filtration plant was established in 1832 in Paisly, Scotland (Pontius, 1990). Only after the transmission of various epidemics, such as cholera and typhoid, through water was realised, more stringent criteria for water quality were established. In the USA the rapid development of communities resulted in many municipal water supplies being erected. Unfortunately the improvement of health and sanitary conditions did not develop at an equally fast rate. Outbreaks of water-born diseases resulted in many deaths. Only at the turn of the century the next milestone in water purification was reached namely the use of chlorine as disinfectant. Since then, the water quality standards have changed several times, becoming more and more stringent due to industrialisation and development, which caused a great amount of water pollution annually. The basic method of water purification today can be summarised by:

- coagulation and flocculation
- filtration
- chlorination

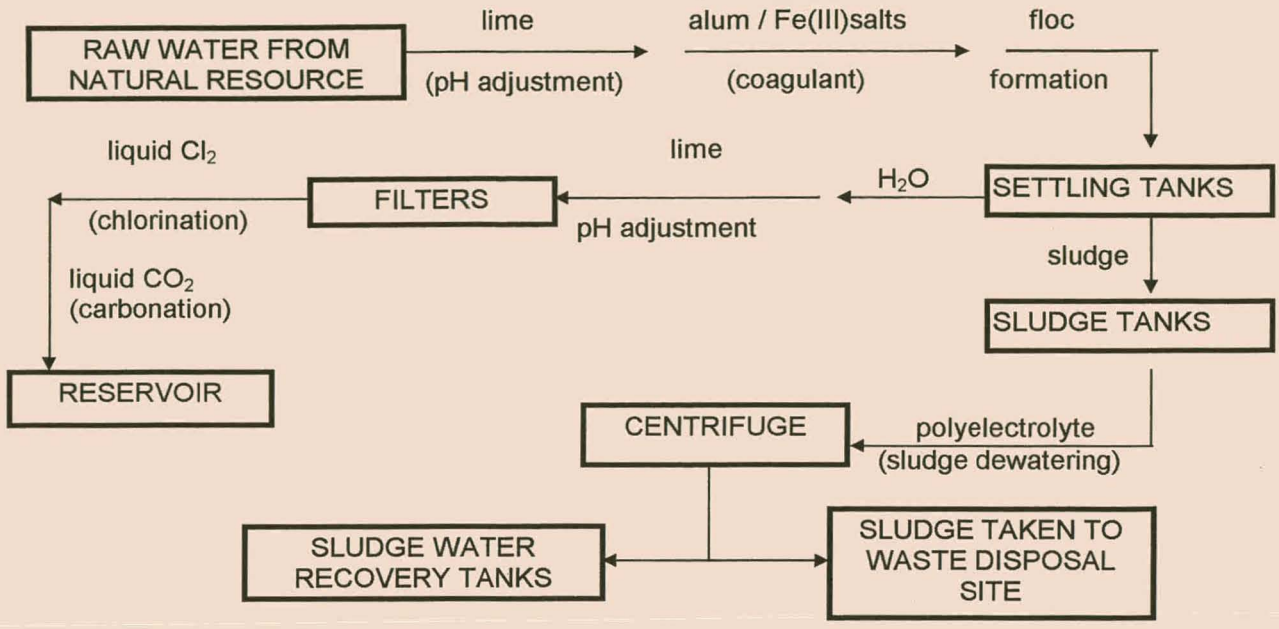

Figure 2.4: Diagrammatic Representation of a Typical Water Treatment Plant

2.4.1 Coagulation and Flocculation

The process of coagulation can be described as the combination of small particles into larger aggregates. Humic substances are stable colloidal particles dispersed in a water medium, each consisting of a negatively charged surface and a diffuse double layer.

These particles can be destabilised by

- compression of the double layer
- adsorption to produce charge neutralisation
- trapping in a precipitate
- adsorption to permit inter-particle bridging

In the water treatment process, charge neutralisation is used to induce the process of coagulation. This is achieved by adding a coagulant to the water. Standard practice is to add either alum ($Al_2(SO_4)_3.14.3H_2O$) or iron (III) salts to destabilise the humic substances, resulting in charge neutralisation and coagulation of the colloids. Coagulation diagrams are drawn up for each water treatment plant. This is a summary of the chemical conditions under which coagulation occurs. The coagulant dosage and pH at which the coagulant should be added are indicated on these diagrams (See Figure 2.5).

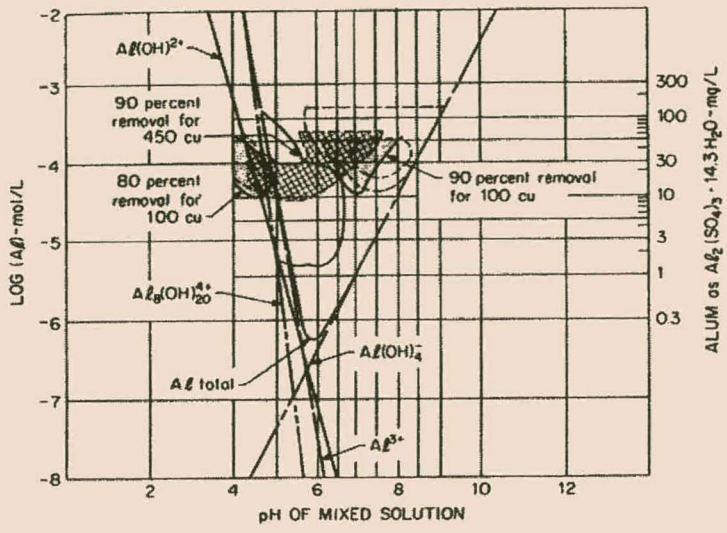

Figure 2.5: A typical alum coagulation diagram for colour removal and its relation to the pH (CU=colour unit) (Pontius, 1990, p.298)

These diagrams can be applied for

- turbidity removal
- colour removal
- direct filtration
- selection of direct mixing devices

The second phase of the coagulation process is referred to as the flocculation process, where smaller particles are transformed into larger aggregates or flocs. These flocs are allowed to settle, thereby separating the water from the humic substances. The settled flocs are referred to as sedimentation. Sedimentation is problematic in terms of sludge disposal. Possible applications have been investigated: the manufacturing of bricks and tiles or in instances where the iron levels are not too high, fertiliser manufacturing from the sludge was assessed (Boucher, 1994).

2.4.2 Filtration

Sand bed filtration is mainly used in the water purification process. The purpose thereof is to remove any remaining suspended particulate matter in the water. The distribution of particle size and physical form of the sand particles are important.

2.4.3 Chlorination

Water-borne diseases pose a serious problem to water used for human consumption. The disinfection of water can be defined as the deliberate reduction of the number of pathogenic microorganisms. Different methods of water disinfection have been established (Pontius, 1990, p.877). They are:

- Chlorination
- chlorine dioxide addition
- ozonation
- ultra violet radiation

For almost a century the predominant method of disinfection of water was through the process of chlorination. Chlorine is administered in a liquid form at low pH after the water has been filtered. Chlorination, however, caused problems by producing DBPs when being administered to water containing traces of organic material. The presence of THMs was discovered in the drinking water only after studies were conducted from 1970 onwards. Humic substances have been shown to be precursors in the formation of THM when it is not completely removed from the water by the process of coagulation. The carcinogenic nature of THMs immediately caused a great health concern. Alternative methods of disinfection therefore had to be investigated.

Disinfection with ultra violet rays has proved to be a good alternative for the conventional disinfection with chlorine (Bernhardt, 1991; Wolfe, 1990). Since 1910 UV irradiation had been used successfully at smaller water treatment plants worldwide. Many limitations existed, however, with regard to the effectiveness and feasibility of such a process when applied on large scale. The following concerns had to be addressed:

- undesirable side reactions of UV-rays with nitrate ions and naturally occurring dissolved organic compounds (DOC)
- the necessity to monitor the disinfection efficiency
- the extent to which the formation of Ca, Fe and Mn coatings inside the UV reactor inhibit the irradiation process
- the generation of undesirable substances in the drinking water by the UV irradiation
- the risk of bacterial regrowth in the water distribution system

Fortunately, in the colder countries, these concerns proved to be exaggerated. In Europe UV disinfection is employed successfully as a means of water disinfection. Lately many household water purification models, based on the principle of UV disinfection, have also surfaced on the market, e.g. the *UV Tech Ultra Violet - Ultra Pure* water purifier.

2.4.4 Membrane Filtration

One of the latest developments for removal of colour from raw water is based on the principle of ultrafiltration, whereby membranes with a specific pore size are utilised to filter out the humic acid colloids (Jacobs, 1997). Unfortunately this process has not yet developed into a cost-effective alternative for current water treatment processes.

2.4.5 The Sirofloc Process

This is a technique whereby colloidal impurities such as colour (humic substances) and turbidity are removed from the water (Hagger, 1996). The process involves the addition of finely divided (1-10μm) magnetite, which is a naturally occurring iron oxide (Fe_3O_4), to raw water. The adsorption of the impurities occur under acidic conditions where the magnetite is positively charged, allowing for excellent adsorption of the negatively charged humic substances to its surface.

The sirofloc process proves to be very versatile, since it not only removes colour and turbidity, but also Fe, Mn, algae, bacteria, viruses and certain heavy metals. The process also operates over a broader pH range than normally possible when employing the standard flocculation process. From an economical point of view this process is also advantageous, since magnetite can be regenerated and recycled. The magnetite containing the adsorbed colloids is regenerated by raising the pH to 11-12 with caustic soda, causing the surface to become negatively charged and the adsorbed colloidal material to be repelled. The magnetite is then washed free of caustic soda and entrained colloidal material and is ready for reuse. The process however produces caustic waste that must be disposed of.

2.4.6 Activated Carbon Adsorption

Various forms of activated carbon are currently used in water purification processes. Granular activated carbon (GAC) and powdered activated carbon (PAC) are used for the removal of organic molecules from polluted waters which exhibit taste, odour, colour, mutagenicity and toxicity effects (Pontius, 1990). At local water purification plants, GAC is used especially for the removal of geosmin, a musty odour product of algae, commonly found in the raw water.

The Brunauer Emmet Teller (BET) surface area for activated carbon materials is typically in excess of $1000m^2/g$. Recently other forms of activated carbon have also been investigated, namely fibrous activated carbon (FAC) in the form of cloths and felt (Le Cloirec, 1997). Initial adsorption kinetic coefficients are higher with fibres than with granules due to the direct connection of micropores on the external surface of fibres. The BET surface area for FAC is improved to $1500m^2/g$.

Although PAC, GAC and FAC allow for the efficient removal of organic micropollutants from water, this process merely transfers the organic micropollutants from one phase to another (Serpone, 1989). Regeneration of the activated carbon is necessary for the cost-effective operation of such a process. The need, therefore, exists to study processes, which involves the chemical destruction of water-born pollutants.

2.4.7 Biological Treatment

Biological treatment of water is focussed mainly on processes for the purification of waste-waters and sewage. Various compounds including phenol, geosmin and methylisoborneol (odour-causing compounds), *p*-nitrophenol, salicylic acid and ammonia can be destroyed by this process (Pontius, 1990) and is based on the consumption of pollutants by specific microorganisms. These microorganisms include the following (Tonkes, 1997):

- algae (e.g. Selenastrum capricornutum)
- bacteria (e.g. Vibrio fischeri)
- crustaceans (e.g. Daphnia magna (fresh water) and Acartia tonsa (marine))
- fish (e.g. Brachydanio rerio (fresh water) and Poecilia reticulata (marine))

Bioreactors employed in these water treatment processes include horizontal-flow anaerobic immobilised sludge reactors (Cadavid, 1997) and anaerobic fluidised bed bioreactors (Cheng, 1997). The combination of anaerobic bioreactors with membranes (Fakhru'l-Razl, 1997) or GAC (Pontius, 1990) are also known.

2.4.8 Advanced Oxidation Processes

The natural process of photolysis as induced by ultra violet sunrays purifies aqueous systems, such as streams, lagoons and lakes (Ireland, 1993). This process results in the breakdown of the organic molecules to form intermediate molecules, which eventually form CO_2 and water. Based on this, researchers have developed several processes, collectively referred to as advanced oxidation processes (AOPs) for the purification of water (Legrini, 1993).

These processes are:

- H_2O_2/UV
- O_3/UV
- H_2O_2/O_3/UV
- TiO_2/UV
- Vacuum Ultra Violet Process (VUV)

H_2O_2/UV, O_3/UV and H_2O_2/O_3/UV are procedures that employ UV photolysis of H_2O_2 and/or O_3 to generate the reactive OH· radical that reacts with the organic molecules. TiO_2/UV, on the other hand, is based on the principle of photocatalytic oxidation, where the semiconductor absorbs the UV rays to generate OH· from the adsorbed H_2O and hydroxide ions. OH· radicals and H_2 molecules are produced during the VUV photolysis when high energy interacts with water.

2.4.9 Purification of Drinking Water vs. Industrial Waste Water

The coagulation process is regarded as an effective process for treating surface and ground water containing NOM, by the local municipal waterworks, and will be applicable for a long period. The use of granular or fibrous activated carbon in conjunction with coagulation will extend the "lifetime" of the coagulation process. The same applies for the sirofloc and membrane processes.

It is doubtful whether the above-mentioned processes can purify water containing NOM and a variety of organic pollutants of industrial origin.

Treatment by means of bioreactors is essentially a slow process, which is inhibited by the presence of certain biocidal pollutants e.g. the chlorophenols. A process, which is capable to purify water containing NOM, organic pollutants, biocides and e.g. microcystin toxins up to potable standard, is obviously desirable.

Photocatalytic oxidation might be capable of achieving this. Although much research has been done in the field of photocatalytic purification of both raw water and water polluted with industrial waste (Hidaka, 1995; Prairie, 1993; Nair, 1993; Mills, 1993), optimisation of the photocatalytic process for the treatment of raw water, containing pollutants, should be embarked on.

REFERENCES

Aguer J.P., Richard C. (1996) Reactive species produced on irradiation at 365nm of aqueous solutions of humic acids. *Journal of Photochemistry and Photobiology A: Chemistry* **93** 193-198

Aguer J.P., Richard C. (1994) Photochemical behaviour of a humic acid synthesized from phenol. *Journal of Photochemistry and Photobiology A: Chemistry* **84** *69-73*

Bernhardt H.(1991) Disinfection of Reservoir Water with UV-rays. *WISA Conference 1991, Proceedings of the Second Biennial Conference. Papers* **1** pp.14-40

Boucher P.S., van Eden J.J. (July 1994) Investigation of Inorganic Materials Derived from Water Purification Processes for Ceramic Applications. *WRC Report no. 538*

Cadavid D.L. Zaiat M., Foresti E. (1997) Paper 5.3: Performance of horizontal-flow anaerobic immobilized sludge (HAIS) reactor treating synthetic substrate subjected to decreasing COD to sulfate ratio's. *International Association on Water Quality (IAWQ)*; GB; International Association on Water Quality Specialized Conference on Chemical Process Industries and Environmental Management: Cape Town, South Africa (8-10 September 1997)

Chen Y., Schnitzer M. (1976) Scanning Electron Microscopy of a Humic Acid and of a Fulvic Acid and its Metal and Clay Complexes. *Soil Sci. Soc. Am. J.* **40** p. 682-686

Cheng S.-S., Wu J.-H., Tseng I.-C., Hwang P.-C. (1997) Paper 5.1: Treatability study of anaerobic fluidized bed bioreactor treating PTA manufacturing wastewater. *International Association on Water Quality (IAWQ)*; GB; International Association on Water Quality

Specialized Conference on Chemical Process Industries and Environmental Management: Cape Town, South Africa (8-10 September 1997)

Chin Y.-P., Aiken G., O'Loughlin E. (1994) Molecular Weight, Polydispersity, and Spectroscopic Properties of Aquatic Humic Substances. *Environ. Sci. & Technol.* **28** p.1853-1858

Fakhru'l-Razi A., Noor M.J.M.M. (1997) Poster Paper 6.9: Treatment of palm oil mill effluent (POME) with membrane anaerobic system (MAS). *International Association on Water Quality (IAWQ)*; GB; International Association on Water Quality Specialized Conference on Chemical Process Industries and Environmental Management: Cape Town, South Africa (8-10 September 1997)

Fukushima M., Nakayasu K., Tanaka S. and Nakamura H. (1995) Chromium (III) binding abilities of humic acids. *Analytica Chimica Acta* **317** 195-206

Fukushima M., Tanaka S., Hasebe K., Taga M., Nakamura H. (1995) Interpretation of the acid-base equilibrium of humic acid by a continuous pK distribution and electrostatic model. *Analytica Chimica Acta* **302** 365-373

Hagger M.J. (1996) Coloured Water Treatment Using the Sirofloc Process. *Poster Presentation: Seminar on "The Treatment of Coloured Water for Potable Use*

Hidaka H., Nohara K., Zhao J., Pelizzetti E., Serpone N. (1995) Photodegradation of surfactants XIV. Formation of NH_4^+ and NO_3^- ion for the photocatalyzed mineralization of nitrogen-containing cationic, non-ionic and amphoteric surfactants. *Journal of Photochemistry and Photobiology A: Chemistry* **91** p.145-152

Ireland J.C. (1993) Microbiological issues related to drinking water disinfection chemistry: opportunites for further TiO_2 research. *Presentation at Conference: Photocatalytic Purification & Treatment of Water & Air* 557-569

Jacobs E.P., Botes J.P. *et al.* (1997) Ultrafiltration in potable water production. *Water SA* **23** 1-6

Kopinke F.-D., Pörschmann J., Stottmeister U. (1995) Sorption of Organic Pollutants on Anthropogenic Humic Matter. *Environmental Science and Technology* **29** No.4 941-950

Kunin R. (1986) The Role of Organic Matter in Water Treatment – A Universal Theory. *Amber-hi-lites* No.179 1-8

Laburn R.J. (1995) Water Supply in South Africa. *J. Water SRT - Aqua* **44** No.4 161-165

Le Cloirec P., Brasquet C., Subrenat E. (1997) Adsorption onto Fibrous Activated Carbon: Applications to Water Treatment. *Energy & Fuels* **11** No.2 p.331-336

Legrini O., Oliveros E., Braun A.M. (1993) Photochemical Processes for Water Treatment. *Chemical Reviews* **93** 671-698

Mills A., Davies R.H., Worsley D (1993) Water Purification by Semiconductor Photocatalysis. Chemical Society Reviews **22** p.417-425

Nair M., Luo Z., Heller A. (1993) Rates of Photocatalytic Oxidation of Crude Oil on Salt Water on Buoyant, Cenosphere-Attached Titanium Dioxide. *Ind. Eng. Chem. Res.* **32** p.2318-2323

Owen D.M., Amy G.L. (1995) NOM characterization and treatability. *Journal AWWA* 46-63

Pontius F.W. (Technical Editor) (1990) Water Quality And Treatment, A handbook of Community Water Supplies 4th Edition New York, N.Y.: McGraw-Hill

Prairie M.R., Evans L.R., Stange B.M., Martinez S.L. (1993) An Investigation of TiO_2 Photocatalysis for the Treatment of Water Contaminated with Metals and Organic Chemicals. *Environ. Sci. Technol.* **27** p.1776-1782

Schnitzer M. and Hansen E.H. (1970) Organo-metallic Interactions in Soils:8. An evaluation of methods for the determination of stability constants of metal-fulvic acid complexes. *Soil Science* **109** 333-340

Schnitzer M. and Khan S.U. (Editors) (1978) Soil Organic Matter Elsevier Scientific Publishing Company

Soil Components Volume 1: Organic Components. (1975) Gieseking J.E. (Editor) Springer-Verlag New York Inc.

Tonkes M., De Graaf P.J.F., Graansma J. (1997) Assessment of complex industrial effluents in the Netherlands using a whole effluent toxicity (or WET) approach. *Oral Presentation at Specialised Conference on Chemical Process Industries and Environmental Management 8-10 September 1997*

Van Der Merwe S.W. (1995) An Overview of Water Supply Management in South Africa. *J. Water SRT - Aqua* **44** No.4 151-160

Warwick P., Hall A. and Read D. (1994) A Comparative Study Employing Three Different Models to Investigate the Complexation Properties of Humic and Fulvic Acids. *Radiochimica Acta* **66/67** 133-140

Wolfe R.L. (1990) Ultraviolet disinfection of potable water. *Envirn. Sci. Technol.* **24** No.6 p.768-773

CHAPTER 3

Photocatalysis

3.1 HETEROGENEOUS PHOTOCATALYSIS

3.1.1 Photocatalytic Oxidation

Heterogeneous photocatalysis is one of the existing AOPs receiving much attention in the research field of water purification. It is a very simple process based on the irradiation of a photocatalyst, usually a semiconductor such as TiO_2, ZnO or CdS, with the consequent production of highly reactive hydroxyl radicals. These hydroxyl radicals can take part in oxidation reactions whereby organic compounds can be completely mineralised to form CO_2 and H_2O. In addition to the oxidation of organic compounds, certain metal ions can be reduced by means of a conduction band electron (e^-_{cb}) formed at the surface of the catalyst compounds (Hoffmann, 1995). The advantage of this process compared to other water treatment processes is therefore that the organic, as well as inorganic, pollutants are destroyed or removed and not merely transferred from one medium to the next. The only disadvantage of heterogeneous photocatalysis is that the redox potential of the specific compound to be oxidised, must lie above that of the valence band of the semiconductor. Similarly, species can only be reduced if their redox potentials lie below that of the conduction band. Heterogeneous photocatalysis has been proven successful in the mineralisation of several classes of compounds. They include chlorinated aromatics, surfactants, pesticides, herbicides, etc. Research in the field of photocatalysis is driven by legislation in industrialised countries where greater emphasis is placed on the simultaneous decontamination and destruction of pollutants in water (Serpone, 1995).

For the process of photocatalytic oxidation to take place, the following is required:

- a photocatalytic n-type semiconductor
- a UV light source (λ < band gap) to create the conduction band electrons (e^-_{cb}) and the valence band holes (h^+_{vb})
- an aqueous medium, since H_2O molecules and OH^- ions are necessary for the production of the OH· radicals

$$H_2O\ (ads) + h^+ \rightarrow OH\cdot\ (ads) + H^+$$

$$OH^- + h^+ \rightarrow OH\cdot\ (ads)$$

- O_2 (g) to prevent the recombination of the e^-_{cb} and h^+_{vb} by trapping the e^-_{cb}

$$O_2(ads) + e^-_{cb} \rightarrow O_2^- (ads)$$

The photocatalytic process can be summarised by the representation in Figure 3.1:

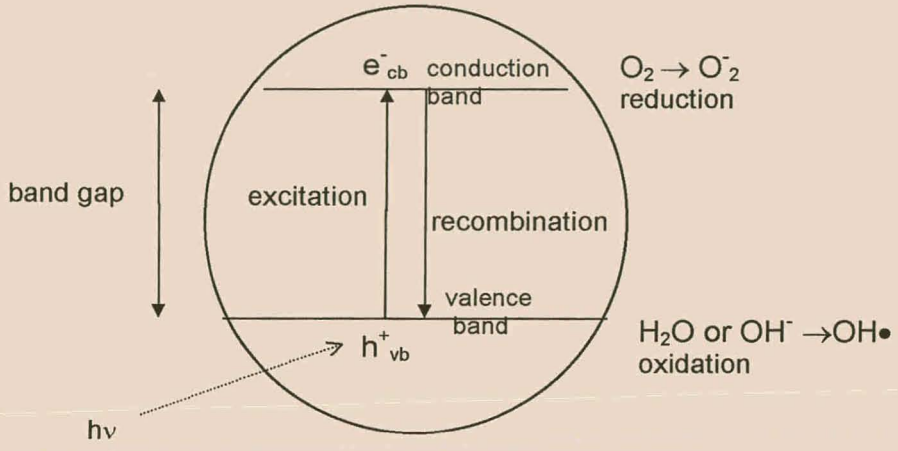

Figure 3.1: Summary of the Photocatalytic Process

When light of a specific minimum energy (i.e. energy greater than the band gap of the semiconductor) falls onto a semiconductor particle, a valence band electron is excited to the conduction band from where certain reactions can take place. The valence band hole reacts with either water or a hydroxyl ion to form the reactive hydroxyl radical necessary for oxidative photocatalysis. If the conduction band electron and valence band hole is not utilised, they recombine and emit light of a specific wavelength.

$$TiO_2 \xrightarrow{h\nu} e_{cb}^- + h_{vb}^+$$

$$H_2O(ads) + h_{vb}^+ \rightarrow OH\cdot(ads) + H^+$$

$$OH^- (ads) + h_{vb}^+ \rightarrow OH\cdot(ads)$$

$$e_{cb}^- + h_{vb}^+ \rightarrow h\nu' \quad (\nu' < \nu)$$

The reaction of the conduction band electron with adsorbed oxygen, O_2 (ads), to produce hydrogen peroxide (H_2O_2) from super-oxide ions (O_2^-), can be summarised by:

$$O_2 (ads) + e_{cb}^{--} \rightarrow O_2^- (ads)$$

$$O_2^- (ads) + H^+ \rightarrow HO_2\cdot$$

$$2(HO_2\cdot) \leftrightarrow H_2O_2 + O_2$$

$$O_2^- (ads) + HO_2\cdot \leftrightarrow O_2 + HO_2^-$$

$$HO_2^- + H^+ \leftrightarrow H_2O_2$$

$$H_2O_2 \rightarrow H_2 + O_2$$

$$H_2O_2 + OH\cdot \leftrightarrow HO_2\cdot + H_2O$$

$$H_2O_2 + HO_2\cdot \rightarrow OH\cdot + H_2O + O_2$$

H_2O_2 may also form hydroxyl radicals by any of the following:

$$H_2O_2 \xrightarrow{h\nu} 2(OH\cdot)$$

$$H_2O_2 + O_2^-(ads) \rightarrow OH\cdot + OH^- + O_2$$

$$H_2O_2 + e_{cb}^- \rightarrow OH\cdot + OH^-$$

3.1.2 Semiconductors

Crystalline minerals are catagorised according to their ability to conduct an electrical current. Three basic types exist, namely conductors, semiconductors and insulators.

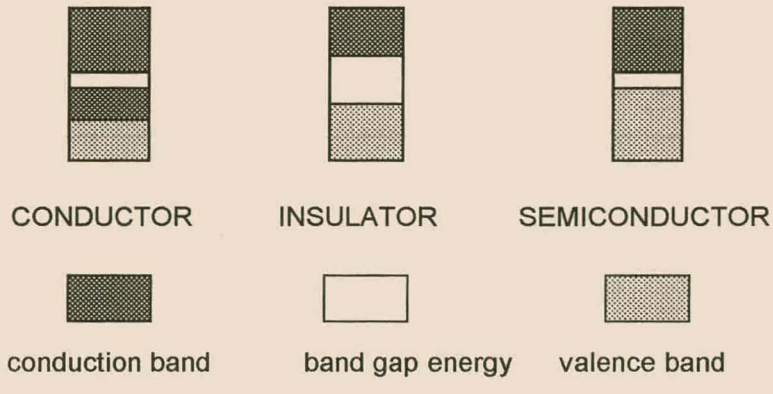

Figure 3.2: Crystalline Mineral Classification (Hand, 1995)

According to the well-known band theory of solids, the valence band (vb) and conduction band (cb) consist of a series of energy levels resulting from the combination of the highest atomic orbitals of the individual atoms. An energy barrier, called the band gap separates the vb from the cb. This band gap is unique for each type of solid. Electrons move about easily in a conductor because of the overlap between the cb and the vb. With the semiconductors and insulators this is not possible, since the vb and cb is separated by the band gap. The size of the band gap indicates whether the solid is an insulator or semiconductor (Serpone, 1989, p.42). Insulators normally have a band gap of approximately 3.5 eV. By doping the semiconductors, the size of the band can either be increased (p-doping) or decreased (n-doping). This allows a wider application of the specific semiconductor.

Table 3.1: Summary of several semiconductors with their band gap energies and wavelength of light equivalent to the band gap (Hand, 1995)

Semiconductor	Semiconductor Type	Band Gap (eV)	Equivalent Wavelength (nm)
SnO_2	n	3.50	354
$KTaO_2$	n	3.50	354
$SrTiO_3$	n	3.40	365
Nb_2O_5	n	3.40	365
ZnO	n	3.35	370
TiO_2 (Anatase)	n	3.20	300
SiC	p	3.00	376
V_2O_5	n	2.80	443
WO_3	n	2.70	459
CdS	n	2.40	516
GaP	p	2.30	539
CdO	n	2.20	563

Semiconductors used in the photocatalytic applications are typically n-type semi-conductors. TiO_2 is the most popular semiconductor used in this field of research.

3.1.3 Titanium Dioxide

Titanium is the ninth most abundant element in nature. It is found in many minerals and occur naturally as an oxide, or an oxide in combination with iron, eg. ilmenite ($FeTiO_3$), rutile

(TiO_2), anatase (TiO_2) and leucoxene ($TiO_2.xFeO.yH_2O$) (Braun, 1997). TiO_2 has three basic crystal structures, namely anatase, rutile and brookite. Since the latter is very scarce, only the anatase and rutile have a significant commercial application. They differ only with respect to their lattice structures, refractive indices (rutile=2.7 and anatase=2.5) and densities.

Two processes exist for the commercial production of TiO_2, namely

- The chloride process
- The sulfate process

The older aqueous sulfate method consists of low-tech, labour-intensive operations performed largely in batch modes, while the newer anhydrous chloride route is composed of high-tech, automated, mostly continuous operations. Both rutile and anatase can be produced via the sulfate process, while only the rutile pigment is produced from the chloride process. Phase conversion from anatase to rutile can be performed. This process requires extremely high temperatures (well over 500°C) as well as effective mineralisers (Braun, 1997).

The commercially available TiO_2 have different crystal structures. Table 3.2 summarises the available types. Degussa TiO_2 was locally available and was therefore used as catalyst for the photocatalytic experiments.

Table 3.2: Summary of Commercially Available TiO_2 (Tanaka, 1993)

TiO_2 Type	Crystal Form	Particle Size (μm)	Specific Surface Area ($m^2.g^{-1}$)
TP-2	Anatase	0.15	17.3
Degussa	Anatase	0.03	57.0
Katayama	Rutile	1.30	2.8
TP-3	Rutile	1.44	4.4
TM-1	Rutile	0.40	6.1

The non-toxic, stable nature of TiO_2, its abundance and therefore low cost, as well as its optical properties made it a good prospect for applications in the chemical industry (Rajeshwar, 1996). Good optical characteristics of TiO_2, namely its high refractive index, particle size and light scattering abilities, allowed for it to be used as a versatile pigment. A few commercial applications of the rutile crystal structure include a whitener in coatings, plastics, printing inks and paper (Judin, 1993).

A further consequence of the good optical properties of TiO_2 is its ultraviolet filtering capabilities over the entire ultraviolet spectrum (UV-A, UV-B and UV-C) (See Figure 3.3). It was however noticed that the anatase crystal form were more photoactive than the rutile crystal form. The ultraviolet filtering capability broadened rutile's commercial application to be used in skin care and cosmetic products, as well as suncreams with a sun protection factor of more than 20. The autoxidation and discoloration of meats and cheeses in grocery stores, as a result of ultraviolet radiation from artificial lighting, could also be prevented now by the addition of TiO_2 (rutile) in the clear plastic wrappings. Even the yellowing and deterioration of mechanical properties of plastics could now be retarded by the addition of TiO_2, which acts as a light stabiliser.

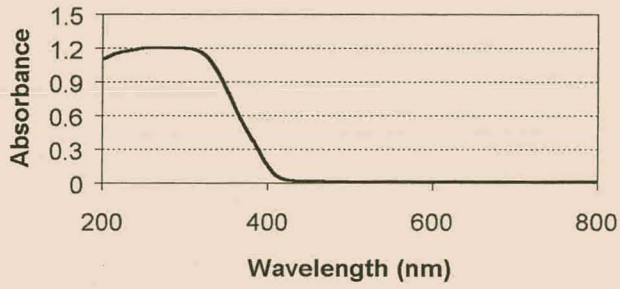

Figure 3.3: UV Absorbance spectrum of TiO_2

The application of TiO_2 as a catalyst in the process of heterogeneous photocatalysis is, perhaps, the most important application of TiO_2 for the future. Many pollutants can now be destroyed instead of just being transferred from one matrix to the next. This process has already found an application in environmental clean-up operations such as oil-spills, where TiO_2-coated microbeads serve as the site for photocatalysis of the oil film (Jackson, 1991). Even continuous-sterilisation systems, based on TiO_2 photocatalysis, have been developed (Matsunaga, 1988). The development of a reactor for the photocatalytic treatment of water for potable use is also receiving much attention.

This efficiency of photocatalysis in the presence of TiO_2 can be improved by the addition of H_2O_2. The purpose of this is twofold. Firstly, it accepts an electron, thereby promoting charge separation and secondly, hydroxyl radicals are simultaneously formed (Tanaka, 1993).

$$O_2 + e^- \rightarrow O_2^-$$

$$O_2^- + H_2O_2 \rightarrow OH\cdot + OH^- + O_2$$

$$H_2O_2 + e^- \rightarrow OH^- + OH\cdot$$

The adsorption of organic molecules onto the surface of TiO_2 in aqueous suspensions is pH dependent. At high pH levels, the adsorption of molecules with electronegative functional groups, e.g. carboxylic groups of humic substances, are suppressed as a result of repulsion caused be the opposing negative charges of the TiO^- species (Tanaka, 1993) (See Figure 3.4). The charge variation of TiO_2 with varying pH levels can be expressed in terms of the following equilibrium:

$$-Ti\text{-}OH_2^+ \overset{H^+}{\Leftrightarrow} -Ti\text{-}OH \overset{H^+}{\Leftrightarrow} -Ti\text{-}O^-$$

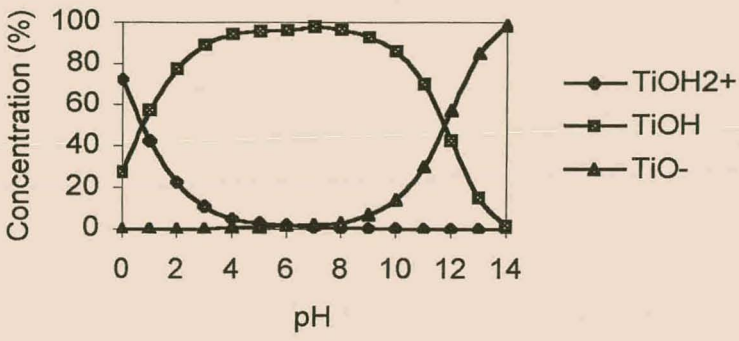

Figure 3.4: Distribution of TiOH-, $TiOH_2^+$- and TiO^-species in aqueous medium (Kriek, 1994, p.48)

Exhibiting semiconductor characteristics, may be the most important feature of TiO_2 for future industrial applications. AOPs are one of the leading fields of research for water purification, with TiO_2 being the most researched semiconductor for photocatalysis. The anatase form of TiO_2 is more efficient as a catalyst in the photocatalytic oxidation of organic molecules. Since the region of light absorption of TiO_2 overlaps with that of sunlight, solar detoxification with TiO_2 is also an attractive option.

3.2 REACTOR DESIGN

Photocatalytic water purification units, based on the fixed-bed reactor (3.2.2), are commercially available (Matrix Photocatalytic Inc.). Information regarding the design of reactors for the application of photocatalytic oxidation is, however, very scarce in literature. Although a vast amount of research has been done in this field, and many experimental results have been published, the lack of information on the efficiency and scaling-up potential of these systems are evident. Apart from information regarding light sources,

reactor volumes, initial concentration of pollutants and other general experimental conditions, no definite specifications for the design of reactor systems are mentioned. This can be attributed to a substantial amount of secrecy that prevails until a specific design is patented (Legrini, 1993). The lack of extensive collaboration between chemists, material scientists and engineers is a further contributing factor. Innovations in photoreactor design and catalyst preparation must continue (Rajeshwar, 1996). Success in the design of reactors lies within the unique combination of the light source, photocatalyst and polluted water. Many of the published photocatalytic experimental results were obtained on small-scale reactors such as batch reactors, annular reactors and cuvettes.

A few basic reactor designs are known:

3.2.1 Annular Reactor

The annular reactor consists of a glass jacket surrounding the UV lamp to facilitate direct contact of the catalyst (e.g. TiO_2) slurry with the lamp. Direct contact can be detrimental since the catalyst adsorbs substantially onto the glass surface, thereby inhibiting UV penetration through the water (Figure 3.5).

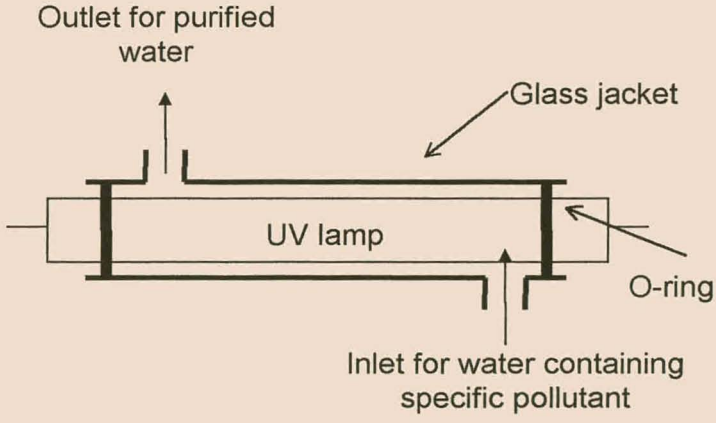

Figure 3.5: Annular Reactor Design

3.2.2 Fixed-bed Reactor

A variation of the annular reactor (Figure 3.5) is the immobilisation of the photocatalyst in a so-called fixed-bed reactor (Figure 3.6). This design facilitates the continuous use of the photocatalyst for the treatment of polluted water and eliminates the tedious process of

filtration to remove the photocatalyst from the purified water. The photocatalyst, eg. TiO_2, is immobilised on inert media such as quartz sand, glass, activated carbon, or noble metal (Haarstrick, 1996).

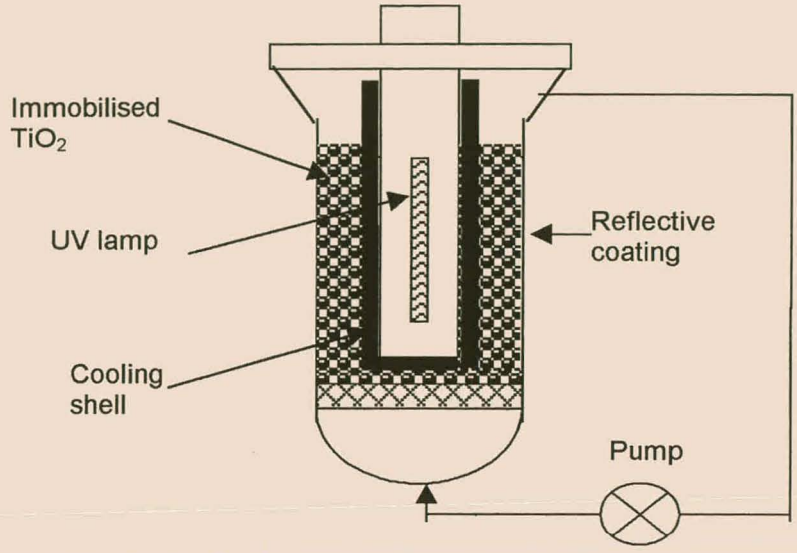

Figure 3.6: Fixed-Bed Reactor (Haarstrick, 1996)

This reactor design does however also have certain drawbacks. The light-utilisation efficiency is decreased by the absorption and scattering of light by the reaction medium and the processing capacities are restricted by the mass transport limitations.

3.2.3 Fiber Optic Cable Reactor

To eliminate the problems experienced with the fixed-bed reactor, Ollis and Marinangeli (1980) proposed the use optical fibres as a means of light transmission to a reactor containing immobilised catalyst (Figures 3.7 and 3.8). The light energy is transmitted to TiO_2 particles, which are chemically anchored to quartz fibre cores, via radial refraction of light out of the fiber (Peill, 1995).

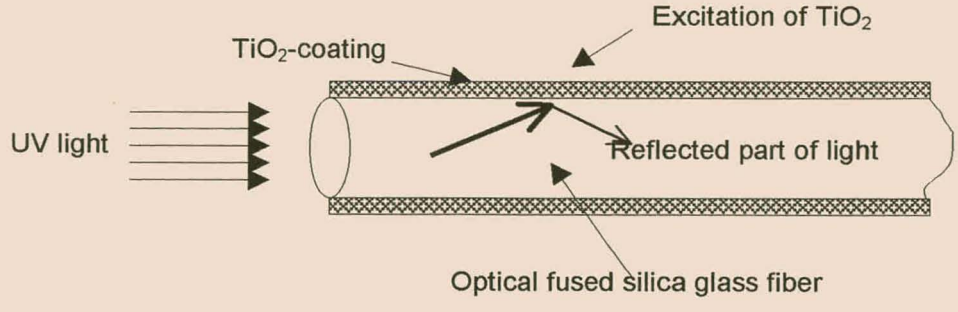

Figure 3.7: An Optical Fiber Coated with TiO_2 (Hofstadler, 1994)

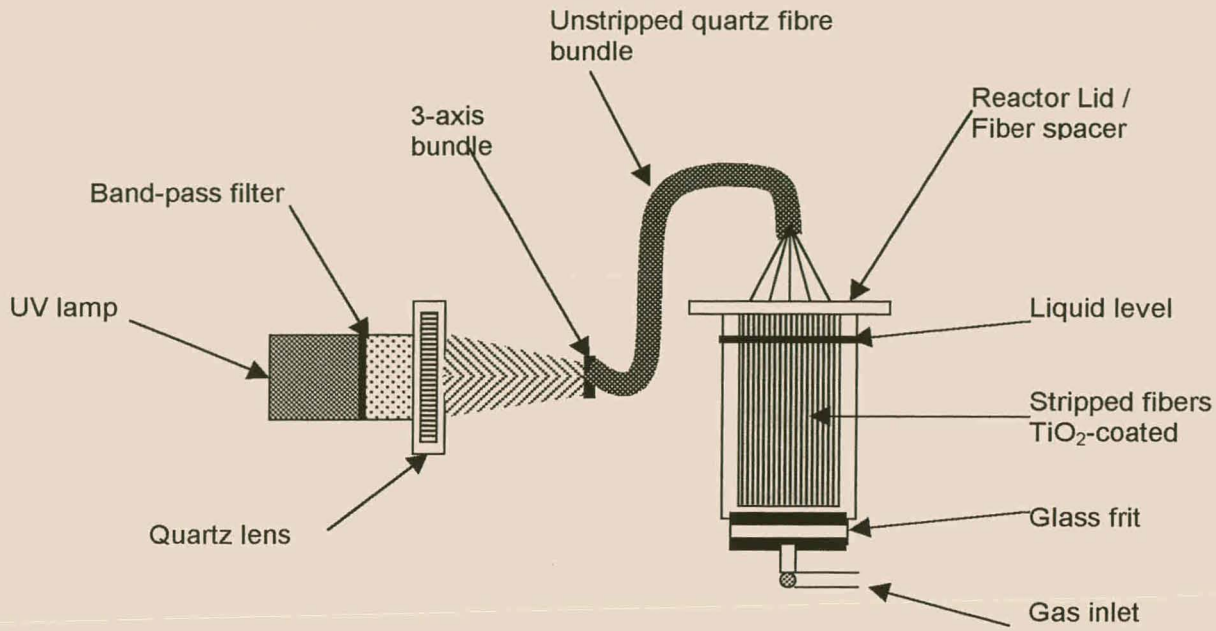

Figure 3.8: Fiber Optic Cable Reactor (Peill, 1995)

Various factors may influence the efficiency of the TiO_2-coated fiber optic cable reactor (Peill, 1995):

- The uniformity and extent of light propagation down the fibre
- The degree of light absorption by the TiO_2 coating of the refracted light
- The ability of the chemical substrates to diffuse into the TiO_2 coating

Peill and Hoffmann have investigated various aspects to develop an optimum fibre optic cable reactor (Peill, 1995; Peill, 1996).

3.2.4 Falling Film Reactor

The conventional falling film reactor system consists of a glass cylinder mounted in a base reservoir, equipped with a peristaltic pump to circulate the TiO_2 slurry through the system (Figure 3.9). The suspension is pumped into the glass cylinder, from where it is allowed to flow over the sides of the cylinder and back into the base reservoir. The cylinder is surrounded by a set of UV lamps (Figure 3.10). The polluted water is therefore exposed to UV irradiation for the duration of the flow of water, alongside the length of the glass cylinder.

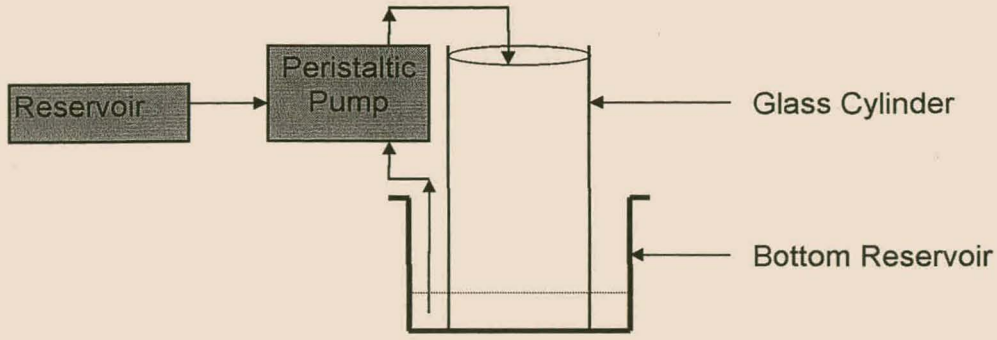

Figure 3.9: Conventional Falling Film Reactor

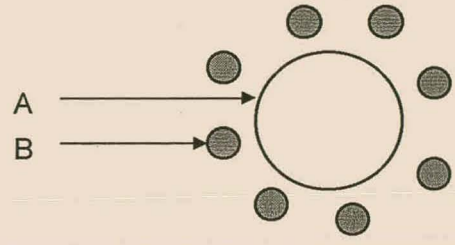

Figure 3.10: Diagram of falling film reactor: top view (A: glass cylinder; B: UV lamps surrounding glass cylinder)

In comparison to the annular reactor, there is no direct contact between the UV lamps and the TiO_2 suspension. The thin film of TiO_2 suspension on the surface of the glass cylinder allows for good penetration of the UV light. The film thickness can be regulated by the flow rate of the slurry through the system.

Based on the principle of the conventional falling film reactor, another type of falling film reactor was designed at the University of Stellenbosch (De Villiers, 1999). It involves a system whereby polluted water is pumped via a peristaltic pump over an inert sheet, hence exposing the pollutant to the UV light (Figure 3.11). The inert sheet (e.g. a fibreglass sheet) enhances the turbulence effect of the water during its gravitational flow, thereby increasing the duration of exposure of the TiO_2 to UV irradiation. Again, no direct contact exists between the UV lamps and the aqueous medium. Two designs exist. Firstly, the slurry type falling film reactor, consisting of a slurry of water and catalyst. Efficient contact is maintained between pollutant and catalyst during photocatalytic oxidation. Unfortunately, separation of the purified water and catalyst, following UV irradiation, poses great difficulty. The second type of this falling film reactor consists of an immobilised bed of catalyst on the sheet, briefly referred to as the fixed bed type. Although poor contact between water and catalyst is sometimes inevitable, separation problems are eliminated utilising this design. A combination of these two types is a well-known design.

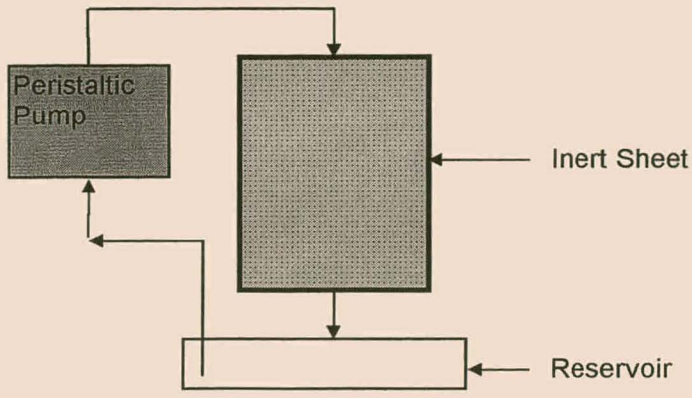

Figure 3.11: Falling Film Reactor

3.2.5 Novel Photocatalytic Reactor

A novel design of a falling film reactor, as designed and constructed at the University of Stellenbosch (De Villiers, 1999) was employed in this study (Figure 3.12). The reactor consisted of an inert fibre glass sheet (the contact matrix for the contaminated water which is exposed to UV light), twelve ultra violet germicidal lamps (a bank of six lamps on either side in a horisontal position to the sheet) and a peristaltic pump to circulate the water through the system. Oxygen bubblers were also inserted in the system to prevent recombination of e^-_{cb} and h^+_{vb} during the photocatalytic process, thereby enhancing the production of hydroxyl radicals. A magnetic stirrer ensured that the TiO_2 remained in suspension in the bottom reservoir.

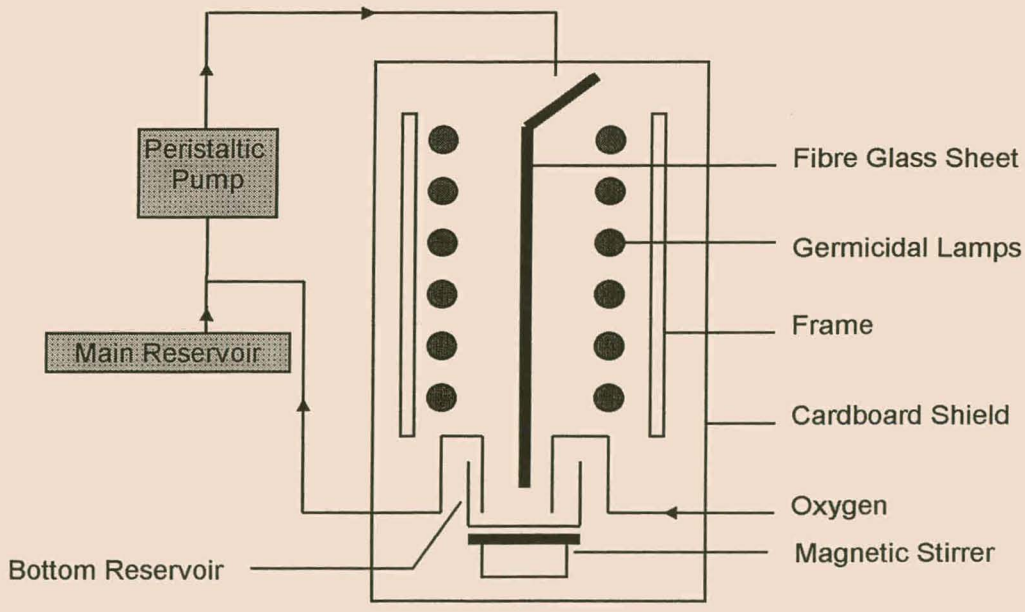

Figure 3.12: A Novel Falling Film Reactor

The simplicity of the design affords a scaling-up potential in three directions. Firstly, scaling-up in the vertical direction, by increasing the length of the sheet and increasing the number of lamps used per bank of lamps, is possible. Increasing the width of the sheet to a maximum of 1.2m (which is the maximum length of commercially available germicidal lamps), allows for the design to be expanded in the lateral direction. Lastly, the reactor can be extended in the horisontal direction by adding more sheets and banks of lamps in series (Figure 3.13).

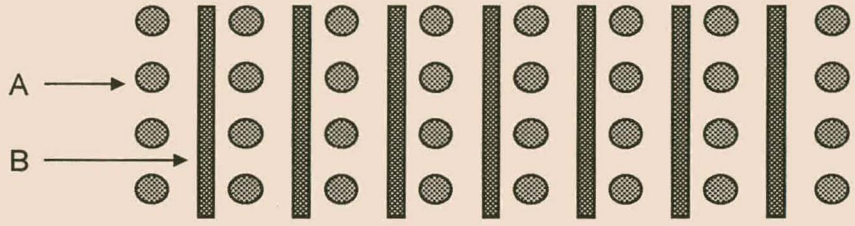

Figure 3.13: Diagram of horizontally scaled-up scenario (A: lamps, B: sheets)

For our purposes a set of twelve commercially available 15 watt germicidal lamps (2.55cm in diameter and 45cm in length), six on either side of the sheet, were used together with a single fibre glass sheet (110cm x 40cm). Optimisation of the single sheet reactor system will provide crucial information regarding further scaling-up procedures (De Villiers, 1999). This novel photocatalytic reactor was used throughout the series of experiments conducted.

REFERENCES

Bennet P.A., Van der Merwe J. (March 1995) Photocatalytic Oxidation - a safe and clean alternative in TOC analysis. *Water Sewage and Effluent* **15** No.1 7-9

Braun J.H. (1997) Titanium Dioxide – A Review *Journal of Coatings Technology* **69** No.868 59-72

De Villiers D. (1999) Design and Evaluation of Photocatalytic Reactors for Water Purification. *PhD Thesis in preparation, University of Stellenbosch.*

Gòreckil T., Boyd-Boland A., (1996) 1995 McBryde Medal Award Lecture: Solid phase microextraction - a unique tool for chemical measurements. *Can. Chem.* **74** 1297-1308

Haarstrick A., Kut O.M., Heinzle E. (1996) TiO_2-Assisted Degradation of Environmentally Relevant Organic Compounds in Wastewater Using a Novel Fluidized Bed Photoreactor. *Environmental Science & Technology* **30** 817-824

Hand D.W., Crittenden J.C. Perram D.L. (1995) Destruction of DBP Precursors Using Photoassisted Heterogeneous Catalytic Oxidation. *Journal American Waterworks Association* **87** Issue 6, pp.84-96

Hoffmann M.R., Martin S.T., Choi W., Bahnemann D.W. (1995) Environmental Applications of Semiconductor Photocatalysis. *Chemical Reviews* **95** p.69-96

Hofstadler K., Bauer R. (1994) New Reactor Design for Photocatalytic Wastewater Treatment with TiO_2 Immobilized on Fused-Silica Glass Fibers: Photomineralization of 4-Chlorophenol. *Environ. Sci.Technol.* **28** p.670-674

Jackson N.B., Wang C.M. et.al. (1991) Attachment of TiO_2 to hollow glass microbeads: Activity of the TiO_2-coated beads in the photoassisted oxidation of ethanol to acetaldehyde. *J. Electrochem. Soc.* **138** No.12 p.3660-3664

Judin V.P.S. (1993) The lighter side of TiO_2. *Chemistry in Britain* **June** 503-505

Kriek R.J. (1994) Skeiding van Pt(IV), Pd(II) en Rh(III) deur Differensiële Fotokatalitiese Reduksie. M.Sc Thesis, University of Stellenbosch

Matrix Photocatalytic Inc., 22 Pegler Street, London, Ontario, Canada N5Z 2B5 (Tel.: +91 519 6608669 Fax: +91 519 6608525)

Matsunaga T., et.al. (1988) Continuous-Sterilization System That Uses Photosemiconductor Powders. *Applied and Environmental Microbiology* **June** p.1330-1333

Ollis D.F., Marinangeli R.E. (1980) *AIChE J.* **26** p.1000

Peill N.J., Hoffmann M.R. (1995) Development and Optimization of a TiO_2-Coated Fiber-Optic Cable Reactor: Photocatalytic Degradation of 4-Chlorophenol. *Environmental Science & Technology* **29** 2974-2981

Peill N.J., Hoffmann M.R. (1996) Chemical and Physical Characterization of a TiO_2-Coated Fiber Optic Cable Reactor. *Environmental Science & Technology* **30** 2806-2812

Rajeshwar K. (June 1996) Photochemical strategies for abating environmental pollution. *Chemistry & Industry* 454-458

Serpone N., Pelizzetti E. (1989) Photocatalysis: Fundamentals and Applications. John Wiley & Sons Inc.

Serpone N. (1995) Brief Introductory remarks on heterogeneous photocatalysis. *Solar Energy Materials and Solar Cells* **38** p.369-379

Tanaka K., Hisanaga T. Rivera A.P. (1993) Effect of crystal form of TiO_2 on the photocatalytic degradation of pollutants *Presentation at Conference: Photocatalytic Purification & Treatment of Water & Air* 169-178

Weng Y.-P., Wang F.-Y., et al. (1993) The Photocatalysis of Anatase Type TiO_2 *Presentation at Conference: Photocatalytic Purification & Treatment of Water & Air* 713-718

CHAPTER 4

Statistical Methods for Optimisation

4.1 OPTIMAL EXPERIMENTAL DESIGN

When complex experimental systems, consisting of many factors, must be optimised, varying each factor individually can become a very tedious and time-consuming process. The individual variation of factors does not allow for any interactions between the factors to be monitored (Braun, 1963).

An alternative approach to the *one-factor-at-a-time* method is to employ a statistical approach for the optimisation. Factors, which might influence the experiments, must be identified and an accurate response to variation in factor values must be measurable. If an experimental approach is well constructed, the number of experiments will be reduced dramatically (Braun, 1963). The basic approach can be divided into three steps, namely

Screening Designs: Screening is the initial step where little is known about the effect of the factors on the response measured. Many factors are examined in order to determine those which exert the greatest effect on the response. Statistical approaches, which can be employed, include the factorial statistical design and Plackett-Burman matrices (Braun, 1963).

Response Surface Designs: From the previous step, the important factors have been identified. These factors are now used to optimise the operating conditions of the system. A model is therefore constructed for optimal experimental results. Typical optimisation procedures include the simplex method and the central composite response surface design.

Verification: The final stage involves execution of the experiment at the predicted best settings to confirm the optimum value of the response predicted at these conditions. Reproducibility of the response can also be determined at these conditions.

Another approach to solving optimisation problems is the *Optimal Experimental Design Pyramid (OED pyramid)* (Ghosh, 1990). The screening design forms the basis of the

pyramid and is employed in the initial stage of the investigation. Progress is made toward the top of the pyramid as more experimental information is generated.

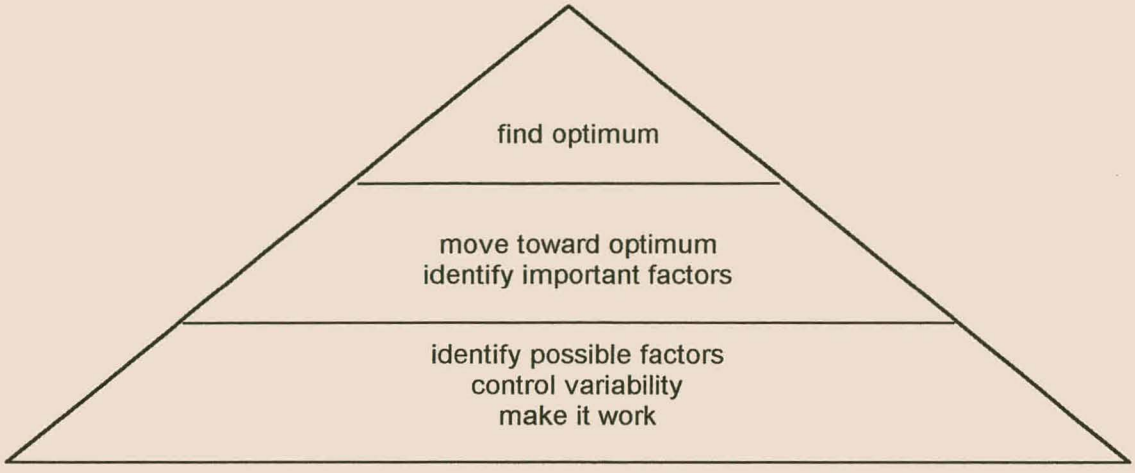

Figure 4.1: Optimal Experimental Design Pyramid (Ghosh, 1990, p.86)

Statistical optimisation of experimental conditions therefore involves much less effort. The sets of experiments are well constructed and the verified end results are reliable. Factor interactions are also investigated.

4.2 EXPERIMENTAL APPROACH

4.2.1 Screening Design: Factorial Statistical Design

The factorial statistical design is one of the more common screening designs available. The purpose is to determine the relative individual influence of the qualitative and quantitative factors on the response measured, as well as the interactions between factors (Morgan, 1995). A *two level two factor factorial design*, for example, consists of two factors, each with a maximum and minimum value. The maximum and minimum levels must be chosen in such a way that a shift in factor value from minimum to maximum would result in a substantial change in the response measured. 2^k (where k = number of factors) experiments must be performed for each factorial design.

A two level two factor factorial (denoted by 2^2 factorial) would therefore consist of factors X_1 and X_2 and would require $2^2 = 4$ experiments. The experiments can be summarised by the following design matrix:

Table 4.1: A Typical Design Matrix for a 2^2 Factorial Design (- : minimum level, +: maximum level, Z: response measured)

Experiment	Factor		Response
	X_1	X_2	Z
1	-	-	Z_1
2	+	-	Z_2
3	-	+	Z_3
4	+	+	Z_4

By employing a statistical computer program, eg. STATGRAPHICS, SAS, QSCA, CARD or STATISTICA, these results can now be processed and interpreted. For our purposes STATISTICA Version 5.1 was employed.

4.2.2 Response Surface Design: Simplex Design

The simplex method can be used for the optimisation of quantitative factors in a particular experimental set-up (Yarbro, 1974). The set of factors, which resulted in the greatest positive response with e.g. a factorial design, is often used as the starting point of a simplex. However, when optimising an analytical reagent, it is preferable not to use the concentration of the reagent as a factor. Concentration effects, which involves movement of the simplex towards maximum concentration, should be avoided (Long, 1969).

The simplex is a geometric figure defined by a number of vertex points equal to one unit more in dimension than the number of factors chosen (Deming, 1973), e.g. a two factor simplex will be represented by a triangle. Each vertex point represents a set of experimental conditions for the entire set of factors. These values are determined in a set way (Long, 1969), namely

- choose the coordinates of vertex 1
- choose step-sizes for each factor
- multiply each step-size by the tabulated values (Table 4.2)
- add this result to vertex 1 to get the values of the new vertex point

Table 4.2: Initial Vertex Locations (Long, 1969)

Vertex	Factor									
No.	A	B	C	D	E	F	G	H	I	J
1	0	0	0	0	0	0	0	0	0	0
2	1.000	0	0	0	0	0	0	0	0	0
3	0.500	0.866	0	0	0	0	0	0	0	0
4	0.500	0.289	0.817	0	0	0	0	0	0	0
5	0.500	0.289	0.204	0.791	0	0	0	0	0	0
6	0.500	0.289	0.204	0.158	0.775	0	0	0	0	0
7	0.500	0.289	0.204	0.158	0.129	0.764	0	0	0	0
8	0.500	0.289	0.204	0.158	0.129	0.109	0.756	0	0	0
9	0.500	0.289	0.204	0.158	0.129	0.109	0.094	0.750	0	0
10	0.500	0.289	0.204	0.158	0.129	0.109	0.094	0.083	0.745	0
11	0.500	0.289	0.204	0.158	0.129	0.109	0.094	0.083	0.075	0.742

The simplex design is based on the principle of rejecting the worse vertex of the geometric figure and calculating a new vertex point (Figure 4.2), until an area of optimum response (a maximum or minimum) is reached. By decreasing the step-size for each factor, this optimum region can then be investigated even further until the exact optimum conditions are determined.

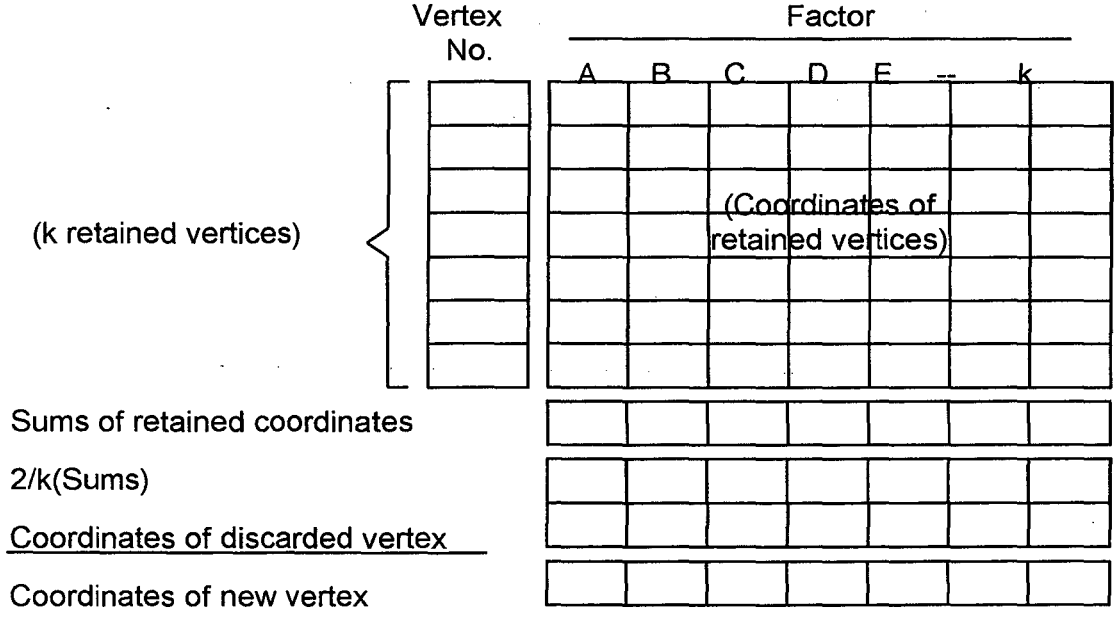

Figure 4.2: Procedure for the Calculation of Succeeding Vertex Points (Long, 1969)

4.2.3 Response Surface Designs: Central Composite Design

A well-known response surface design is the central composite design. This design consists of a complete 2^k factorial, with additional axial points (denoted by a) along the coordinate axes, as well as a center point. The center points is repeated two or three times in order to determine the reproducibility of the specific system under investigation. The axial points can be located at arbitrary distances from the center point, depending on the analysis being performed. However, for the design to be rotatable, the axial distance from the center point must be $a=F^{1/4}$, where F is the number of factorial points ($F=2^k$). Rotatability is a desirable property for any design,allowing for the response to be estimated with equal precision at all points in the factor space that are equidistant from the centre of the design (Mason, 1989).

The following steps (Mason, 1989) construct a central composite design:

- a complete 2^k factorial layout (with k factors)
- 2k axial points along the coordinate axes
- m repeat observations at the design center
- randomise the experiment to eliminate "bias effects"

The total number of runs in a central composite design is based on the complete factorial design:

$$n=2^k + 2k + m$$

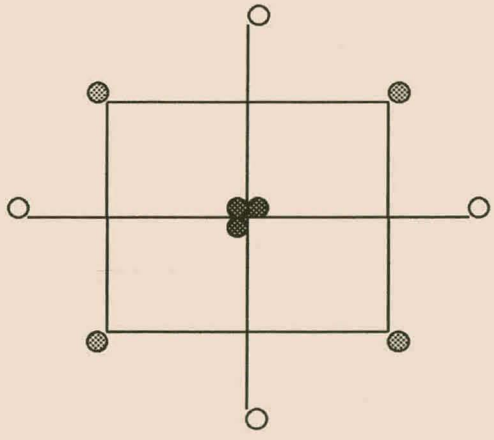

Figure 4.3: Typical Central Composite Design for two factors (◍ 2^k factorial design; ● center points; ○ axial points)

The data obtained can now be analysed by means of one of the above mentioned statistical programs.

4.2.4 Response Surface Methodology

The experimental region for a chosen system is characterised by the manner in which the factors influence the specific response function. Graphic representations of these experimental regions provide a clearer image of the variation of the response as a function of the chosen factors (Figure 4.4).

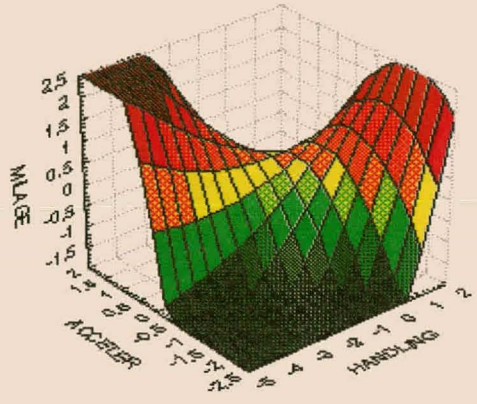

Figure 4.4: A Typical Saddle Response Surface

Mathematical modelling is employed to determine the basic shape of the response surface. This is done by constructing a quadratic polynomial for the response in terms of two factors (X_1 and X_2). The general form of a quadratic polynomial in terms of two factors can be represented by:

$$Z = \beta_0 + \beta_1 X_1 + \beta_2 X_2 + \beta_{11} X_1^2 + \beta_{22} X_2^2 + \beta_{12} X_1 X_2$$

where,

Z: response function
X_1, X_2: experimental factors
β_0: intercept on response axis
β_1, β_2: gradient for each factor
β_{11}, β_{22}: parabolic character of the surface for each factor
β_{12}: interaction term; combined effect of the two factors

These polynomials can be generated with any of the above mentioned statistical computer programs.

For further discussions of statistical methods of optimisation see:

- Box G.E.P., Draper N.R. (1986) Empirical Model-Building and Response Surfaces. John Wiley & Sons
- DeVor R.E., Chang T.-H., Sutherland J.W. (1992) Statistical Quality Design and Control: Contemporary Concepts and Methods. Macmillan Publishing Company
- Miller J.C., Miller J.N. (1984) Statistics for Analytical Chemistry. John Wiley & Sons

4.3 EXPERIMENTAL APPROACH

The OED pyramid approach was chosen for the optimisation of the photocatalytic destruction of humic substances in raw water. An accurate response measurement to a change in parameter value therefore had to be identified. A dual approach was employed. TOC and $CHCl_3$ measurements were used as a response. These analytical methods are discussed in Chapter 5. The optimisation can be summarised as follows:

- **Screening Designs:** A 2^3 factorial approach was employed to identify any significant factors.
- **Response Surface Designs:** The factors identified in the screening designs were then further optimised firstly by means of the central composite approach.

REFERENCES

Box G.E.P., Draper N.R. (1986) Empirical Model-Building and Response Surfaces. John Wiley & Sons

Braun A.M., Jakob L. (1963) Advances in Photochemistry **18** Chapter 2

Deming S.N., Morgan S.L. (1973) Simplex Optimisation of Variables in Analytical Chemistry. *Analytical Chemistry* **45** 278A-283A

De Villiers D. (1999) Design and Evalutaion of Photocatalytic Reactors for Water Purification. *PhD Thesis in preparation, University of Stellenbosch*

DeVor R.E., Chang T.-H., Sutherland J.W. (1992) Statistical Quality Design and Control: Contemporary Concepts and Methods. Macmillan Publishing Company

Ghosh S. (Editor) (1990) Statistical Design and Analysis of Industrial Experiments, Chapter 3, New York, N.Y.: Dekker

Legrini O., Oliveros E., Braun A.M. (1993) Photochemical Processes for Water Treatment. *Chemical Reviews* **93** 671-698

Long D.E. (1969) Simplex Optimisation of the Response from Chemical Systems. *Analytica Chimica Acta* **46** 193-206

Mason R.L., Gunst R.F., Hess J.L. (1989) Statistical Design and Analysis of Experiments with Applications to Engineering and Science. New York, N.Y.: Wiley

Miller J.C., Miller J.N. (1984)Statistics for Analytical Chemistry. John Wiley & Sons

Morgan E., (1995) Chemometrics: Experimental Design. John Wiley & Sons (Eng.)

Rajeshwar K. (June 1996) Photochemical strategies for abating environmental pollution. *Chemistry & Industry* 454-458

Yarbo L.A., Deming S.N. (1974) Selection and Preprocessing of Factors for Simplex Optimisation. *Analytica Chimica Acta* **73** 391-398

CHAPTER 5

Analytical Protocol

Since this project, at a later stage, ran concurrently with a WRC project, directed toward the characterisation of coloured waters in terms of trihalomethane formation potential and other simpler methods, it was decided to use the analytical protocol as developed by the writer of this thesis.

5.1 ANALYTICAL PROTOCOL

5.1.1 UV Spectroscopy

Since a pronounced chromophore exhibits an absorption at 254 nm for HA and FA compounds, UV spectroscopy is a logical option for monitoring the reduction of HA and FA content of coloured water. Hence, by following the reduction in UV absorbance at 254 nm, the removal of colour from the treated water can be determined.

A double-beam GBC 920 UV/VIS spectrophotometer, equipped with a deuterium lamp, a quartz iodide lamp and 1 cm quartz cuvettes were used for all UV analysis.

5.1.2 TOC Analysis

The destruction efficiency was also measured in terms of the reduction in total organic carbon (TOC) content of the treated water. A low temperature TOC analyser (ANATOC) was employed (Bennet, 1995). The operation of the ANATOC is based on the photocatalytic oxidation of the organic content of each sample. A catalyst suspension of 0.2% $^{w}/_{v}$ TiO_2 in combination with an ultra violet source (two 8-watt blacklight fluorescent tubes) was employed. The organic content is decomposed in the aqueous medium to yield CO_2, H_2O and the acid, base or salt of any of the inorganically bound compounds. The resulting CO_2 gas is captured in a conductivity cell, which yields the corresponding conductivity signal. The latter takes into account the following CO_2 – HCO_3^- - H_2CO_3 equilibria according to the pH of the sample:

$$CO_2 + H_2O \rightarrow H_2CO_3$$
$$H_2CO_3 \rightarrow H^+ + HCO_3^-$$

Calibration of the ANATOC is done with a standard 200mg C/L solution of benzoic acid. pH dependency of CO_2 is an important factor to consider (See Figure 5.1). For accurate determination of TOC content, it was therefore necessary to adjust the pH of each sample to a value below pH 5 to ensure that only CO_2 is present in the sample. Suggested pH levels were between 3.5 and 4. pH adjustments were done with 0.1M solutions of perchloric acid and NaOH to obtain the required pH 3.5. A standard sample injection volume of 1000µL was used throughout the TOC analyses. TOC content was determined in terms of mg C/L.

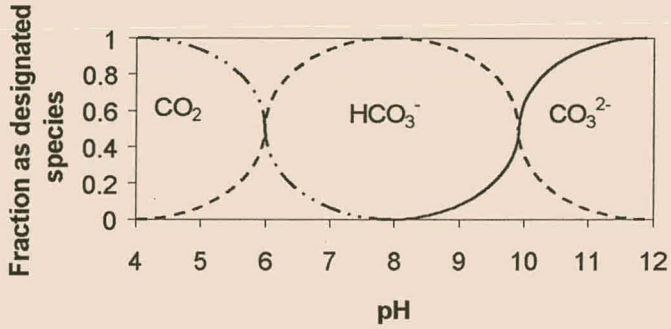

Figure 5.1: Distribution curves for CO_2 species as a function of pH

5.1.3 Trihalomethane Formation Potential Analysis

THMs are produced in drinking water when chlorine is added for disinfection (See 2.4.3). Various models are used to predict THM formation, however, THM concentrations cannot be calculated accurately from these models. A method to determine the formation potential of the THMs is believed to be of much greater value than predicting THM concentrations (Greenberg, 1992, p.5-44). Various factors must be accounted for during these procedures in order to obtain meaningful and reproducible results. They include:

- temperature
- reaction time
- chlorine dose and residual chlorine
- pH

It is known that elevated temperatures and pH values, as well as longer reaction times, enhance THM formation (Greenberg, Clesceri, Eaton, 1992, p.5-45).

Various definitions of THM formation potentials are in existence, i.e.

- ***Trihalomethane formation potential (THMFP):*** THMFP represents the concentration of THMs formed in water samples buffered at pH 7.0, containing an excess of free chlorine with a chlorine residual of 1 to 5 mg/L after being kept for 7 days at 25°C. This process is not a pure simulation of the actual standard water treatment process, but provides a useful indication of possible THM precursors.

- ***Basic trihalomethane formation potential (BTHMFP):*** BTHMFP is identical to the THMFP, except that the water sample is buffered at pH 9.2, simulating lime softened or naturally high pH, thereby accelerating THM formation. BTHMFP is very similar to the maximum trihalomethane formation potential, the only differences being the reagent preparation procedures and required residual chlorine concentration.

- ***Ultimate trihalomethane formation potential (UTHMFP):*** UTHMFP potential estimates the highest possible THM concentrations that could be produced at the extreme conditions of a public water supply system. These results may be of regulatory or monitoring value.

- ***Maximum trihalomethane potential (MTHMP):*** MTHMP is determined by taking triplicate samples from a point in the distribution system that reflects maximum residence time, consequently storing them for 7 days at or above 25°C and determining the total THM concentration if a detectable free chlorine residual remains in one of the samples.

- ***Simulated distribution system trihalomethane concentration (SDSTHMC):*** SDTHMC is represented by the THM concentration in a previously chlorinated water sample after storage that represents the time and conditions in the utility's distribution system. These samples include existing THMs plus THMs produced during storage.

The BTHMFP method was chosen for the proposed statistical optimisation of the photocatalytic reactor for the destruction of humic and other natural organic substances. A response function was defined in terms of the THMFP, which is represented by the following equation:

$$THMFP\ (\mu g/L) = CHCl_3\ (\mu g/L) + CHCl_2Br\ (\mu g/L) + CHClBr_2\ (\mu g/L) + CHBr_3\ (\mu g/L)$$

The protocol can be summarised as follows:

5.1.3.1 Distilled Water

Deionised water was obtained by passing distilled water through a MILLI-Q deioniser. This water was checked thoroughly for the absence of Cl_2 and THMs

5.1.3.2 Cl_2 Water Preparation

Cl_2 water must be administered to the treated water samples to simulate the disinfection of treated water. The method chosen entailed dosing with dissolved chlorine.

Reagents (See 5.3 for preparation of reagents):

Cl_2 (g)
Ammonium iron (II) sulfate solution
DPD reagent solution
Phosphate buffer solution

Procedure:

Cl_2 (g) is bubbled through an amber glass bottle filled with distilled water. Free active chlorine was determined via a standard DPD titration method (Merck p.47-50) and entailed the following:

A 100 mL of Cl_2 test water was introduced into a narrow-necked flask (150 mL capacity) and 5 mL of both DPD reagent solution and a phosphate buffer solution were added. The resultant solution was titrated against a standard ammonium iron (II) sulfate solution until a colourless or an unchanging faint pink solution was obtained. The titration was executed using magnetic stirring equipment. A microburette with injection tube and nozzle was used to transfer the ammonium iron (II) sulfate titrant to the titrating flask, directly under the surface of the liquid. A maximum limit of 3 mL or more of ammonium iron (II) sulfate was regarded acceptable for reaching the end-point of the titration. In the case of exceeding this limit, titrations were repeated, using a smaller volume of Cl_2 water, diluted to 100 mL with double-distilled water.

Calculation:

1 mL ammonium iron (II) sulfate solution $\cong$ 0.1 mg free active chlorine

$$\text{mg/L free active chlorine} = \frac{a \times 0.1 \times 1000}{b} \qquad (1)$$

a = mL of ammonium iron (II) sulfate solution consumed
b = mL of test water used

Cl_2 water prepared by means of the above method has a high free active chlorine concentration. It was found that a typical dilution with a resulting consumption of less than 3 mL of ammonium iron (II) sulfate solution was approximately 300 µL of Cl_2 water diluted to 100 mL with double distilled water.

This determination for each sample was carried out in triplicate and the average was taken as the concentration of free active chlorine.

5.1.3.3 Basic Trihalomethane Formation Potential Method

Determination of BTHMFP required all treated water to be treated with Cl_2 water prepared by the method described in 5.1.3.2. The Cl_2 dosage is based on the organic and ammonia-nitrogen (NH_3-N) demand of the raw and treated water samples and is calculated from equation 2 (Krasner, 1996).

Reagents (See 5.3 for preparation of reagents):
Nessler's reagent
Borate buffer
Cl_2 water

Calculations:

$$Cl_2(mg/L) = 3 \times TOC(mg/L) + 7.6 \times NH_3\text{-}N(mg/L) \quad (2)$$

$$C_1V_1 = C_2V_2 \quad (3)$$

C_1: Cl_2 (mg/L) from titration of the stock solution
V_1: volume of concentrated free chlorine to be added to the test water
C_2: answer of equation (2)
V_2: 20.5 mL

Procedure

The TOC content is determined for each sample as a prerequisite for equation 1. Each water sample is further tested with Nessler's reagent for the presence of ammonium salts. This is done by the addition of a few drops of reagent to the test water. The formation of an orange-brown precipitate indicates a positive test. The amount of ammonium salts can be

determined quantitatively by means of a method described by Merck (p.7-12). A negative test reduces equation (2) to the following expression:

Cl_2 (mg/L) = 3 x DOC (mg/L)

20 mL's of treated water is transferred to an amber glass bottle equipped with a hole cap, teflon septum and a magnetic stir bar. Amber glass samples bottles were required to prevent UV induced reactions in the water samples. 0.5 mL of borate buffer is added to adjust the pH to 9.2. The volume of Cl_2 water required to disinfect the treated water samples is calculated by means of equations (2) and (3).

Sample bottles are placed in a thermoregulated water bath at 25°C on a non-electric magnetic stirrer for a period of 3 days to induce THM formation. The standard residence time is usually 7 days, but in this case THMFP is only a qualitative representation of the efficiency of the photocatalytic reactor. Practical considerations therefore resulted in the period being reduced to 3 days.

5.1.3.4 Analysis of Trihalomethanes via Solid Phase Microextraction

Quantification of THMs, as formed during the chlorination as described in 5.1.3.3, is very important. In the past, trace amounts of compounds in natural liquid samples required isolation from the liquid phase followed by preconcentration and ultimately analysis (Gòrecki, 1996). The isolation of organic compounds usually entailed one of the following extraction procedures:

- liquid-liquid extraction (LLE)
- solid phase extraction (SPE)
- headspace extraction

These extraction methods exhibited many drawbacks. LLE is a process that requires large quantities of high purity solvents, which resulted in high costs and disposal problems. In addition, LLE methods are very laborious and reproducibility is not guaranteed (Gòrecki, 1996).

SPE, a more contemporary approach to extraction, is based on the adsorption of analytes onto a specially formulated material, usually packed in cartridge form. Although not as time-consuming as LLE methods, hazardous solvents are still required to remove trapped

analytes from the cartridges prior to chromatographic analyses. When further pre-concentration of samples is required, solvent-impurities may introduce unwanted concentration effects and consequently hamper the analysis. The greatest drawback of SPE is the strong dependence of breakthrough volume on the matrix composition (Gòrecki, 1996).

Headspace extraction is limited to volatile and semivolatile analytes. Reproducible results are not guaranteed (Gòrecki, 1996).

New extraction and sampling preparation technology has, however, been developed recently: *solid phase microextraction* (SPME). SPME is basically a miniaturisation of the process of solid phase extraction of analytes from aqueous medium (Gòrecki, 1996). The SPME device (Figure 5.2), as developed by Supelco (Shirey, 1995), consists of a phase-coated polymeric fibre contained within a syringe. Extraction of the desired compounds is achieved by exposing the fibre to the sample (in a vial), thereby facilitating the adsorption of analytes onto the fibre coating. Upon completion of the adsorption phase, the fibre is withdrawn into the needle, removed from the sample vial and introduced into the GC via its injector where the adsorbed analytes are thermally desorbed and subsequently analysed.

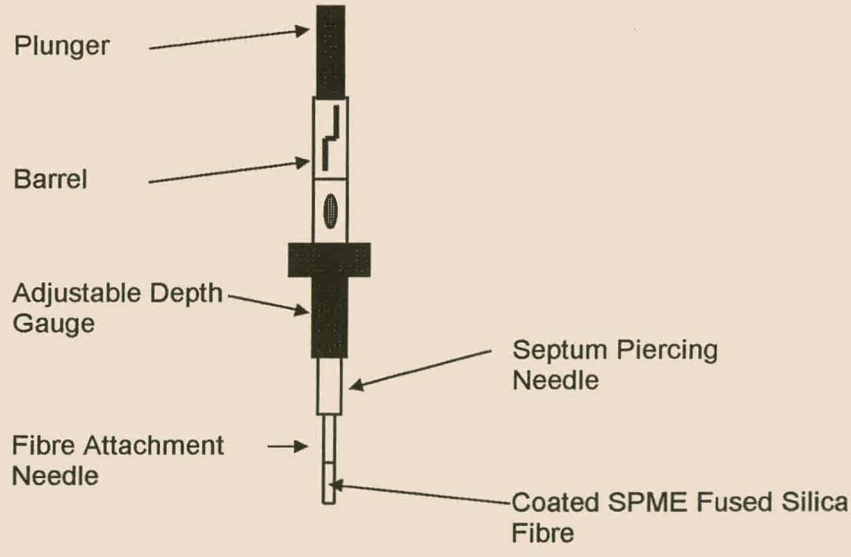

Figure 5.2: A standard SPME device

A range of polymeric fibres, consisting of a variety of stationary phases with different thickness coatings, is available for the analysis of organic analytes. They include the following types:

- 100μm Polydimethylsiloxane
- 30μm Polydimethylsiloxane
- 7μm Polydimethylsiloxane
- 85μm Polyacrylate
- 65μm Carbowax / divinylbenzene
- 65μm Polydimethylsiloxane / divinylbenzene

The extraction and analysis of semivolatiles in aqueous medium (e.g. $CHCl_3$) are usually done utilising a 100μm polydimethylsiloxane (PDMS) fibre.

The mechanism and factors influencing extraction efficiency by means of PDMS fibres are discussed in Chapter 7.

5.2.1 Solid Phase Microextraction Process for Analysis of THMs

Since excess free active Cl_2 in the vial will damage the PDMS fibre after repeated extraction, a procedure to remove this excess by ascorbic acid was developed.

Reagents (See Reagents for preparation):

30% Ascorbic acid solution

Methylene chloride solution

Calculations:

Volume of Ascorbic Acid (mL) = 1.2 x Cl_2 (mg/L) + 1.1 (4)

Cl_2 (mg/L): value calculated from equation (2)

Procedure:

From equation (4) the volume of 30% ascorbic acid solution required to react with excess free active Cl_2 in solution was calculated. Sample bottles were removed from the water bath and the calculated volume of ascorbic acid was added with a micro syringe. Finally an internal standard (40μL of CH_2Cl_2) solution was added to each sample to facilitate a more accurate determination of the THM analytes via GC analysis (Christian, 1986) (See equation 5). Samples were allowed a 10 minute equilibration time before extraction of analytes by means of SPME was ensued (See Figure 5.3).

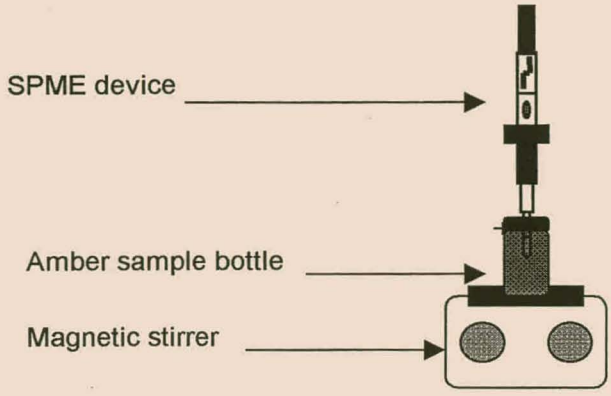

Figure 5.3: Extraction of VOCs with SPME

Selected Adsorption conditions:

Adsorption time = 20min

Adsorption = headspace

Adsorption temp = 20°C

Stirring Rate = 500 rpm

These conditions were selected for optimum adsorption.

5.2.2 Solid Phase Microextraction Desorption Process and GC/MS Analysis

A Fisons GC, series 8000, coupled to a mass spectrometer, series MD 800, was used for separation and subsequent analysis of extracted THMs. It was required that the plunger of the SPME device was retracted to withdraw the PDMS fibre into the septum-piercing needle before removal of the SPME device from a particular sample bottle. After transfer to the GC, all volatiles were concentrated at the beginning of the GC column by means of cryo trapping with CO_2 (dry). A septum-piercing needle at the bottom end of the SPME device was used to pierce the GC septum. Finally the plunger was pushed down to expose the PDMS fibre to the high temperature of the injector block of the GC/MS.

Selected Desorption conditions:

Desorption temp = 200°C

Desorption time = 2min

Cryo trapping = 2min

GC column Specifications:

Type = non-polar

Length = 40 m

Internal diameter = 0.32mm

Stationary phase = PS 255

Film Thickness = 1.2μm

Selected GC Temperature Program:

Temp 1=45°C

Duration=4 min

Rate=9°C/min

Temp 2=120°C

Duration=3 min

Selected MS scan program:

Mass range = 50-255 mass units

(According to the mass variation of the anticipated THM analytes.)

Peaks were integrated electronically and were reported in terms of total ion count (TIC).min.

5.2.3 Determination of Trihalomethane Concentrations

For each sample of raw and treated water that was analysed, a standard solution of THMs containing the internal standard (CH_2Cl_2) was subjected to a similar procedure. The concentrations of the relevant species were calculated using equation 5.

Reagents (See Reagents for preparation):

Standard THM solution: Chloroform
Bromodichloromethane
Dibromochloromethane
Bromoform

Methylene chloride

Borate buffer

Calculations:

$$\text{THM conc.}\,(\mu g/L) = \frac{\text{Peak Area (sample)}}{\text{Peak Area (std)}} \times \frac{\text{Peak Area } (CH_2Cl_2/\text{std})}{\text{Peak Area } (CH_2Cl_2/\text{sample})} \times \text{THM conc. (std)} \quad (5)$$

THM conc. ($CHCl_3$) = 75 μg/L

THM conc. ($CHCl_2Br$) = 200 μg/L

THM conc. ($CHClBr_2$) = 250 μg/L

THM conc. ($CHBr_3$) = 30 μg/L

Procedure

20 mL of a standard THM mixture were introduced into an amber glass sample bottle together with 40μL methylene chloride (internal standard). The pH of the standard THM solution was adjusted with 0.5 mL borate buffer. Analysis for THMs in this standard mixture was performed in a similar fashion to that of the THMs in the raw and treated water samples.

Chromatograms of both the unknown sample and the standard were integrated electronically. The resulting peak areas, together with the concentration of the standard THM under investigation, were subsequently substituted into equation (5) for the calculation of the unknown concentration.

5.3 REAGENTS FOR PREPARATION OF SAMPLES

5.3.1 pH Adjustments

pH adjustments during photocatalysis: 0.1M NaOH and 0.1M HCl (Merck) solutions
pH adjustments during TOC analysis: 0.1M NaOH and 0.1M $HClO_4$ solutions

5.3.2 Borate Buffer

A Borate buffer solution was used to maintain a pH of 9.2 during the chlorination of all water samples. For this purpose, 30.9 g anhydrous H_3BO_3 (Merck pro analysi) and 10.8g NaOH (Merck pro analysi) were dissolved in deionised water and diluted to 1L. The buffer was kept refrigerated at 4°C.

5.3.3 DPD titration reagents

Ammonium iron (II) sulfate solution: 1.106g of Ammonium iron(II) sulfate GR were dissolved in freshly boiled and cooled deionised water. 2ml 1M sulfuric acid was added and diluted up to 1000ml with deionised water.

DPD reagent solution: 0.11g of N,N-diethyl-1,4-phenylenediammonium sulfate GR were dissolved in deionised water, together with 2ml 1M sulfuric acid and 2.5ml 0.02M Titriplex III solution, and diluted to 100ml. Prepared DPD reagent is light sensitive, hence was stored in a brown bottle in the dark to prevent discoloration.

Phosphate buffer solution: 46g of Potassium dihydrogen phosphate GR and 24g tri-Sodium phosphate 12-hydrate (LAB) were dissolved in 1000ml deionised water.

Sulfuric acid 1M: The contents of one ampule of 0.5M Sulfuric acid Titrisol concentrated solution for the preparation of 1L of 1N solution were diluted to 500ml with deionised water.

Titriplex III solution 0.02M: 200ml 0.1M Titriplex III metal (pM) indicator was diluted to 1000ml with deionised water.

5.3.4 Nessler's reagent (Basset, 1979)

35 g of Potassium iodide were dissolved in 100 mL of water. This was followed by the addition of 4% Mercuric chloride solution, while stirring or shaking, until a faint red precipitate remained (about 325 mL were required). A solution of 120 g of Sodium hydroxide in 250 mL of water was then added (while stirring), and diluted to 1 L with distilled water. More mercuric chloride solution was added until permanent turbidity was obtained. The mixture was allowed to stand for one day after which the clear liquid was decanted from sediment. The solution was kept stoppered in a dark-coloured bottle (Bassett, 1979).

5.3.5 30% Ascorbic acid

The solubility of ascorbic acid in water is approximately 30% ($^{m}/_{v}$). To prevent contamination of treated water samples, ascorbic acid (Merck, pro analysi) was used. 30g of ascorbic acid were added to 70 mL distilled water.

5.3.6 Methylene chloride

A 50 mg/L methylene chloride solution was prepared by diluting 0.367 mL of methylene chloride to 1 litre with distilled water.

5.3.7 Standard THM Mixture

"Environmental standard solutions" (Supelco) were used for the preparation of standard solutions of THMs. Each ampoule contained 1 mL 5000 µg/mL of the given THM in methanol. A dilution of one ampoule to 100 mL with distilled water yielded a 50 mg/L THM solution.

For all 4 THMs under investigation (i.e. $CHCl_3$, $CHCl_2Br$, $CHClBr_2$ and $CHBr_3$), the contents of the corresponding ampoule was quantitatively transferred to a 100 mL volumetric flask using distilled water.

- **Mixture**

From these prepared, diluted THM solutions the following amounts were used for a 1 L dilution mixture:

$CHCl_3$:	1.5 mL 50 mg/L solution
$CHCl_2Br$:	4 mL 50 mg/L solution
$CHClBr_2$:	5 mL 50 mg/L solution
$CHBr_3$:	0.6 mL 50 mg/L solution

This combination yielded the following concentrations:

$CHCl_3$	:	75 µg/L
$CHCl_2Br$	:	200 µg/L
$CHClBr_2$	:	250 µg/L
$CHBr_3$	:	30 µg/L

5.4 RAW WATER SAMPLES

Raw water samples (with a substantial colour) were collected from a lagoon at Betty's Bay (in the South Western Cape region) and the Simonstown storage dam. These samples were considered to be a representative sample of raw water containing a high level of humic acids. The collected water samples were stored at 4°C in the dark to prevent biological activity from altering the humic content. Water samples required for the photocatalytic experiments were allowed to stabilise at room temperature (±20°C) before use. Analysis of the Betty's Bay and Simonstown raw water yielded the following results for the following water quality characteristics:

Table 5.1: Characterisation of Betty's Bay and Simonstown Raw Water (Analysis done by Scientific Services, Cape Metropolitan Council)

Determination	Raw Water	
	Betty's Bay	Simonstown
Physical and General		
Electrical Conductivity (mS/m @ 20°C)	26.7	24.6
pH	6.54	5.71
Turbidity (NTU)	1.15	1.35
Colour (Pt std)	200	280
Organic		
Oxygen Absorbed (4hrs at 27°C) (mg/L)	2.284	1.5
Alkalinity		
Total Alkalinity as $CaCO_3$ (mg/L)	6.0	3.0
Mineral		
Chloride (Cl^-) (mg/L)	73.0	68.0
Sulphate (SO_4^{2-}) (mg/L)		11.4
Calcium (Ca) (mg/L)	6.00	6.19
Magnesium (Mg) (mg/L)	5.15	4.25
Sodium (Na) (mg/L)	37.13	35.49
Potassium (K) (mg/L)	0.33	0.85
Trace Metals		
Aliminium (Al) (mg/L)	0.29	0.51
Iron (Fe) (mg/L)	0.397	0.518
Manganese (Mn) (mg/L)	0.002	0.023

REFERENCES

Basset J., Denney R.C., Jeffery G.H., Mendham J. (Editors) (1979) Vogel's Text-Book of Quantitative Inorganic Analysis: Theory and Practice; 4th Edition; Longmans, Green and Co.

Christian G.D., O'Reilly J.E. (Editors) Instrumental Analysis (1986) 2nd Edition *Allyn and Bacon Inc.*

Gòrecki T., Boyd-Boland A., Zhang Z., Pawliszyn J. (1996) 1995 McBryde Medal Award Lecture: Solid phase microextraction – a unique tool for chemical measurements. *Can. J. Chem.* **74** p.1297-1308

Krasner S.W., Crouè J.-P., Buffle J., Perdue E.M. (1996) Three Approaches for Characterizing NOM. *Journal AWWA* **June** pp.66-79

Merck E. The Testing of Water. *Darmstadt*

Greenberg A.E., Clesceri L.S., Eaton A.D. (Editors) (1992) Standard Methods for the Examination of Water and Watewater 18th Edition (p.5-45)

CHAPTER 6

Experimental Investigation with Photocatalytic Reactor

The experimental photocatalytic reactor, as described in Chapter 3, was employed for all photocatalytic destruction experiments. Degussa P-25 TiO_2, with an average particle size of 5.00 μm and surface area of 44.18m^2/g, was used as semiconductor catalyst (Kriek, 1994). It was administered either in the form of a *slurry* combined with an *immobilised bed*, or strictly as an immobilised bed type. Two reactor operation modes were employed. These included a *single pass mode*, where a particular water sample was pumped from a main reservoir, through the reactor, into the base reservoir. Samples were extracted from the base reservoir. The sequence was repeated to simulate a coupled series of fiberglass sheet reactors. The second mode entailed recirculation of the water in a closed loop through the reactor utilising a peristaltic pump. Small aliquots were taken at set time intervals. Photocatalytic reactor efficiency was monitored utilising either UV spectroscopy, TOC content or THMFP determinations (See Chapter 5).

6.1 PRELIMINARY INVESTIGATION

6.1.1 Objective

The objective was to determine the feasibility of using the existing photocatalytic reactor as a means for destroying NOM in raw water.

For this reason a synthetic humic acid solution (Fluka) was prepared and subjected to photocatalytic treatment. Thereafter a raw water sample was treated in similar fashion to investigate the destruction of natural organic matter in raw water.

6.1.2 Procedure

General Experimental Conditions:

TiO_2 concentration	:	1g/L
O_2	:	2.5 L/min (via bubblers)
Analyte 1	:	Synthetic 0.001% ($^M/_V$) Fluka humic acid solution spiked in distilled water

Analyte 2	:	Simonstown raw water
Analyte Volume	:	3 liters
pH	:	Natural (pH=6.2)
Operation Mode	:	Single Pass
Catalyst Application	:	Immobilised bed
Flow Rate	:	2 L/min
Analysis	:	Spectrophotometric
Response	:	UV absorbance at 254 nm

The synthetic humic acid suspension was photocatalytically treated in the reactor using 3 single passes. A 20 mL sample was collected beforehand, as well as after each completed single pass. The samples were filtered through a double layer of Whatman Nr.42 filter paper to remove any retained TiO_2.

The raw water sample was treated in a similar fashion.

6.1.3 Results and Discussion

UV/VIS spectra were recorded for the collected samples over a wavelength range of 200-900nm. Typical spectra are shown in Figure 6.1. The photocatalytic degradation of the humic acid and natural organic material in raw water were presented as normalised values, i.e. C_N/C_o=(Absorbance after pass N)/(Initial Absorbance), in Figure 6.2.

Table 6.1: Absorbance results as a function of single pass number

Single Pass Number (N)	UV Absorbance at 254 nm	
	Fluka Humic Acid	Raw Water
0	0.1152	1.2050
1	0.0773	0.6635
2	0.0630	0.5131
3	0.0594	0.4028

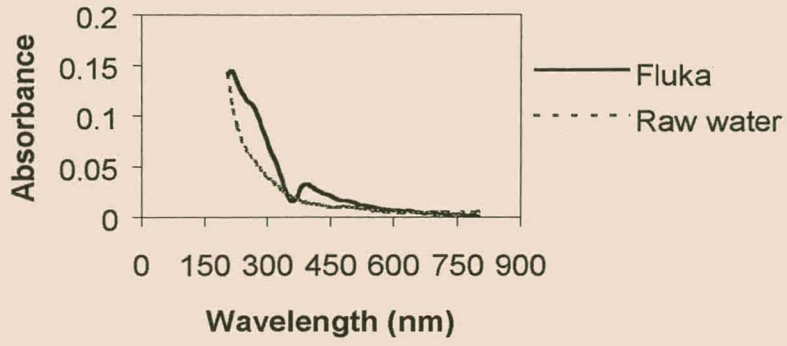

Figure 6.1: Absorbance spectra for synthetic HA (Fluka) and raw water

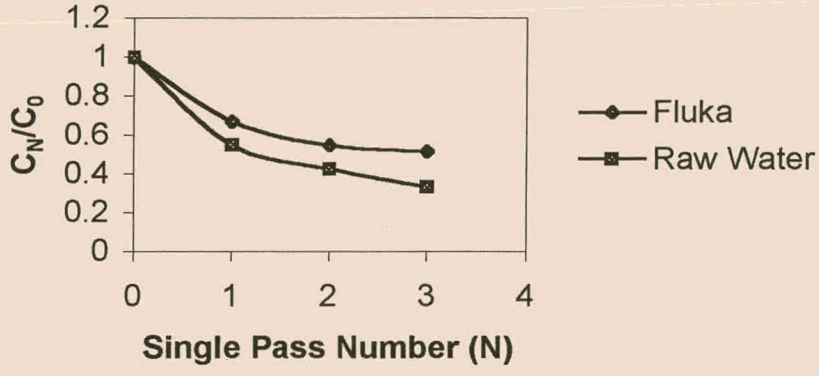

Figure 6.2: Normalised photocatalytic degradation curves based on absorbance at 254nm

Conclusion:

From the above curves it was clear that for both the synthetic humic acid sample, as well as the raw water sample, a visible reduction in ultraviolet absorbance at 254 nm is obtained with photocatalytic treatment.

It can therefore be concluded that the experimental photocatalytic reactor is capable of colour removal from NOM laden water. Removal of organic load (e.g. TOC), however, needs to be verified.

6.2 RESPONSE MEASUREMENTS OF NOM

6.2.1 Objective

Using 3 separate analytical responses to measure photocatalytic efficiency might yield great disparity in results due to calibration error, human error, and day-to-day variation in external conditions. It was therefore necessary to investigate the extent of agreement between the 3 selected methods, toward the analysis of NOM in raw water.

6.2.2 Procedure

General Experimental Conditions:

Analyte	:	Simonstown raw water
Calibration Series	:	20%; 40%; 60%; 80%; 100%
Analyte Volume	:	3 liters
pH	:	Natural, otherwise as prescribed by method
Analysis	:	TOC content
	:	UV Spectroscopy
	:	THMFP
Response	:	UV (at 254 nm)
	:	TOC
	:	THMFP

A calibration series was constructed using Simonstown raw water. A 100% concentration value represented the raw water per se and the corresponding lower percentages indicated distilled water dilutions thereof. Analytical determinations for UV absorbance (254nm), TOC and THMFP were executed according to standard methodology as described in Chapter 5.

TOC values obtained (Table 6.2(a)) for the calibration series were used to calculate corresponding Cl_2 demand in each sample. The Nessler's reagent tested negative for the presence of ammonia-nitrogen compounds in all cases (5.1.3.2), hence the Cl_2 demand calculation simplified to the following expression:

Cl_2 demand = 3 x TOC (mg/L)

6.2.3 Results and Discussion

UV absorbance and TOC values are given in Table 6.2(a), while THM results are summarised in Table 6.2(b).

Table 6.2(a): Calibration Results for UV and TOC analysis

Raw water Concentration (%)	UV Absorbance (254 nm)	TOC content (ppm C)
0	0	0
20	0.150	6.5
40	0.382	11.9
60	0.664	16.3
80	0.880	20.3
100	1.139	26.4

Table 6.2(b): Calibration Results for THMFP

Raw water Conc. (%)	$CHCl_3$ (mg/L)/100	$CHCl_2Br$ (mg/L)/100	$CHClBr_2$ (mg/L)	$CHBr_3$ (mg/L)	THMFP (mg/L)
0	0.00	0.00	0	0	0
20	7.00	1.20	1	0	821
40	16.96	2.52	4	0	1952
60	36.18	5.46	9	0	4173
80	52.00	7.00	13	0	5913
100	83.40	11.38	18	0	9496

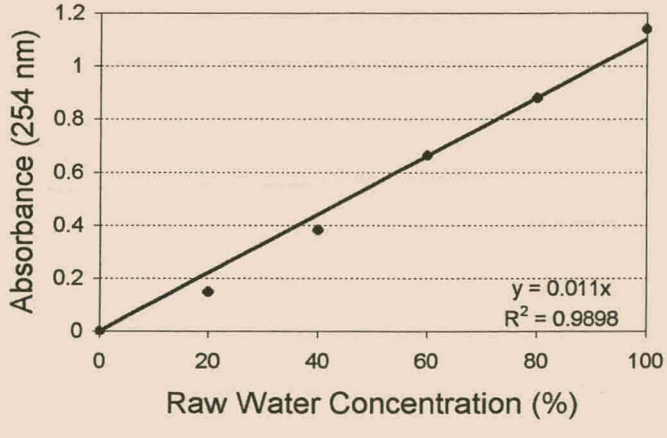

Figure 6.3(a): UV Spectrophotometric Calibration Curve

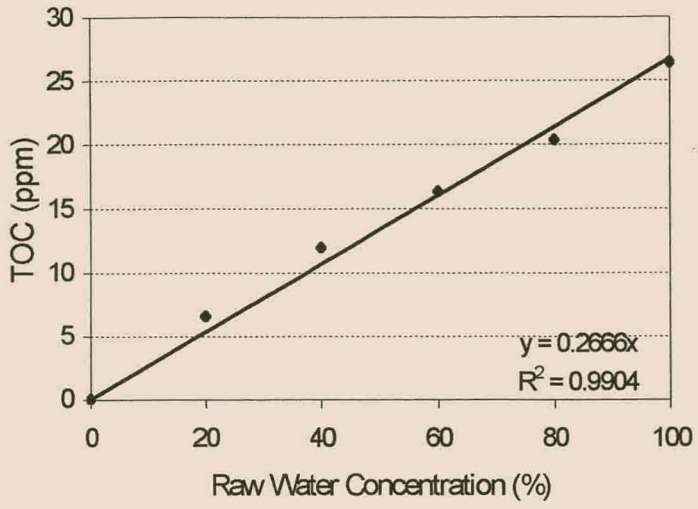

Figure 6.3(b): TOC Calibration Curve

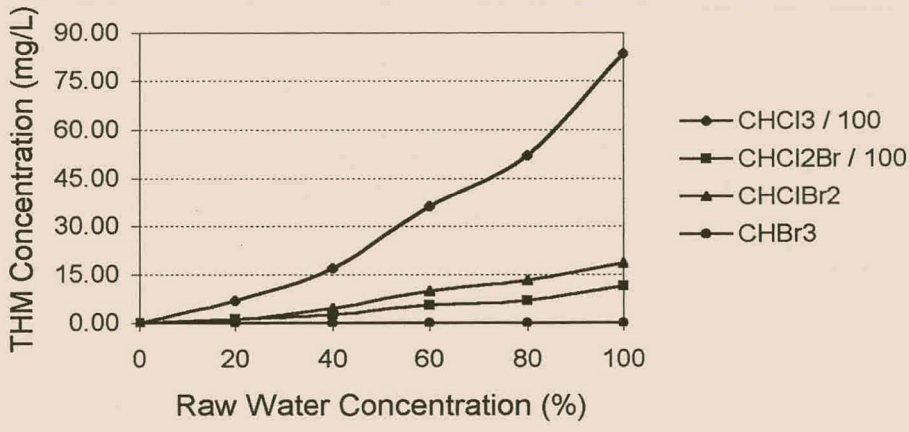

Figure 6.3(c): THM Calibration Curve

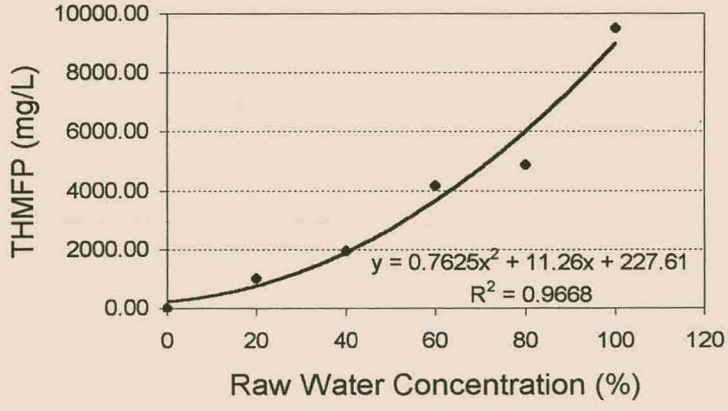

Figure 6.3(d): THMFP Calibration Curve

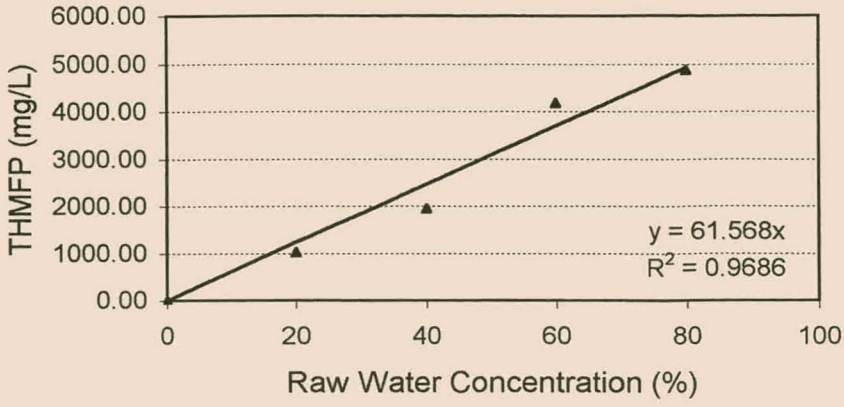

Figure 6.3(e): Linear THMFP Calibration Curve

Discussion:

- The UV calibration curve was linear over the region of investigation, hence measuring the absorbance at 254 nm is considered an efficient method for monitoring colour removal in water.

- The TOC calibration series correlated well with the UV calibration curve.

- The 4 THM species were not generated by Cl_2 treatment to the same extent. $CHCl_3$ was formed in great excess compared to the other THM species. Depending on the presence of bromide ions in the raw water, the mono- di- and tri-bromo species were formed in a decreasing ratio. This is in accordance with other investigations carried out in this laboratory.

- A linear calibration, using THMFP, as a response signal, could not be achieved. Instead a quadratic increase of THMFP with an increase in the raw water concentration was observed. (See Figure 6.3(d))

- Since it has been established that the response of the detection system is linear with respect to individual THM concentrations (Chapter 7) the non-linearity in e.g. Figure 6.3(d) is difficult to explain.

- If the point corresponding to undiluted water is ignored, the response can be regarded as linear (Figure 6.3(e)). Since treated water samples will contain a NOM concentration less than 100%, this linear region corresponds well with the region of interest for treated water samples.

6.3 RESPONSE MEASUREMENTS OF NOM PHOTOCATALYTIC DEGRADATION PRODUCTS

6.3.1 Objective

It is well known that humic substances have very large and complex molecular structures. Photocatalytic degradation of these large organic molecules yields smaller molecules. Efficient photocatalytic oxidation leads to complete breakdown of the organic content in the raw water with the concomitant mineralisation (low TOC) effect. These partially oxidised molecules may differ substantially from the original organic material in the raw water. As mentioned before, it was important to determine whether correlations existed between the 3 analytical methods used to monitor degradation efficiency. A series of photocatalytic experiments were consequently conducted to assess this possibility.

6.3.2 Procedure

General Experimental Conditions:

TiO_2 concentration	:	See Table 6.3
Analyte	:	Simonstown raw water
O_2	:	2.5L/min (via bubblers)
Analyte Volume	:	3 liters
pH	:	See Table 6.3
Flow Rate	:	See Table 6.3
Operation Mode	:	Recirculation
Catalyst Application Mode	:	Immobilised Bed
Sampling Time Interval (min)	:	0;5;10;20;30
Analytical Methods	:	UV Spectroscopy
	:	TOC
	:	THMFP
Response	:	UV absorbance at 254 nm
	:	TOC content
	:	THMFP

A series of 8 experiments were conducted. 3 Factors were varied according to a 2^3 factorial design format to create a systematic variation in experimental conditions. These factors were:

- TiO_2 concentration
- pH of analyte
- Pump speed of analyte through the reactor

The experimental design matrix below (Table 6.3) contains the combination of factor levels for each of the 8 runs.

Table 6.3: Factorial Design Matrix

Run	Factor		
	TiO_2 (g/L)	pH	Flow Rate (l/min)
1	10	8	2
2	10	8	1
3	10	3	2
4	10	3	1
5	1	8	2
6	1	8	1
7	1	3	2
8	1	3	1

50 mL samples were collected at various time intervals, including a zero-time sample, which was collected prior to commencement of a particular irradiation run. Samples were filtered with Whatman No.42 filter paper. Each sample was devided into 3 portions to facilitate measurements of the 3 different responses.

6.3.3 Results and Discussion

All UV absorbance, TOC and THMFP response measurements (obtained via the corresponding analysis) were normalised in order to facilitate comparisons. Normalisation was performed as follows:

$$\text{Normalised Signal} = \frac{C_t}{C_0}$$

where,

C_t=Response measurement at time interval t=t

C_0=Response measurement at time interval t=0

Results for e.g. UV measurement are summarised in Table 6.4.

Table 6.4: Results by UV measurement of 2^3 Factorial Design

Run	Sampling Time (min)				
	0	5	10	20	30
1	1	0.666	0.509	0.337	0.128
2	1	0.465	0.459	0.166	0.076
3	1	0.312	0.273	0.195	0.124
4	1	0.326	0.307	0.195	0.110
5	1	0.513	0.500	0.238	0.149
6	1	0.657	0.587	0.399	0.245
7	1	0.291	0.306	0.176	0.141
8	1	0.287	0.281	0.200	0.122

Results from each run were represented separately such that response values for the same sample could be compared.

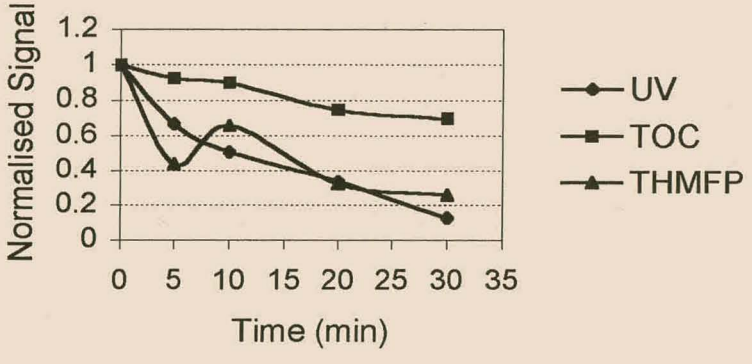

Figure 6.4 (a): Run 1

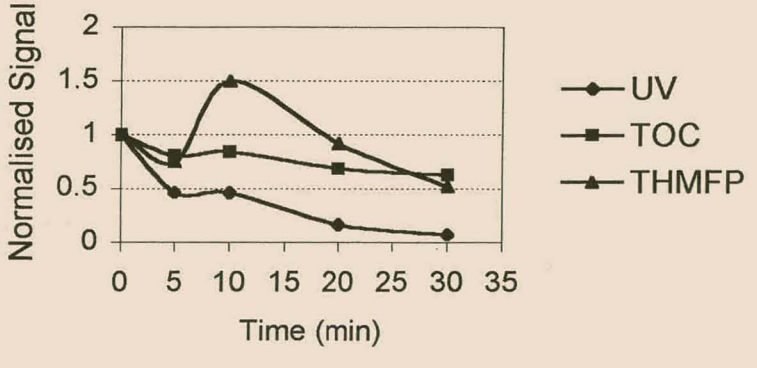

Figure 6.4 (b): Run 2

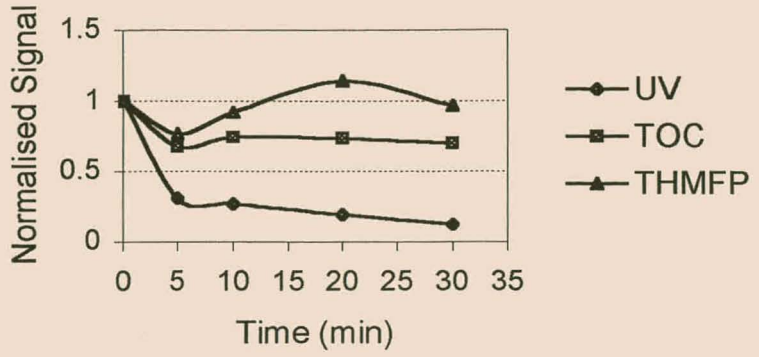

Figure 6.4 (c): Run 3

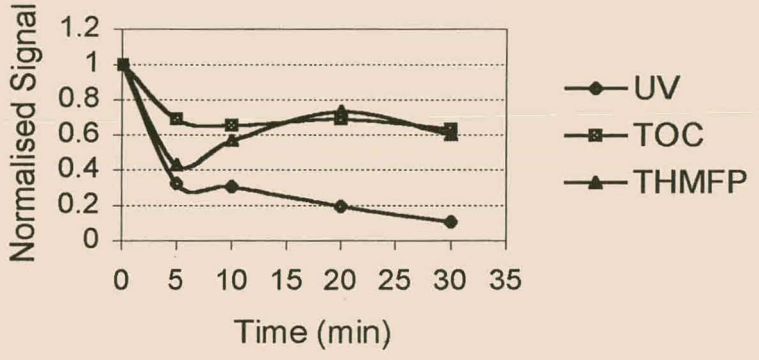

Figure 6.4 (d): Run 4

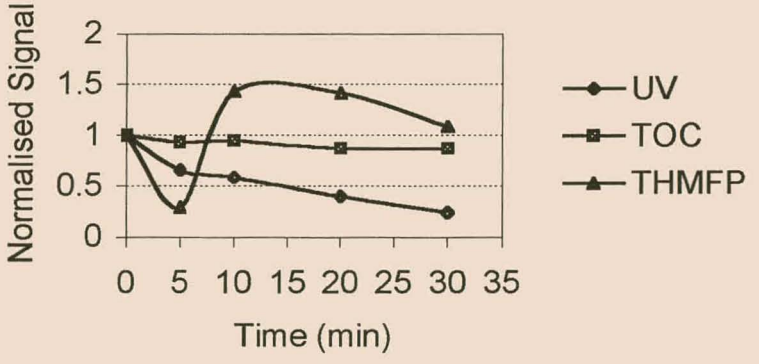

Figure 6.4 (e): Run 5

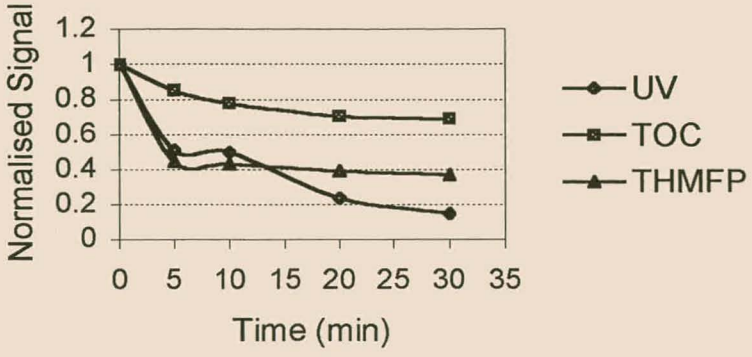

Figure 6.4 (f): Run 6

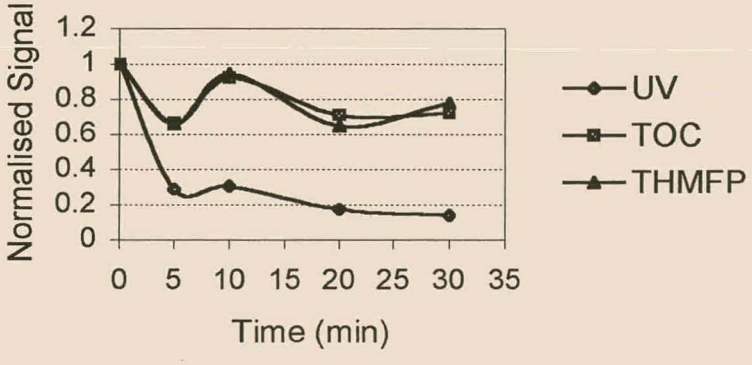

Figure 6.4 (g): Run 7

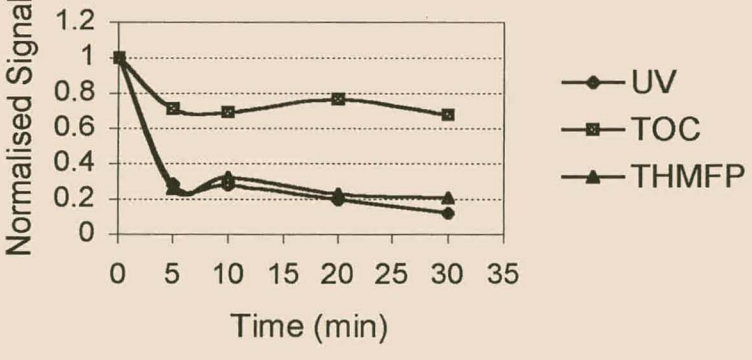

Figure 6.4 (h): Run 8

Remarks:

- UV absorbance at 254 nm is a good indicator of colour removal by the photocatalytic process. Colour removal as such, however, is not an indicator of removal of other (smaller) organic species.

- A significant increase in the THMFP is observed after about 5 minutes reaction time.
- Flow rate has a significant effect on THMFP (Figure 6.4(a) and (b)).
- pH has a significant effect on THMFP (Figure 6.4(a) and (c)).
- TiO_2 has significant effect on THMFP (Figure 6.4 (a) and (e)).
- TOC show generally a slow decrease.

Discussion:

- The initial decrease in THMFP before 5 minutes reaction time can be attributed to adsorption of humic substances onto the glass fibre.
- The increase in THMFP after 5 minutes reaction time can be attributed to photocatalytic breakup of the humic substances into smaller intermediate molecules.
- The stability of large, complex humic structures lead to initial resistance against complete mineralisation during the photocatalytic degradation process. Intermediate organic species are formed as a result of partial photocatalytic oxidation. It can be postulated that these intermediates have $-CH_2(COOH)$ and $-C(COOH)CH_3$ - functional groups, which caused an unexpected increase in THMFP response due to an increased reactivity of the smaller intermediate molecules.
- It was therefore decided to discard UV absorbance for response measurements and to continue with TOC and THMFP in the optimisation studies of photocatalytic destruction of NOM.

6.4 OPTIMISATION OF PHOTOCATALYTIC REACTOR FOR THE DESTRUCTION OF NATURAL ORGANIC MATTER

6.4.1 Recirculation Mode

Factors involving the specific sample to be treated were identified for optimisation. The OED pyramid approach was followed (4.1).

6.4.1.1 Factorial Design

6.4.1.1.1 Objective

A 2^3 factorial design was chosen for the optimisation of factors that could possibly influence the photocatalytic efficiency of the reactor (4.2.1).

6.4.1.1.2 Procedure

General Experimental Conditions:

TiO_2 concentration	:	See Table 6.5
Analyte	:	Betty's Bay raw water
Analyte Concentration	:	See Table 6.5
Analyte Volume	:	3 liters
pH	:	See Table 6.5
Flow Rate	:	2 L/min
Catalyst Application	:	Combined slurry and immobilised bed
Operation Mode	:	Recirculation
O_2	:	2.5L/min (via bubblers)
Sampling Intervals (hrs)	:	0 and 2
Analytical Methods	:	TOC Analysis
Response	:	% reduction

The following factors were selected for the factorial experiment:

- TiO_2 Concentration
- Raw water Concentration
- pH of Analyte

The effect of variation of these factors was monitored as a function of a defined response function. Since the reactor was applied in degradation experiments, the response used was the TOC reduction (%) after a pre-selected time interval. The response function can be defined by the following equation:

$$\%\,\text{Reduction} = \frac{C_0 - C_t}{C_0} x100$$

where

C_0= TOC content at time interval t=0 (in ppm C)

C_t= TOC content at time interval t=t (in ppm C)

The factorial design matrix (Table 6.5) are given below:

Table 6.5: Factorial Design Matrix

Run	Factor		
	TiO_2 (g/L)	PH	Raw Water Conc. (%)
1	10	6.5	100
2	10	6.5	50
3	10	3.0	100
4	10	3.0	50
5	1	6.5	100
6	1	6.5	50
7	1	3.0	100
8	1	3.0	50

50 mL samples were collected, at set intervals as before, including a zero-time sample. Samples were filtered with a double layer of Whatman No.42 filter paper.

6.4.1.1.3 Results and Discussion

Response values are summarised in Table 6.6. The optimisation results were analysed and interpreted using the statistical computer program, STATISTICA 5.0, which is capable of yielding regression coefficients etc. with respect to the specific experimental design results.

Table 6.6: Factorial Design Response Values

Run	TOC (ppm) t=0 hrs	TOC (ppm) t=2hrs	% Reduction
1	25.06	3.70	92
2	10.97	4.16	62
3	21.39	4.60	84
4	7.89	4.07	52
5	16.39	2.03	87
6	7.89	4.69	52
7	14.19	4.93	12
8	8.33	3.03	4

An ANOVA analysis was performed to determine the significance of the various factors under investigation. The significance was described in terms of a null-hypothesis probability (p), where the boundary level of significance was assigned to be p=0.1. For p<0.1, the null

hypothesis is proved to be invalid. Variation of such a factor would exert a significant effect on the response measured. If $p>0.1$, the opposite is proved, and the corresponding factor can be discarded within the constraints of the particular experimental design.

Response surface methodology usually requires the combination of a mathematical model with the chosen experimental design and corresponding response data. Polynomials of linear or quadratic form can be used. In this case, a quadratic polynomial model indicated no significant factors via the ANOVA analysis. By using a linear model for data processing, we assumed that no interactions occurred between the relevant factors. The response measured could be expressed in terms of the following equation:

$$Z = \beta_0 + \beta_1 X_1 + \beta_2 X_2$$

where
Z=response function
X_1, X_2=experimental factors
β_0=intercept on response axis
β_1, β_2=gradient for each factor

The following null-hypothesis probabilities were calculated by STATISTICA (See Table 6.7):

Table 6.7: ANOVA results

Factor	p-Value
TiO_2	0.506
pH	0.716
NOM concentration	0.0447

Remarks

- Only the NOM concentration revealed a probability less than 0.1 and was therefore classified as being significant. Therefore, an increase in NOM content resulted in greater % TOC reduction. Similar response increases with increase in pollutant concentration(s) have been observed for other photocatalytic oxidation investigations.

- Relative to the NOM concentration, the other 2 factors exerted no significant effect on the response within their respective regions of variation.

In order to investigate the effects of the other 2 factors in the absence of the dominating effect of the NOM concentration factor, the 2^3 factorial design was divided into two separate 2^2 fractional factorial matrices. Each 2^2 fractional matrix represented only one of the 2 selected NOM concentration levels.

From Table 6.5 the fractional factorial matrices consisted of the following runs:
100% NOM content: 1, 3, 5, 7
50% NOM content: 2, 4, 6, 8

The fractional factorial results were processed and interpreted via STATISTICA 5.0, assuming a linear mathematical model:

$$Z = \beta_0 + \beta_1 X_1 + \beta_2 X_2$$

where
Z=response function
X_1, X_2=experimental factors
β_0=intercept on response axis
β_1, β_2=gradient for each factor

Table 6.8: ANOVA results

Factors	p-Value	
	100% NOM Content	50% NOM Content
TiO_2	0.612763	0.736302
pH	0.313539	0.683166

The following regression coefficients were obtained for the linear model:

50% NOM Content:
$Z=62.39+0.73*X_1 - 2.32*X_2$

100% NOM Content
$Z=56.09+0.60*X_1 +4.16*X_2$

Where
Z=TOC Reduction (%)
X_1=TiO_2 concentration
X_2=pH

Remarks:

- Both NOM concentration scenarios, yielded null-hypothesis probabilities with values greater than 0.1, indicating the insignificance of the individual factors with the constraints of the design. (Table 6.8)

- The response intercept (β_0) is in the same range for both NOM content scenarios.

- β_1, the gradient for the TiO_2 concentration, has a positive value for both cases. Further, an increase in TiO_2 concentration implicates an increase in the % TOC reduction.

- The gradient (β_2) for the pH factor showed opposing values for the 2 scenarios in terms of the sign of the coefficient. A positive gradient was observed for a high NOM content, while a negative gradient was observed at low pH values.

- From the β_1 and β_2 values the following conclusion was drawn for the 2 scenarios: At high NOM content an increase in both TiO_2 and pH would lead to improved reduction in TOC levels, while high TiO_2 and low pH levels would yield optimum destruction of NOM substances at low NOM content.

- The variation in optimum pH could be explained in terms of the ionisation of the functional groups on NOM molecules (See Chapter 2, Figure 2.3). In addition, TiO_2 exhibits a charge variation as a function of pH according to the following equilibria (3.1.3):

$$\text{-Ti-OH}_2^+ \overset{H^+}{\Leftrightarrow} \text{-Ti-OH} \overset{H^+}{\Leftrightarrow} \text{-Ti-O}^-$$

  Interaction between these ionised species explains the resultant behaviour.

6.4.1.2 Central Composite Designs (CCD)

The unusual effect of pH on the tendency toward optimum TOC reduction indicated that it affected either the ionisation of the TiO_2 particles, or the functional groups on the NOM substances. A response surface design was therefore used for the optimisation of these factors, resulting in a condition for maximum TOC reduction.

6.4.1.2.1 Objective

The objective of this study was to optimise the TOC reduction rate in terms of pH and TiO_2 concentration as experimental factors, by using a central composite response surface design.

6.4.1.2.2 Procedure

Since the fulvic acid (FA) fraction of NOM is soluble over the entire pH range, and the humic acid (HA) fraction is only soluble from pH greater than 7 (2.3), two regions of interest were identified for the optimisation of the pH level, namely pH 3-6 and pH 6-9. This was combined with the variation in TiO_2 concentration. Two CCDs (4.2.3) were therefore generated. The corresponding α-parameter was set at $\alpha=2^{0.5}$

A shorter sampling time interval was used compared to previous experiments. This was done in view of optimising the initial rate of photocatalytic oxidation as it pertains to the original water sample containing a relative HA content of 100%.

General Experimental Conditions:

TiO_2 concentration	:	See Table 6.9
Analyte	:	Betty's Bay raw water
Analyte Volume	:	3 liters
pH	:	See Table 6.9
Flow Rate	:	2 L/min
Catalyst Application	:	Combined slurry and immobilised bed
Operation Mode	:	Recirculation
O_2	:	2.5L/min (via bubblers)
Sampling Intervals (min)	:	0 and 15
Analytical Method	:	TOC Analysis
Response	:	% reduction

The reproducibility within the CCD is determined in triplicate by performing the center runs, i.e. Run 1, 6 and 11.

The response chosen for the statistical manipulation of data, was similar to that used for the factorial design, namely % reduction of TOC content after time interval t=15. Since it was already known that interactions were absent between these factors, a linear mathematical

model was chosen for each pH region, with the aim of generating the corresponding response surfaces (See factorial design for equation).

Table 6.9: Experimental Design Matrix for Two 2 Factor Central Composite Designs

Run	pH Range 3-6		pH Range 6-9	
	pH	TiO_2 (g/L)	pH	TiO_2 (g/L)
1	4.50	6.00	7.50	6.00
2	3.00	2.00	7.50	11.66
3	6.00	2.00	9.00	2.00
4	3.00	10.00	9.62	6.00
5	6.00	10.00	9.00	10.00
6	4.50	6.00	7.50	6.00
7	2.38	6.00	6.00	40.00
8	6.62	6.00	5.38	6.00
9	4.50	0.34	6.00	2.00
10	4.50	11.66	7.50	0.34
11	4.50	6.00	7.50	6.00

6.4.1.2.3 Results and Discussion

6.4.1.2.3.1 pH range 3-6

Table 6.10: Experimental Results

Run	TOC (ppm) t=0 min	TOC (ppm) t=15 min	% Reduction
1	23.7	15.9	33
2	26.6	16.3	39
3	27.6	17.2	38
4	24.8	23.0	7
5	25.8	17.7	32
6	27.7	18.7	32
7	27.9	22.5	19
8	23.0	16.6	28
9	27.3	18.2	33
10	25.4	19.0	25
11	27.5	16.5	40

Table 6.11: ANOVA results (pH 3-6)

Factor	p-Value
pH	0.729246
TiO_2 Concentration	0.085310

The following equation represented the linear model for the assigned pH region:

$Z=53.58+0.812*X_1 -1.67*X_2$

X_1=pH
X_2=TiO_2 concentration

Remarks:

- From the probabilities calculated, the TiO_2 factor proved to be significant, while pH exerted no significant effect on the response.
- The response surface equation indicated a negative gradient for the TiO_2 factor. This was contradictory to the findings from the fractional factorial designs.

6.4.1.2.3.2 pH Range 6-9

Table 6.12: Experimental Results

Run	TOC (ppm) t=0 min	TOC (ppm) T=15 min	% Reduction
1	20.9	17.7	16
2	16.8	14.6	13
3	16.9	15.0	11
4	22.2	15.2	31
5	23.1	18.5	20
6	24.0	12.8	46
7	18.9	12.4	35
8	20.5	18.2	11
9	22.0	18.2	17
10	24.1	15.6	36
11	23.7	18.4	22

Table 6.13: ANOVA results (pH 6-9)

Factor	p-Value
pH	0.132414
TiO_2 Concentration	0.092344

The following equation represented the linear model for the assigned pH region:

$Z=42.59+1.65*X_1 -3.86*X_2$

$X_1=TiO_2$ concentration

$X_2=pH$

Remarks:

- From Table 6.13 it could be deduced that the variation of TiO_2 has statistical significance, while the pH factor did not play a significant role, albeit yielding a probability very close to 0.1.

- The negative gradient of the pH factor, from the regression, suggested that an increase in pH reduced the TOC reduction efficiency. This could be explained in terms of the distribution of TiO_2 species across the entire pH range. (3.1.3) From pH 4 onward, an increasing % of the TiO^- species is present in the TiO_2 suspension. This negative charge repels the OH^- ion at the surface of the catalyst, subsequently decreasing the photocatalytic efficiency of the system.

6.4.1.3 Superimposed Model

In order to obtain a more thorough picture of the response variation over the entire pH range (i.e. from pH 3 to pH 9) the 2 central composite designs were merged, thus generating an unique superimposed model.

6.4.1.3.1 Objective

The purpose of this investigation was therefore to assess the possibility of using a superimposed model to generate an optimised response surface over the entire pH range of interest.

6.4.1.3.2 Procedure

The results from the above central composite designs (Tables 6.10 and 6.12) were combined and reinterpreted using STATISTICA.

6.4.1.3.3 Results and Discussion

A linear-quadratic model was selected whereby 2-way interactions were included. The corresponding response function was represented by the following polynomial equation:

$$Z = \beta_0 + \beta_1 X_1 + \beta_2 X_2 + \beta_{11} X_1^2 + \beta_{22} X_2^2 + \beta_{12} X_1 X_2$$

where,

Z: response function

X_1, X_2: experimental factors

β_0: intercept on response axis

β_1, β_2: gradient for each factor

β_{11}, β_{22}: coefficients for quadratic main effects

β_{12}: interaction term; combined effect of the two factors

The corresponding ANOVA results are summarised below:

Table 6.14: ANOVA results (L: linear; Q: quadratic)

Factors	p-Value
pH (L)	0.105317
pH (Q)	0.002244
TiO_2 Concentration (L)	0.611924
TiO_2 Concentration (Q)	0.507704
PH (L) by TiO_2 Concentration (L)	0.006017

The following regression equation was generated:

$$Z=17.15+11.47*X_1 - 1.48*X_1^2 - 4.07*X_2 - 0.09*X_2^2+0.82*X_1*X_2$$

Where

X_1=pH

X_2=TiO_2 concentration

A rising ridge type response surface was generated and clearly illustrated the 2-way interactions as observed. The corresponding contour plot confirmed the existence of the ridge and an optimised pH-TiO_2 condition.

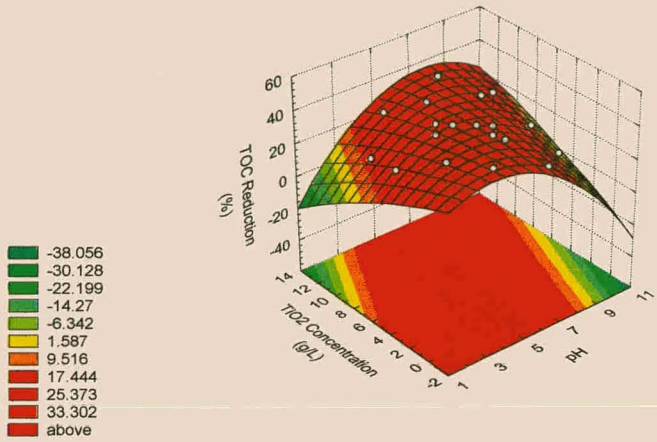

Figure 6.5: Response Surface

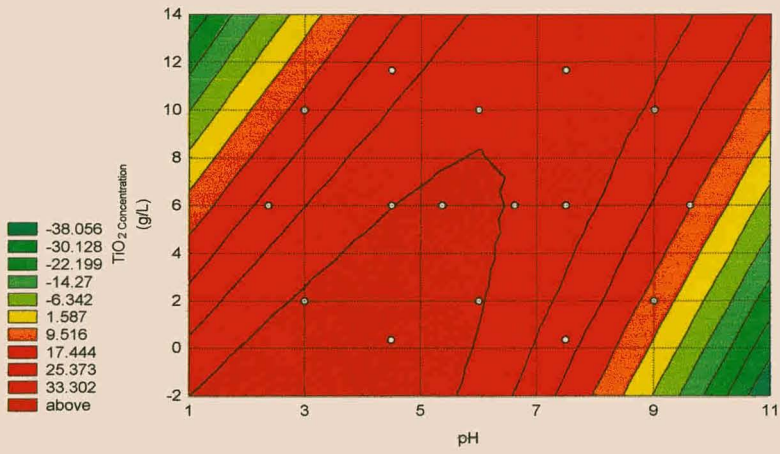

Figure 6.6: Contour Plot

Remarks:

- From Table 6.14, the significance of both the quadratic pH effect (X_1^2), as well as the 2-way effect between pH and TiO_2 (X_1X_2) was clear.

- The significance of these factors would consequently result in a curved response surface.

- The β_{11} and β_{22} coefficients characterise the parabolic nature of the response surface. The calculated negative values for those coefficients therefore corresponded with the convex nature of the response surface. (Figure 6.5)

- β_{12} (the interaction term), which proved to be significant caused asymmetry of the ridge across the surface. An optimised tendency was observed diagonally across the surface, from low pH (at low TiO_2) to high pH (at high TiO_2).

- The calculated optimum condition from the contour plot is reported as:
  TiO_2=7.80 g/L
  pH=6.20

6.4.2 Single Pass Mode

The single pass mode comprised a procedure whereby a water sample was pumped once from the main external reservoir, through the reactor, to the base reservoir within the reactor (See Figure 3.11). A sample was taken from the base reservoir (after each pass) to determine NOM degradation via photocatalytic oxidation. Thereafter the water sample was returned to the main reservoir for the start of the next single pass.

The single pass number is indicated by the symbol N. Each single pass represented a residence time of approximately 4 seconds. This was the approximated time available for UV irradiation as the water layer moved down the fibreglass sheet towards the base reservoir.

6.4.2.1 Objective

In view of a prospective scaling-up of the existing photocatalytic reactor for potable water treatment, it was essential to optimise the shortest pathway for the production of purified water. In contrast to the recirculation mode, the single pass mode was regarded as more feasible towards scaling-up procedures. As far as the single pass mode was concerned, it was necessary to determine the number of passes required to reach an acceptable level of NOM purified water.

6.4.2.2 Procedure

General Experimental Conditions:

TiO_2 concentration	:	1g/L
Analyte	:	Simonstown raw water
Analyte Volume	:	3 liters
pH	:	Natural
Flow Rate	:	2 L/min
Catalyst Application	:	Immobilised bed
Operation Mode	:	Single Pass Mode
O_2	:	2.5L/min (via bubblers in bottom reservoir)
Analytical Method	:	UV Spectroscopy
Responses	:	UV absorbance at 254 nm
	:	TOC

UV absorbance was chosen at the time when its inadequacy was not realised. A ten single pass experiment was performed with 50 mL samples extracted before and after each single pass. A control experiment was performed in conjunction with the single pass photocatalytic experiment. This comprised the same procedure as done with the photocatalytic experiment, but with the exclusion of UV irradiation in each single pass. The control was necessary to determine the extent of mass transfer via adsorption onto the TiO_2-coated fiberglass sheet in comparison with actual destruction or removal of humic materials by means of photocatalysis (when UV irradiation occurred).

6.4.2.3 Results and Discussion

Table 6.15 contains the response values for the single pass series. The results were normalised in the graphic presentation, thereby facilitating comparison of the 2 experimental modes.

Table 6.15: Single Pass Mode Results

Single Pass No. (N)	Response			
	TOC (ppm)		UV absorbance @ 254nm	
	Photocatalytic	Control	Photocatalytic	Control
0	41.6	33.9	1.230	1.188
1	37.7	30.6	0.795	0.742
2	27.0	28.7	0.463	0.642
3	21.2	25.6	0.289	0.648
4	21.6	25.5	0.178	0.678
5	18.9	25.4	0.139	0.728
6	18.1	26.7	0.104	0.798
7	17.2	28.4	0.0903	0.683
8	17.3	27.7	0.0950	0.704
9	17.4	28.0	0.0797	0.865
10	19.4	28.4	0.0798	0.758

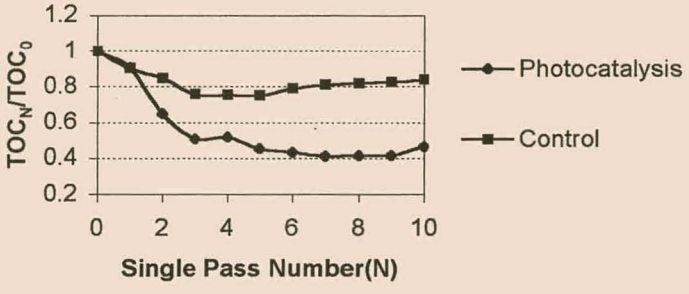

Figure 6.7: Normalised TOC Response Results

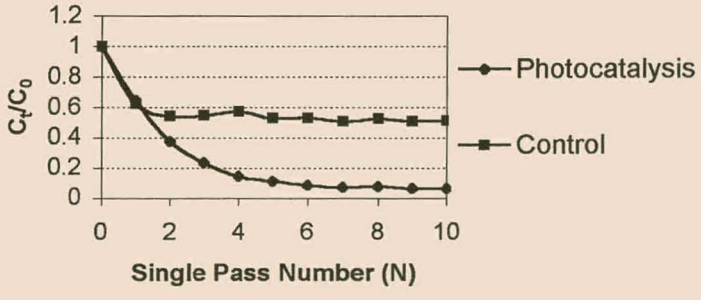

Figure 6.8: Normalised UV Absorbance Results

Remarks:

- The results as depicted in Figure 6.7 and 6.8 confirmed enhanced removal rates of NOM from the water sample with the addition of photocatalysis.

- Mass transfer of NOM to the fibre glass sheet (via adsorption) occurred during the first 3 passes of the control experiment. Single passes 4 to 10 showed no further adsorption.

- The corresponding photocatalytic degradation rate was characterised by first order exponential decay according to the following equations:
  $C(N)=C_0.e^{-kN}$
  $\ln C(N)/C_0=-kN$
  k=first order decay constant
  N=single pass number

6.5 CONCLUSIONS

From the preliminary experiments conducted, it was clear that the experimental reactor (with immobilised bed catalyst) was able to photocatalytically degrade NOM in raw water.

The reduction in NOM was succesfully monitored using 3 different analytical methods, i.e. UV Spectroscopy, TOC analysis and THMFP determinations. UV absorbance at 254 nm is sufficient to monitor colour removal. The last two analytical methods showed good correlation when determining intermediate degradation products in photocatalytically treated water. THMFP determinations, however, were too time-consuming to be used in reactor optimisation studies.

The 2^3 factorial design indicated that the NOM content was the dominant factor for optimum degradation efficiency. Increased NOM content improved the degradation efficiency. Furthermore, scientific publications have advised the omission of concentration as factor from experimental design type optimisations (Long, 1969).

Since the structural characteristics of both TiO_2 and NOM substances facilitated surface modification by pH variation, pH was identified as an important factor to consider for optimum TOC degradation in NOM laden water. From the superimposed model, a rising ridge was

observed as response surface. The ridge stretched diagonally across the pH range 3 to approximately 7. The amount of TiO_2 that was required for optimum TOC degradation was therefore dependent on the pH of the raw water. These results pertained to the photocatalytic treatment of NOM laden water in a catalyst type of reactor where TiO_2 was immobilised on glass fibre.

Clearly if reactors, as depicted in Figure 3.13, are serially coupled and operated on the single pass mode, the pH can be lowered and the amount of TiO_2 per sheet increased, as the water progresses through the reactor system.

The choice of operation mode plays an important role when determining the efficiency of a process, since the production rate of potable water is a crucial factor. Both the recirculation and single pass modes were investigated. Encouraging results were achieved within the first 5 passes of the single pass mode, even without employing an optimised system. This mode seemed promising for scaling-up and should receive further attention. The recirculation mode proved to be less time-efficient, when compared the single pass mode in terms of reaching a particular level of NOM removal. Moreover, recirculation mode reactors are unsuitable to scaling-up due to volumetric limitations.

From the results obtained it was evident that the existing experimental photocatalytic reactor has shown the potential to be developed as an effective water treatment unit. Such a scaling-up attempt would, however require extensive collaboration between chemists, engineers and water treatment specialists, accompanied by sound financial back-up of a large company or government body.

REFERENCES

Kriek R.J. (1994) Skeiding van Pt(IV), Pd(II) en Rh(III) deur Differensiële Fotokatalitiese Reduksie. M.Sc Thesis, University of Stellenbosch

Long D.E. (1969) Simplex Optimization of the Response from Chemical Systems. *Analytica Chimica Acta* **46** p.193-206

CHAPTER 7

Solid Phase Microextraction

Although the THMFP determinations proved to be too time-consuming for reactor optimisation investigations, it was necessary to develop a solvent-free analytical protocol for these determinations.

The general awareness of pollution and hazards caused by solvents used for extraction processes has initiated a trend toward the development of solvent-free sample preparation methods. Although several solvent-free methods have been known for some time, the enforcement of more stringent regulations on scientists and industry has prompted the shift in emphasis.

7.1 SOLVENT–FREE SAMPLE PREPARATION

Solvent-free sample preparation can be categorised according to the separation medium employed in the process, namely:

- gas-phase extraction
- membrane extraction
- sorbent extraction

7.1.1 Gas-phase Extraction

3 typical methods of gas-phase extraction include

- Static headspace sampling
- Purge and trap / Dynamic headspace sampling
- Supercritical fluid extraction (SFE)

Static headspace analysis has been used for decades for the analysis of VOCs in food, beverages, etc. This is however a low sensitivity analytical method, where no concentrating effect occurs. A further disadvantage is that "exhaustive extraction" is not possible by means of

this method. Small amounts of analyte are therefore extracted at a time, reducing the sensitivity considerable. Careful calibration, where equilibration times between gas and liquid phase should be taken into consideration, is therefore required (Poole, 1991, p.818; Zhang, 1994).

Dynamic headspace analysis (i.e. purge and trap method) allows for quantitative extraction of analytes. With this analytical method carrier gas is bubbled through an aqueous sample, forcing the analyte from the aqueous medium into the gas phase. Thereafter, the analyte is collected using a cold trap or a sorbent trap. Foaming, cross-contamination and stripping gas flow rates, rendering the technique incompatible with on-line operation, constitutes the major problem areas when using dynamic headspace analysis (Poole, 1991, p.824; Zhang, 1994).

Since supercritical fluids exhibit both gas-like mass transfer and liquid-like solvating characteristics SFE are a very efficient solvent-free sample preparation method. High costs of instrumentation and high purity gas are however limiting factors (Poole, 1991, p.601; Zhang, 1994).

7.1.2 Membrane Extraction

This technique involves 2 simultaneous processes, namely a polymeric extraction from the sample matrix and a gas extraction from the polymeric phase. Despite decades of development of this technology, little information is available on its application for sample preparation in chromatography. Presently, hollow fibres have replaced the use of supported membrane sheets. This approach facilitated good comparison with headspace methods, resulting in a significantly better surface-area-to-volume ratio and yielding improved mass transfer rates. Unfortunately polar compounds can not be analysed with membrane extraction, which limits the application prospects of the technique (Zhang, 1994).

7.1.3 Sorbent Extraction

The principle of using sorbent material for the extraction of analytes from aqueous media was developed several years ago. By employing different sorbents, a variety of analytes can be extracted from aqueous or gaseous medium. Solid phase extraction (SPE) is one such a sorbent extraction techniques, which have shown an extensive application in sample preparation for analysis. Despite its advantages (Chapter 5), this method still exhibits some limitations, e.g.

it requires environmentally hazardous solvents for the extraction of analyte from the sorbent. Moreover, SPE cartridges are often blocked as a result of oily components (Gòrecki ,1996) (Zhang, 1994).

In order to overcome the limitations of SPE, the geometry of the sorbent has been improved. The sorbent is coated onto a fine rod of fused silica fibre, changing the geometry to a cylindrical shape. This approach induces rapid mass transfer during extraction and desorption without encountering the problem of plugged cartridges. The miniaturisation of SPE was aptly named SPME, i.e. solid-phase microextraction (See Chapter 5) (Gòrecki, 1996).

7.1.4 SPME

For clarity the diagrammatic representation of the SPME device (Figure 5.3) is repeated below.

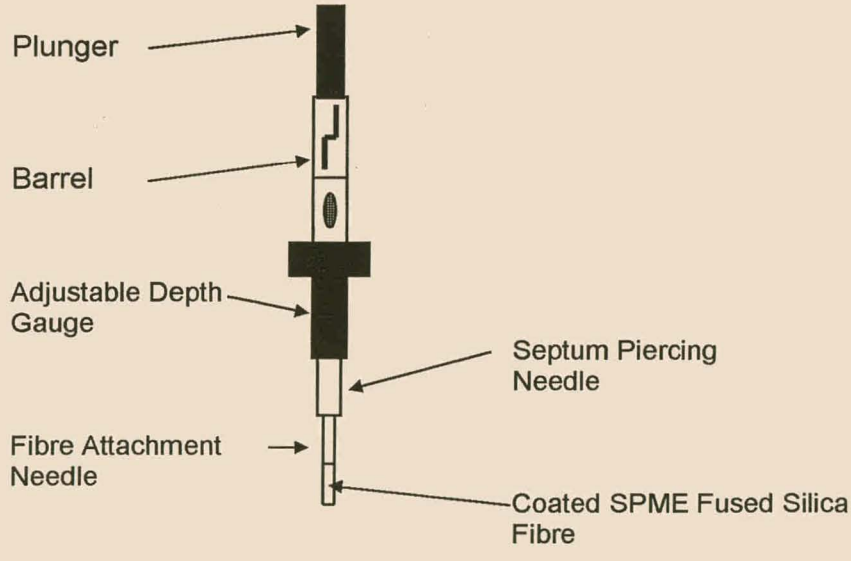

Figure 7.1: SPME Device

The SPME analytic method consists of 2 processes, namely:

- The partitioning of analytes between the fibre coating and the sample matrix at low temperature.
- Desorption of the concentrated analyte in the injection port of an analytical instrument for analysis at high temperature (e.g. GC).

When the partitioning of analytes between the sample matrix and polymeric coating of the fibre occurs, the amount of analyte absorbed onto the fibre at equilibrium can be presented by the following equation (Eisert, 1996):

$$n = \frac{K_{fs}V_fC_0V_s}{K_{fs}V_f + V_s} \quad (1)$$

where,
n=mass of analyte absorbed by the fibre coating
V_f, V_s=volumes of fibre coating and sample respectively
K_{fs}=partition coefficient of analyte between fibre coating and sample matrix
C_0=initial concentration of analyte in sample matrix

Since the sorbents selected for fibre coatings have a strong affinity for organic compounds, K_{fs} values for analytes are large, implicating a very high concentrating effect. This leads to good sensitivity. K_{fs} values are however not large enough to ensure exhaustive extraction of the analytes from the sample matrix. SPME, like headspace analysis, is therefore based on an equilibrium process. Proper calibration prior to analysis is therefore required for quantitative analysis of analytes.

Since the sample volume, V_s, is much larger than that of the polymeric fibre coating, we can assume that $V_s >>> K_{fs}V_f$. Equation 1 therefore simplifies to give the following relationship:

$$n = K_{fs}V_fC_0 \quad (2)$$

Equation 2 clearly indicates a linear relationship between the amount of analyte absorbed by the fibre coating and the initial concentration of the analyte in the sample matrix, when assuming a large sample volume.

The simplicity of the relationship between analyte extracted and initial analyte concentration, together with its simple geometry, makes this method well suited to field sampling and analysis. The method has been used with great success for the extraction of samples from lakes, soil, air, etc. *The mainstay of its success can be ascribed to the fact that sampling, extraction, concentration and injection have been merged into a single device.*

Several factors influence the efficiency of extraction of analytes from the sample matrix. Each one will be discussed below (Zhang, 1994; Zhang, 1993; Eisert, 1996).

7.1.4.1 Agitation of sample matrix

As mentioned before, SPME is an equilibrium process, thus the rate of extraction of analytes is directly influenced by the diffusion rate of the analyte. Two scenarios exist, namely a static and dynamic scenario. During the static scenario the transport of analyte to fibre is limited by diffusion of the analyte in both the aqueous sample phase and the aqueous fibre phase. This result in long equilibrium times.

When the dynamic scenario applies, extensive stirring of the sample matrix is done. This allows for faster mass transfer of the analyte in the aqueous medium compared to that in gas or polymer phases, rendering the limitations of diffusion ineffective. Magnetic stirring or sonication can therefore be employed to reduce equilibrium times considerably.

7.1.4.2 Extraction matrix

Samples can be extracted directly from the aqueous medium, or via the headspace above. Semivolatile compounds are analised from the aqueous medium, while VOCs are, as a rule of thumb, extracted from the headspace. Since the kinetics in solution are slow compared to that in the gas-phase, the extraction matrix employed directly influences equilibrium times. Equilibrium between analytes in the gas-phase and the polymeric fibre are achieved within minutes, while equilibrium in the aqueous medium could take more than 1 hour. To avoid very long extraction times, a fixed time could be selected for extraction from the aqueous medium whereby a certain percentage of the equilibrium amount would be extracted.

A means of overcoming the kinetic limitations of diffusion is to heat the sample during the extraction of the analyte. As the temperature rises, more VOCs are released from the sample matrix into the headspace above, thereby facilitating headspace extraction. However, during quantitative analysis of analytes, it is important to control the extraction temperature very carefully, since the slightest variation in temperature would influence the amount of analyte present in the headspace above the sample matrix. An accurate temperature control unit should

only be employed in cases where sensitivity is very low. These units, however, will escalate the cost of analysis.

7.1.4.3 pH

The extraction efficiency of neutral forms of analytes, by means of a non-ionic polymeric fibre coating, is greater than that for ionised species. The pH of the sample matrix should therefore be adjusted to a level where the relevant species to be analysed carries no charge.

7.1.4.4 Ionic Strength

The sensitivity of an extraction could be improved greatly by adjustment of the ionic strength of the sample matrix. As the ionic strength of the sample matrix increases, the partitioning of polar organic compounds onto the polymeric fibre coating, increases. K_{fs} is therefore dependent on the ionic strength of the sample matrix. Ionic salts prescribed for variation of ionic strength are NaCl or Na_2SO_4.

7.1.4.5 Sample Volume

From equation 1 and 2 we can deduce that this factor should not influence equilibrium times. Naturally, the sensitivity of an analysis could be improved with larger sample volumes.

7.1.4.6 Adsorption temperature

As discussed previously, the adsorption temperature of the sample matrix influences the kinetics of adsorption of the analyte. The dependency of the partitioning coefficients on temperature therefore allows for an optimum extraction temperature for the analyte. It is however important to realise that an increase in temperature beyond the optimum conditions, would result in a reduction in partitioning coefficients, with a consequent decrease in the amount of analyte extracted.

7.1.4.7 Desorption temperature

Since the extraction process is based on adsorption of the analyte onto the fibre at relatively low temperatures and desorption from the fibre at relatively high temperatures, the high temperature of a GC injector block (ca. 200°C) is ideal for desorption of the analyte followed by direct GC analysis. Temperature ranges and recommended desorption temperatures have been suggested for each type of fibre available (Eisert, 1996).

7.1.4.8 Matrix Effects

SPME has proven to be less effective when applied for environmental analysis. The observed deteriorated efficiency was ascribed to the competition for absorption onto the fibre of foreign compounds in the sample matrix. The fibre selected for a specific analysis should be selective toward the specific analyte to be analised.

7.1.4.9 Polymeric Fibre

As mentioned in Chapter 5, a number of fibres are available for the analysis of different analytes. Polarity and fibre thickness determine the application of each fibre. New fibres are being developed continuously and the trend seems to move in the direction of custom-made fibres for specific groups of analytes.

7.2 OPTIMISATION OF SPME FOR ANALYSIS OF $CHCl_3$

Since various factors (7.1.4.1-7.1.4.9) have an influence on SPME, this analytical method had to be optimised for optimal extraction of THMs from samples and ultimately the THMFP calculations (See Chapter 5 & 6).

Factorial design optimisation experiments were used to determine the significant factors. All preliminary experiments for THMFP determinations were performed by monitoring only the production of $CHCl_3$ after chlorination.

7.2.1 Experimental Optimisation of SPME

The experimental conditions of the chlorination process restricted some of the factors mentioned previously (See Chapter 5). Factors relevant to the THMFP analysis were identified and optimised with respect to the production of $CHCl_3$, utilising a 2^4 factorial design.

7.2.1.1 Factorial Design 1

7.2.1.1.1 Objective

A 2^4 factorial design was employed to investigate the effect of variation of certain factors on the $CHCl_3$ extraction efficiency as the measured response.

7.2.1.1.2 Procedure

As discussed previously, the utilisation pre-defined conditions are advised for SPME analysis of specific groups of analytes. Consequently the following factors were fixed at set conditions for the analysis of THMs:

Constant factors:

- Agitation: Samples were stirred during extraction, thereby reducing the equilibrium time considerably.
- Extraction matrix: Extraction from the headspace above the sample matrix was employed.
- Sample volume: 4mL vials were used with a sample volume of 1mL to allow for headspace analysis.
- Fibre: A 100 μm PDMS fibre was used for extraction of VOCs.

The following factors were selected for optimisation in the factorial design:

Varied Factors:

- Desorption temperature
- Extraction temperature
- Extraction time
- pH

The response selected for the factorial design was the peak area obtained for the $CHCl_3$ peak.

General Experimental Conditions

Analyte	:	50 mg/L $CHCl_3$ stock solution
SPME fibre	:	100µm PDMS fibre
Sample matrix pH	:	Table 7.1
Sample volume	:	1mL
Agitation	:	Magnetically stirred (250 rpm)
Extraction matrix	:	Headspace
Extraction time	:	Table 7.1
Extraction temperature	:	Table 7.1
Desorption temperature	:	Table 7.1
Response	:	Peak Area of $CHCl_3$

Table 7.1: Factorial Design Matrix

Run	Factors			
	Desorption Temp. (°C)	Extraction Temp. (°C)	Extraction Time (min)	pH
1	200	20	10	3
2	200	20	10	12
3	200	20	30	3
4	200	20	30	12
5	200	50	10	3
6	200	50	10	12
7	200	50	30	3
8	200	50	30	12
9	270	20	10	3
10	270	20	10	12
11	270	20	30	3
12	270	20	30	12
13	270	50	10	3
14	270	50	10	12
15	270	50	30	3
16	270	50	30	12

Analysis of $CHCl_3$ was done with SPME coupled to GC/MS. Peak areas were reported as TIC.min.

7.2.1.1.3 Results and Discussion

$CHCl_3$ peak areas are summarised in Table 7.2.

These results were interpreted using the STATISTICA package.

Table 7.2: Factorial Design Response Values

Run	$CHCl_3$ Peak area (TIC.min)	Run	$CHCl_3$ Peak area (TIC.min)
1	4633311	9	4529395
2	4898494	10	4663280
3	5863563	11	5128126
4	5420441	12	5102006
5	16737269	13	19446228
6	19687878	14	24476766
7	23569980	15	21491592
8	23353542	16	19885546

Table 7.3: ANOVA results

Factor	Null-hypothesis probability
Desorption temperature (1)	0.650
Extraction temperature (2)	**0.000**
Extraction time (3)	0.121
pH (4)	0.692
1 by 2 interaction	0.964
1 by 3 interaction	**0.072**
1 by 4 interaction	0.613
2 by 3 interaction	0.781
2 by 4 interaction	0.266
3 by 4 interaction	0.346

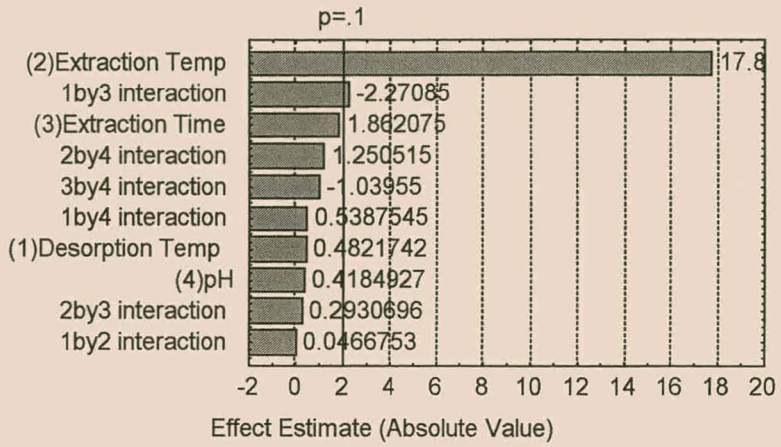

Figure 7.2: Pareto Chart

Conclusions:

- From the results in Table 7.3, it could be deduced that only the extraction temperature and the 2-way interaction between the desorption temperature and extraction time were significant. The variations of the other factors proved to be insignificant in terms of their effects on the response measured.

- The Pareto chart illustrated very clearly that the effect of an increase in the extraction temperature on the response measured dominated the entire optimisation. This observation is in accordance with the Pareto Principle.

- It was therefore concluded that the only factor exerting a significant influence on the response measured, was the variation in adsorption temperature. As discussed earlier, an increase in this factor would nullify the kinetic limitations of the diffusion of the analyte to the polymeric coating of the fibre.

- Since the desorption temperature did not play a significant role, it was decided to restrict this factor to its lowest level, i.e. 200°C, thereby limiting exposure to high temperatures, hence preventing premature fibre decomposition.

- An increase in pH of the sample matrix indicated a small positive effect on the response measured. This suited the analytical method for analysis of THMs very

well, since the sample matrix was buffered at pH 9.2 for the duration of the chlorination process prior to the analysis of THMs.

7.2.1.2 Second Factorial Design

7.2.1.2.1 Objective

A fractional factorial experiment was executed, and the results combined with a fractional factorial section from the previous factorial design (Run 1-8). This was done to investigate the effect of variation in ionic strength of the sample matrix, together with extraction temperature, extraction time and pH, on the extraction efficiency. These 2 fractional factorial designs were combined to form a full 2^4 factorial design.

7.2.1.2.2 Procedure

The first 8 runs from the previous factorial design were incorporated into this factorial design. The significance of the 4 factors was investigated.

Varied factors:

- Ionic strength
- Extraction temperature
- Extraction time
- pH

General Experimental Conditions

Analyte	:	50 mg/L $CHCl_3$ stock solution (See Chapter 5)
SPME fibre	:	100μm PDMS fibre
Sample matrix pH	:	Table 7.4
Sample volume	:	1mL
Agitation	:	Magnetically stirred (250 rpm)
Extraction matrix	:	Headspace

Extraction time	:	Table 7.4
Extraction temperature	:	Table 7.4
Ionic strength	:	saturated with NaCl
Desorption temperature	:	200°C
Response	:	Peak Area of $CHCl_3$

The amount of NaCl required for a saturated solution at a specific temperature was obtained from Figure 7.3, namely

- 20°C : 0.36 g/mL
- 50°C : 0.37 g/mL

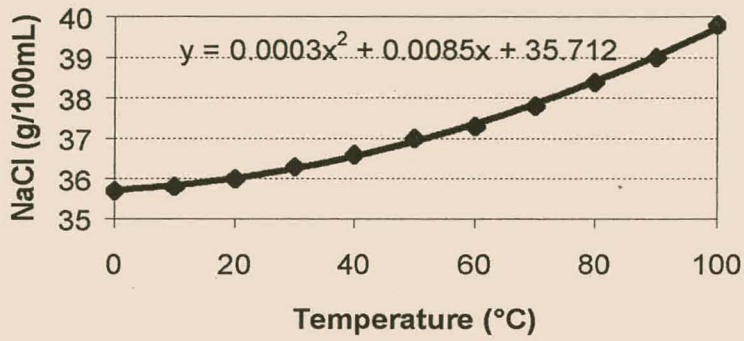

Figure 7.3: Solubility of NaCl as a function of temperature (Elvers, 1993, p.319)

Table 7.4: Factorial Design Matrix

Run	Factors			
	Ionic strength Saturation with NaCl (%)	Extraction temp (°C)	Extraction time (min)	pH
1	0	20	10	3
2	0	20	10	12
3	0	20	30	3
4	0	20	30	12
5	0	50	10	3
6	0	50	10	12
7	0	50	30	3
8	0	50	30	12
9	100	20	10	3
10	100	20	10	12
11	100	20	30	3
12	100	20	30	12
13	100	50	10	3
14	100	50	10	12
15	100	50	30	3
16	100	50	30	12

7.2.1.2.3 Results and Discussion

Results obtained are summarised in Table 7.5 below.

Table 7.5: Factorial Design Response Values

Run	$CHCl_3$ Peak area (TIC.min)	Run	$CHCl_3$ Peak area (TIC.min)
1	4633311	9	25270184
2	4898494	10	30540170
3	5863563	11	28811474
4	5420441	12	40537040
5	16737269	13	15554029
6	19687878	14	17841180
7	23569980	15	20534934
8	23353542	16	23486422

The quadratic model with 2-way interactions was selected for interpretation of optimisation data using STATISTICA.

$$Z = \beta_0 + \beta_1 X_1 + \beta_2 X_2 + \beta_{11} X_1^2 + \beta_{22} X_2^2 + \beta_{12} X_1 X_2$$

where,

Z: response function

X_1, X_2: experimental factors

β_0: intercept on response axis

β_1, β_2: gradient for each factor

β_{11}, β_{22}: coefficients for quadratic main effects

β_{12}: interaction term; combined effect of the two factors

Table 7.6: ANOVA results

Factor	Null-Hypothesis Probability
Extraction temperature (1)	0.158
Extraction time (2)	**0.014**
pH (3)	**0.098**
Ionic strength / Saturation with NaCl (4)	**0.000**
1 by 2 interaction	0.802
1 by 3 interaction	0.609
1 by 4 interaction	**0.000**
2 by 3 interaction	0.586
2 by 4 interaction	0.444
3 by 4 interaction	**0.088**

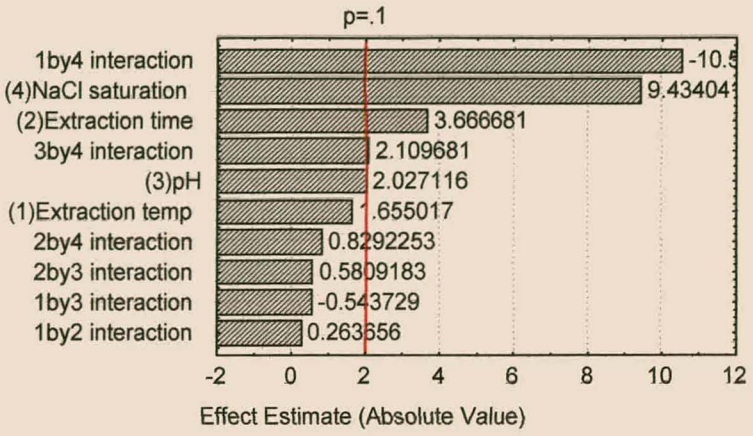

Figure 7.4: Pareto chart

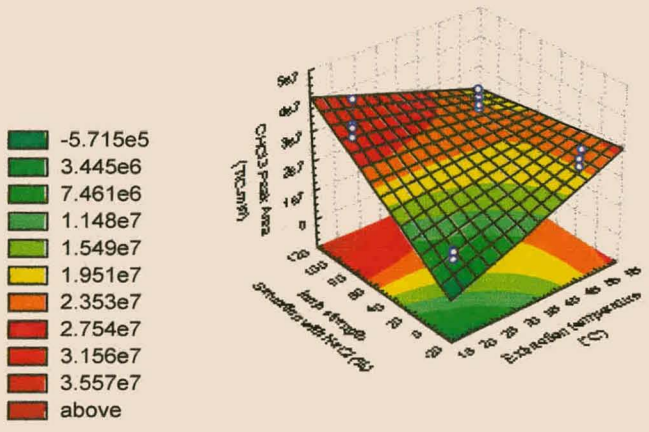

Figure 7.5: Response Surface

Conclusions:

- In contrast to the previous factorial design, the variation in ionic strength of the sample matrix resulted in more factors and 2-way interactions exerting a statistically significant effect on the measured response.

- Three factors, namely extraction time, pH and ionic strength were significant, with the ionic strength factor having the most significant effect when varied from 0% saturation with NaCl to 100% saturation with NaCl.

- The significance of the extraction temperature, from the previous factorial design, has been negated by the saturation effect with NaCl. This was confirmed with the very large 2-way interaction between these 2 factors. From Figure 7.5 it could therefore be concluded that, at low extraction temperature, an increase in ionic strength of the sample matrix would result in an improved response measurement, while at higher extraction temperature an increase in ionic strength had no significant effect on the response measured.

- An increase in the extraction time resulted in an improved response measured. This was anticipated in light of the time required for equilibrium to be reached between the relevant phases.

7.3 REPRODUCIBILITY

Reproducibility of an analytical method is of paramount importance when developing such a procedure for quantitative analysis.

7.3.1 Objective

The objective of this investigation was to determine the reproducibility of the analytical method in terms of the internal standard (CH_2Cl_2) used (See Chapter 5).

7.3.2 Procedure

The reproducibility was investigated for 3 scenarios, namely

- No agitation without NaCl saturation
- Agitation without NaCl saturation
- Agitation with NaCl saturation

General Experimental Conditions:

Analyte	:	50 mg/L CH_2Cl_2 stock solution
SPME fibre	:	100µm PDMS fibre
Sample matrix pH	:	Natural
Sample volume	:	1mL
Agitation	:	Table 7.7
Extraction matrix	:	Headspace
Extraction time	:	10 minutes
Extraction temperature	:	20°C
Ionic strength	:	Table 7.7
Desorption temperature	:	200°C
Instrumentation	:	SPME device coupled with Fisons GC/MS
Response	:	Peak Area of CH_2Cl_2

7.3.3 Results and Discussion

Reproducibility was expressed in terms of the standard deviation, as well as % relative standard deviation. These statistical calculations can be expressed by the following equations (Brewer, 1980):

$$s = \left(\frac{\sum d_i^2}{n-1} \right)^{1/2}$$

where,

s=standard deviation

$d = x_i - \bar{x}$

d=deviation

x_i=given result

$\bar{x}$ = mean

n=number of results

$$rsd(\%) = \frac{s}{\bar{x}}(100)$$

where,

rsd(%)=relative standard deviation, percent

Table 7.7: Reproducibility Results

Conditions	No agitation / No NaCl	Agitation / No NaCl	Agitation / NaCl
CH_2Cl_2 Peak area (TIC.min)	8.71×10^5	9.85×10^5	1.29×10^6
	1.03×10^6	1.03×10^6	1.28×10^6
	9.98×10^5	1.00×10^6	1.25×10^6
	9.36×10^5	9.82×10^5	1.29×10^6
	9.38×10^5	9.74×10^5	2.69×10^5
Average Peak area	9.54×10^5	9.94×10^5	1.27×10^6
STD deviation	6.06×10^4	2.15×10^4	1.48×10^4
%RSD	6.35	2.16	1.16

Conclusion:

- Relatively low % RSD values were obtained (See Table 7.7). A value lower than 10% is acceptable.

7.4 CONCLUSIONS

From the reproducibility test, it can be deduced that SPME, when employed correctly, can be used for quantitative analysis. Experimental design optimisation proved to be an acceptable approach for ascertaining the most efficient conditions for SPME analysis.

From the factorial design results produced, the following conditions were selected for the monitoring of the amount of $CHCl_3$ produced:

- Extraction matrix=headspace
- pH=9.12 (determined by borate buffer used in chlorination process)
- agitation=magnetic stirring
- sample volume=1 mL
- extraction time=30 minutes
- extraction temperature=20°C
- ionic strength=saturation with NaCl (3.6 g/mL)
- desorption temperature=200°C

REFERENCES

Brewer S. (1980) Solving Problems in Analytical Chemistry. John Wiley & Sons, Inc.

Eisert R., Levsen K. (1996) Solid-phase microextraction coupled to gas chromatography: a new method for analysis of organics in water. *Journal of Chromatography A* 733 p.143-157

Elvers B., Hawkins S., Russey W., Schulz G. (1993) Ullmann's Encyclopedia of Industrial Chemistry, Fifth Completely Revised Edition, **A24**, p.319

Gòrecki T., Boyd-Boland A., Zhang Z., Pawliszyn J. (1996) 1995 McBryde Medal Award Lecture: Solid phase microextraction – a unique tool for chemical measurements. *Can. J. Chem.* **74** p. 1297-1308

Poole C.F., Poole S.K. (1991) Chromatography Today. Elsevier Science Publishers

Zhang Z., Pawliszyn J. (1993) Headspace Solid-Phase Microextraction. *Anal.Chem.* **65** p.1843-1852

Zhang Z., Yang M.J., Pawliszyn J. (1994) Solid-Phase Microextraction: A Solvent-Free Alternative for Sampling Preparation. *Analytical Chemistry* 66 No.10 p.844A-853A

CHAPTER 8

THM Analytical Protocol

8.1 INTRODUCTION

From the experiments conducted during the optimisation of SPME for the adsorption and GC analysis of $CHCl_3$, it became apparent that the method had the potential to be developed into a protocol for the analysis of treated water. The following four THM species were investigated for inclusion in the protocol:

- chloroform ($CHCl_3$)
- bromodichloromethane ($CHCl_2Br$)
- dibromochloromethane ($CHClBr_2$)
- bromoform ($CHBr_3$)

Due to the carcinogenic nature of these compounds, a progressive trend towards more stringent drinking water standards with respect to the maximum acceptable concentration (MAC) of total THM (TTHM) content in drinking water, have been observed.

In 1992 the World Health Organisation (WHO) adopted the following MAC values for THMs (Table 8.1):

Table 8.1: MAC values for THMs (Casey, 1997)

THMs	MAC value (µg/L)
$CHCl_3$	200
$CHCl_2Br$	60
$CHClBr_2$	100
$CHBr_3$	100

A further restriction was imposed. The WHO demanded that the sum of the ratios of the species to their respective MAC values should be less than one. The USEPA finally adopted a MAC of 80 µg/L for TTHM with the option of reducing it to a level of 40 µg/L.

The aim of this part of the thesis was therefore the development of a method for the determination of the THMFP for treated water samples. This would facilitate the evaluation of the efficiency of water treatment processes with respect to the amount of THMs likely to form as a result of the disinfection process. The following aspects required investigation:

- quenching of the chlorination process prior to the determination of THMFP
- linearity of the chromatographic response over the entire concentration range for the four selected THM species
- factors influencing the adsorption of volatiles onto the SPME fibre
- refinement of the chlorination process for raw and treated water samples
- the protocol for analysis of THMs had to be tested

8.2 QUENCHING OF THE CHLORINATION PROCESS

Reproducible THMFP results required the quenching of the chlorination process prior to the analysis of THMs. Ascorbic acid was suggested for quenching the chlorination process whereby excess free chlorine is removed (Van Steenderen, 1988). This is based on a chemical reaction between the two compounds. To avoid the introduction of excess ascorbic acid in the test water, it was necessary to determine the minimum amount of ascorbic acid required for removing a specified amount of free active chlorine.

8.2.1 Objective

The objective of this investigation was therefore to determine the relationship between the amount of concentrated ascorbic acid required rendering a specific concentration of free Cl_2 inactive in the sample matrix.

8.2.2 Procedure

General Experimental Conditions

Cl_2 concentration : 109 mg/L; 66.5 mg/L; 43.6 mg/L; 24.5 mg/L; 10.9 mg/L
Ascorbic Acid concentration : 30% ($^{M}/_{V}$)

Chlorine water samples of varying concentration were prepared and treated with specified volumes of 30% ascorbic acid solution. The DPD-titration method (5.1.3.2) was employed to determine whether all the free active chlorine was destroyed after the addition of ascorbic acid.

8.2.3 Results and Discussion

The following relationship was established (Figure 8.1):

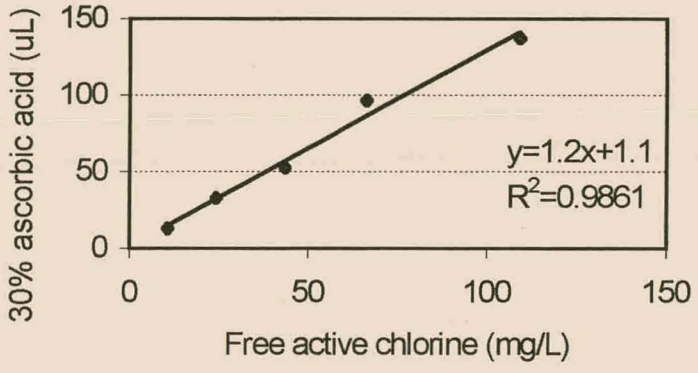

Figure 8.1: Relationship between ascorbic acid and free active chlorine

Remarks:

- From Figure 8.1 the amount of 30% ascorbic acid required to remove a specified amount of free active chlorine from solution could easily be calculated. (See equation 1)

- The following linear relationship was derived from it:
  30% ascorbic acid (μL) = 1.2 x free active Cl_2 (mg/L) + 1.1

- In order to avoid a DPD titration on each sample after chlorination, it was decided to treat all chlorinated water samples with an ascorbic acid volume equivalent to the initial concentration of free chlorine. Thereby any remaining free chlorine would be removed.

8.3 THM CALIBRATIONS

8.3.1 Objective

The linearity of the response as measured over the entire concentration range for the four THM species had to be investigated. Calibration data were therefore acquired for the THM species under investigation. Linearity would enable one to use equation 5 (5.2.3) for the calculation of the concentration of the relevant THM species without having to calibrate the SPME device for each sample under investigation.

8.3.2 Procedure

General Experimental conditions:

THM conc. (stock solution)	:	50 mg/L THM species (5.3.7)
THM conc. (calibration standards)	:	See Table 8.2 below
Sample volume	:	20 mL
Dilution matrix	:	distilled water
Instrumentation	:	SPME device equipped with 100μm PDMS fibre
	:	Fisons GC/MS

Table 8.2: THM calibration series

THM species	Concentration (μg/L)				
$CHCl_3$	150	50	20	5	
$CHCl_2Br$	100	50	20	10	5
$CHClBr_2$	100	50	20	10	5
$CHBr_3$	50	15	10	5	

SPME experimental conditions:

Sample volume	:	20 mL
Adsorption time	:	30 minutes
Adsorption temperature	:	20 °C
Adsorption agitation	:	magnetically stirred
Adsorption matrix	:	immersed in solution
Desorption temperature	:	200 °C

Desorption time	:	duration of run
Fibre type	:	polydimethylsiloxane fibre

Each peak was integrated electronically and the concentration was reported in terms of peak area (TIC.min).

8.3.3 Results and Discussion

The following calibration results were obtained for the 4 THM species (Table 8.3):

Table 8.3: Calibration data

$CHCl_3$		$CHCl_2Br$		$CHClBr_2$		$CHBr_3$	
Conc. µg/L	Peak Area (TIC.min)	Conc. µg/L	Peak Area (TIC.min)	Conc. µg/L	Peak Area (TIC.min)	Conc. µg/L	Peak Area (TIC.min)
150	604263	100	139238	100	115817	50	585995
50	185469	50	72450	50	54362	15	182625
20	90510	20	34572	20	24948	10	119655
5	35648	10	20624	10	12039	5	63902
		5	9738	5	8439		

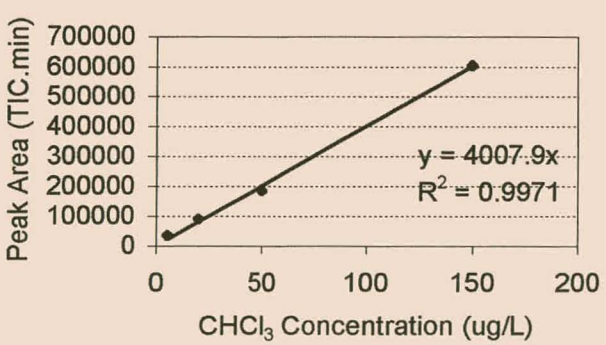

Figure 8.2(a): Calibration curve of $CHCl_3$

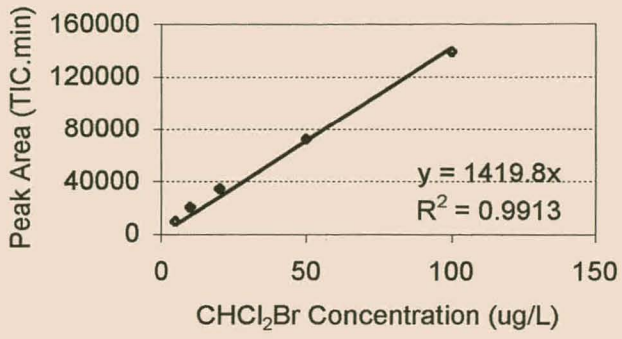

Figure 8.2(b): Calibration curve of $CHCl_2Br$

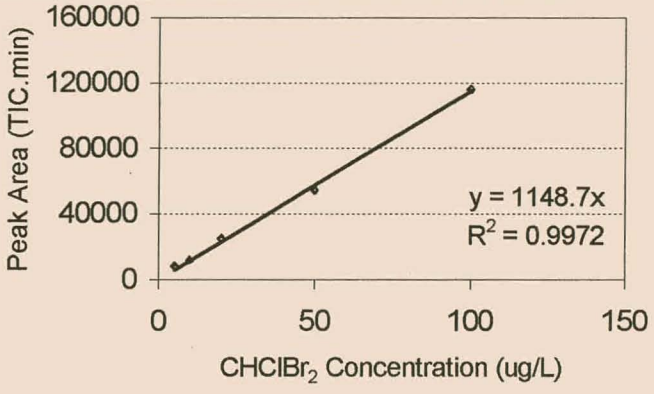

Figure 8.2(c): Calibration curve of $CHClBr_2$

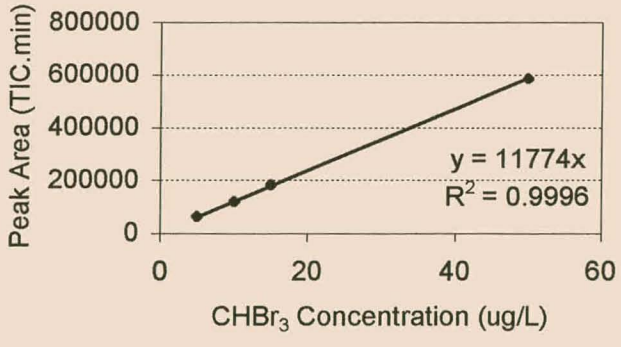

Figure 8.2(d): Calibration curve of $CHBr_3$

Remarks:

- The above calibration curves clearly indicate linearity for all four THM species over the concentration range under investigation.

- This result allows for the accurate determination of the relevant THM concentrations by means of the method of spiking with an internal standard. Equation 5 (5.2.3) could therefore be used for the calculation of the THM concentrations, without calibration prior to each sample analysis. CH_2Cl_2 was chosen as internal standard, since its peak in the gas chromatogram was well separated from the rest.

8.4 SPME EXTRACTION OPTIMISATION

8.4.1 Influence of foreign matter in the analyte matrix

8.4.1.1 Objective

This investigation had a dual purpose. Firstly the effect of foreign matter, such as NOM, on the effectiveness of the extraction of THMs from the analyte matrix, was investigated. This was achieved by comparing the linearity of calibration curves of the THM species for both the distilled water matrix and the raw water matrix scenario. Secondly it was investigated whether the presence of all 4 THM species in the same matrix affected the linearity of the individual calibration curves.

8.4.1.2 Procedure

General Experimental conditions:

THM stock solution	:	4 x 1 mL of 50 mg/L THM stock solution diluted to 200 mL
Calibration series	:	25 µg/L; 50 µg/L; 75 µg/L; 100 µg/L; 125 µg/L; 150 µg/L
Sample volume	:	20 mL
Dilution matrix	:	distilled water
	:	Swellendam raw water
Internal Standard	:	CH_2Cl_2
Instrumentation	:	SPME device equipped with 100µm PDMS fibre
	:	Fisons GC/MS

A synthetic (distilled water) and real (raw water) matrix were used for the preparation of the calibration solutions from the 50 mg/L THM stock solutions (See 5.3.7). 1 mL of each of the four 50 mg/L standard THM solutions was added to a 200 mL volumetric flask and diluted to 200 mL with the appropriate dilution matrix for the preparation of the additional stock solutions. Calibration standards were prepared from these stock solutions. All four THMs were therefore analysed simultaneously from the same calibration solution. The SPME experimental conditions were similar to that used in 8.3.1 above. Each sample was buffered at pH 9.18 with borate buffer. A micro syringe was used for the addition of the internal standard solution.

8.4.1.3 Results and Discussion

Results are summarised in Table 8.4(a) and (b).

Table 8.4(a): Peak Areas of Raw Water Matrix (ND: Not Detected)

[THM] (µg/L)	Peak Area $CHCl_3$	Peak Area $CHCl_2Br$	Peak Area $CHClBr_2$	Peak Area $CHBr_3$	Peak Area CH_2Cl_2
0	ND	ND	ND	ND	1168455
25	168594	141882	204851	540488	1154205
50	306684	258773	438557	1313197	1220418
75	509785	401042	646562	2105562	1180234
100	624618	617444	962286	2219028	1256410
125	705299	658550	939479	2098089	1131247
150	1065589	1103494	1742025	4347874	1147908

Table 8.4(b): Peak Areas of Distilled Water Matrix (ND: Not Detected)

[THM] (µg/L)	Peak Area $CHCl_3$	Peak Area $CHCl_2Br$	Peak Area $CHClBr_2$	Peak Area $CHBr_3$	Peak Area CH_2Cl_2
0	ND	ND	ND	ND	1178641
25	175455	135282	184020	479763	1126824
50	361077	313693	493284	1070065	1230433
75	408639	390756	638942	1406225	1274904
100	722763	631120	976096	1898877	1196700
125	649045	691511	962009	2137076	1105976
150	1069425	1052866	1562056	3038998	1272646

Curves were generated for both matrix scenarios (Figure 8.3(a)-(d)).

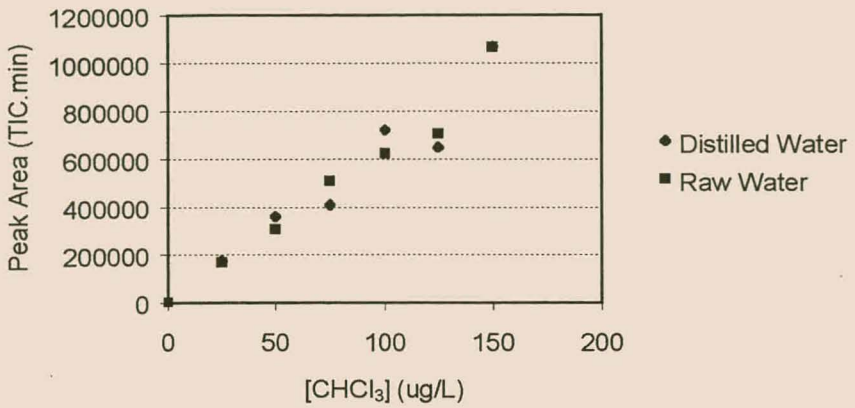

Figure 8.3(a): Chloroform Calibration

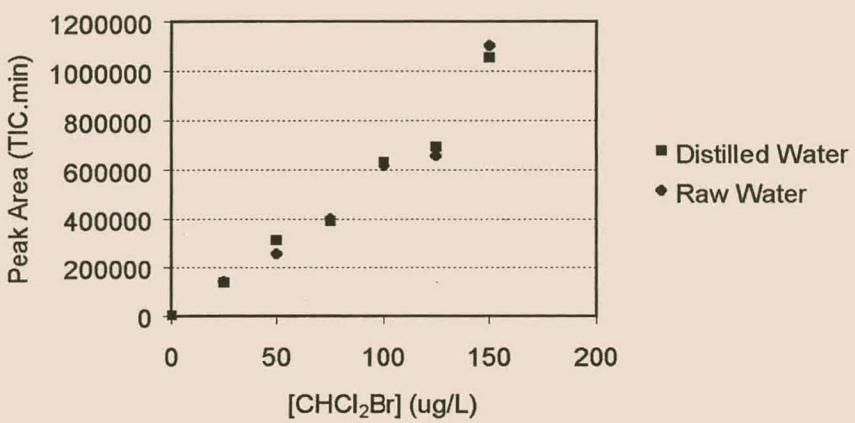

Figure 8.3(b): Bromodichloromethane Calibration

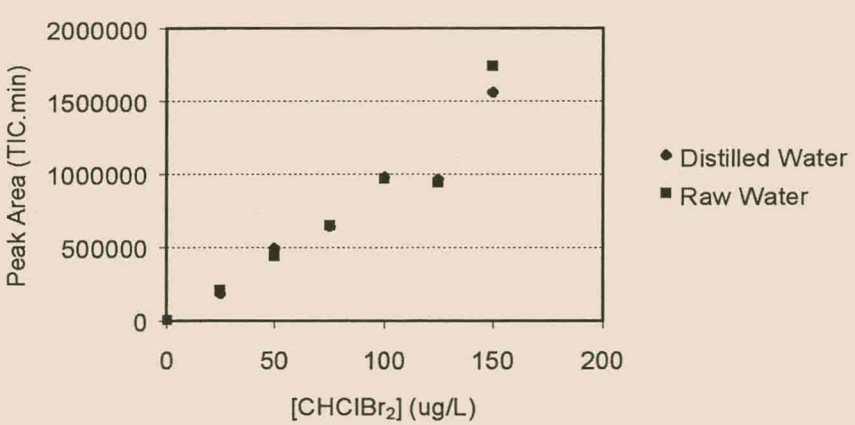

Figure 8.3(c): Dibromochloromethane Calibration

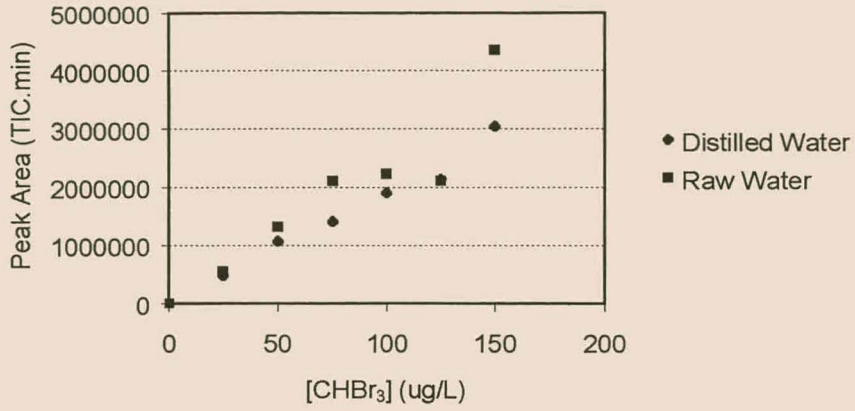

Figure 8.3(d): Bromoform Calibration

Remarks:

- One can conclude that the analyte matrix had no influence on the extraction efficiency of the THMs by means of SPME.
- The presence of more than one THM species in the sample matrix did not effect the linearity of the calibration curves.
- The development of an analytical protocol (using synthetic samples) for the analysis of analytes from an unknown matrix is therefore feasible.

8.5 SPME EXTRACTION OPTIMISATION OF THMs IN MULTI COMPONENT SYSTEMS

The THMs under investigation should demonstrate similar optimised conditions for SPME adsorption and analysis. However, hasty extrapolation of the $CHCl_3$ adsorption results (from the previous chapter), could yield incorrect results. An approach similar to that of the $CHCl_3$ optimisation was therefore applied to determine the optimal conditions for the effective extraction of THMs in a multi component system.

8.5.1 Orthogonal Array

8.5.1.1 Objective

During this study a statistical experimental design approach was followed to optimise the SPME extraction process. An 8.4.2.3 orthogonal array, consisting of 8 runs, 4 factors, 2 levels and a strength of 3, was used to investigate the effect of various factors on the extraction efficiency of the SPME fibre.

8.5.1.2 Procedure

General Experimental conditions:

THM stock solution	:	Standard THM mixture (5.3.7)
Sample volume	:	20 mL
Instrumentation	:	SPME device equipped with 100μm PDMS fibre
	:	Fisons GC/MS

Although many factors could potentially influence the extraction efficiency, not all were simultaneously optimised. Several factors were kept at constant levels, either for convenience, or because of experimental constraints resulting from the chlorination process.

Constant Factors:

- agitation by means of magnetically stirring the sample (250 rpm)
- sample volume = 20 mL (sample bottle restriction)
- pH = 9.18 (conditions for chlorination process)
- desorption temperature = 200 °C (7.2.1.1.3)

Larger sample volumes were used since extraction of THMs occurred directly from the chlorination sample bottle.

Variable Factors:

- Adsorption temperature
- Adsorption time
- Saturation with NaCl
- Extraction matrix: headspace analysis versus immersion

The amount of NaCl required for saturation of the samples at the selected temperatures was calculated from the solubility curve of NaCl (Chapter 7, Figure 7.2), namely:

- 20°C : 7.2 g/20mL
- 50°C : 7.4 g/20mL

Table 8.5 contains the orthogonal array design matrix for the above optimisation procedure.

The response was measured in terms of peak area of each THM species, expressed in terms of TIC.min.

Table 8.5: Orthogonal Array Design Matrix

Run	Factors			
	Ads. Temp. (°C)	Ads. Time (min)	NaCl (%)	Headspace (H) / Immersion (I)
1	20	30	0	H
2	20	30	100	I
3	20	60	0	I
4	20	60	100	H
5	50	30	0	I
6	50	30	100	H
7	50	60	0	H
8	50	60	100	I

The standardised GC/MS method (5.2.2) was used for the determination of THMs.

8.5.1.3 Results and Discussion

The following response values were obtained for the experimental procedure (Table 8.6).

Table 8.6: Response measurements

Run	Response: Peak Area (TIC.min)			
	$CHCl_3$	$CHCl_2Br$	$CHClBr_2$	$CHBr_3$
1	456471	803463	1517618	481736
2	1902237	7267574	9768754	2101376
3	277743	1101243	1534753	430237
4	2839544	6401410	9581642	1875560
5	395620	1191422	1329928	1054832
6	2251235	6082606	9658907	2100481
7	513171	1317404	2003983	550891
8	987993	3598833	5257197	1300883

The data obtained was interpreted by means of STATISTICA V5.0. Since no interactions were revealed in the quadratic model, a linear model was employed for the interpretation of data.

Table 8.7: ANOVA Results

Factor	Response: p-value			
	$CHCl_3$	$CHCl_2Br$	$CHClBr_2$	$CHBr_3$
Ads. Temp.	0.434	0.415	0.431	0.912
Ads. Time	0.810	0.474	0.457	0.205
NaCl saturation	0.0231	0.0132	0.00887	0.0158
Ads. Matrix	0.189	0.714	0.365	0.909

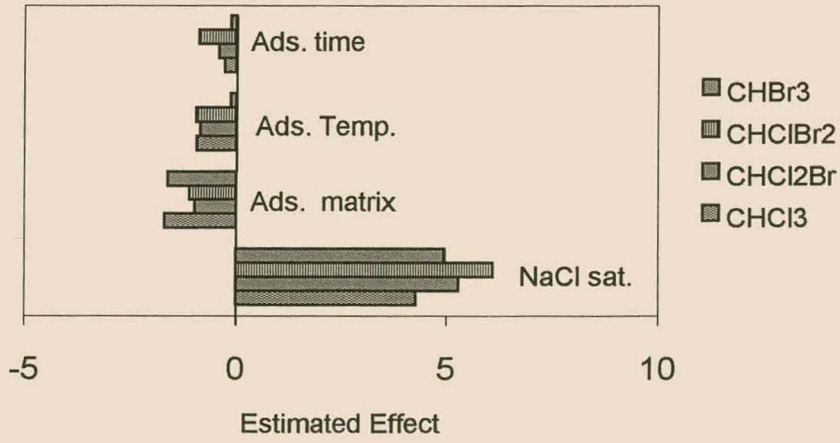

Figure 8.4: Pareto Chart

Remarks:

- From the ANOVA table, the dominant significance of saturating the samples with NaCl was clear. The other factors showed no significance within the experimental design.

- The presence of a salt such as NaCl in the analyte matrix, increases the ionic strength of the water, thereby increasing the partitioning of organic compounds into the PDMS fibre (7.1.4.4).

- The Pareto chart (Figure 8.4) confirmed this finding. However, from the Pareto chart it also became apparent that saturation with NaCl was the only factor, which positively affected the response. The other factors, although not having a significant effect on the response, all indicate a small negative influence on the response when increasing the factor value from the lower to upper level.

- The negative effect caused by changing the adsorption matrix from the headspace to the aqueous matrix, confirmed the reduction in distribution constants of the THMs for the liquid and gas phases, as determined by Pawliszyn and co-workers (Eisert, 1996) (See Table 8.8).

- From 7.2.1.1.3 it is known that an increase in adsorption temperature would volatilise more of THMs, thereby resulting in increased peak areas. However, saturation with NaCl causes the opposite to occur. The estimated effect, as indicated by the Pareto chart, was therefore negative. The thermodynamic explanation for this is given in Atkins, 1978, p.216. When an involatile solid is added to a volatile solvent, the entropy in the solvent is raised and the tendency of the solvent to evaporate is decreased. The colligative effect of sodium chloride dissolved in water in elavation of the boiling point and depression of the freezing point is supported by freezing point depression data in *The Chemical Rubber Company (1968)*.

- In general, it was concluded that the 4 THM species responded in a similar fashion toward variation in the levels of experimental factors. Conclusions drawn from the 2^4 factorial designs (7.2.1.1 and 7.2.1.2) could therefore be extrapolated from $CHCl_3$ to the other species.

Table 8.8: Distribution Constants (K_{ow}: octanol-water partitioning coefficient; K_{aq}: aqueous-fibre partitioning constant; K_g: gaseous-fibre partitioning constant) (Eisert, 1996)

THMs	Log K_{ow}	Log K_{aq}	Log K_g
$CHCl_3$	1.97	2.6	2.6
$CHCl_2Br$	1.88	2.7	3.4
$CHClBr_2$	2.08	3.5	3.0
$CHBr_3$	2.30	2.8	3.5

The predominant effect of the saturation of the aqueous matrix with NaCl precluded the true estimation of the effects of the other factors. Hence, it was decided to optimise these factors by varying them one-at-a-time.

8.5.2 Agitation

It was found that without extensive stirring of aqueous solutions (static case), the time for reaching equilibrium could take very long (Eisert, 1996). It was therefore decided to use extensive stirring (dynamic case) during adsorption to ensure short equilibrium times. This scenario is favorable for both headspace and immersion adsorption.

8.5.2.1 Objective

The aim of this investigation was to determine whether a variation in the stir speed would influence the efficiency of the extraction process.

8.5.2.2 Procedure

General Experimental Conditions:

THM stock solution	:	Standard THM mixture (5.3.7)
Sample volume	:	20 mL
Salt	:	NaCl
Instrumentation	:	SPME device equipped with 100µm PDMS fibre
	:	Fisons GC/MS

SPME Experimental Conditions:

- sample volume : 20 mL
- adsorption time : 30 minutes
- adsorption temperature : 20 °C
- adsorption agitation : 0 rpm; 250 rpm; 500 rpm; 750 rpm; 1000 rpm
- adsorption matrix : immersed in solution
- desorption temperature : 200 °C
- desorption time : 2 minutes
- fibre type : PDMS fibre

The experiment was conducted for two extreme ionic strength scenarios namely one with saturation with NaCl and the other without any addition of salt. An equilibration period of 5 minutes was maintained before extracting the THMs. The response was expressed in terms of peak area for the relevant THM species.

8.5.2.3 Results and Discussion

Response measurements (peak areas) for the relevant THMs are summarised in Table 8.9(a)-(b) and the stir speed effect in Figures 8.5(a) and (b).

Table 8.9(a): Response measurements: No salt added

Stir speed (rpm)	Peak Area (TIC.min) $CHCl_3$	Peak Area (TIC.min) $CHCl_2Br$	Peak Area (TIC.min) $CHClBr_2$	Peak Area (TIC.min) $CHBr_3$
0	583999	1712161	2397697	620468
250	608842	1420455	2258181	527002
500	626383	1482431	2364753	497209
750	559375	1515297	2289078	483317
1000	648289	1417332	2220201	475598

Table 8.9(b): Response measurements: Salt saturation

Stir speed (rpm)	Peak Area (TIC.min) $CHCl_3$	Peak Area (TIC.min) $CHCl_2Br$	Peak Area (TIC.min) $CHClBr_2$	Peak Area (TIC.min) $CHBr_3$
0	1369557	3730367	7261031	1588777
250	1700678	4949196	9617454	2495228
500	1668871	4619704	9049920	2155017
750	1921375	4909831	9360515	2193699
1000	2008694	5114804	9658788	2311248

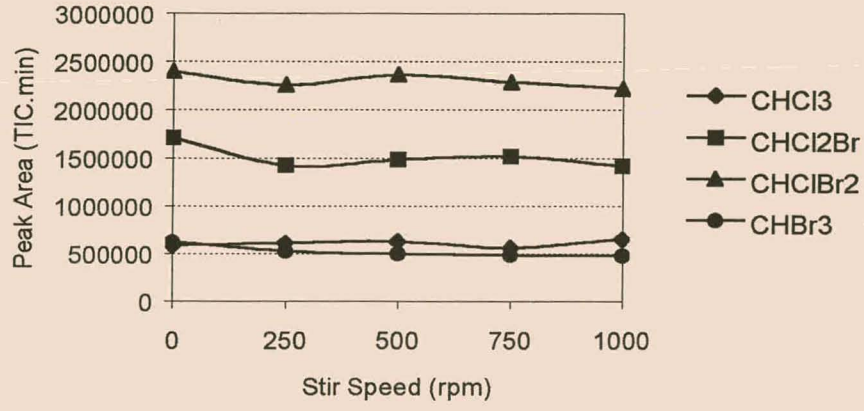

Figure 8.5(a): Stir speed effect: No salt added

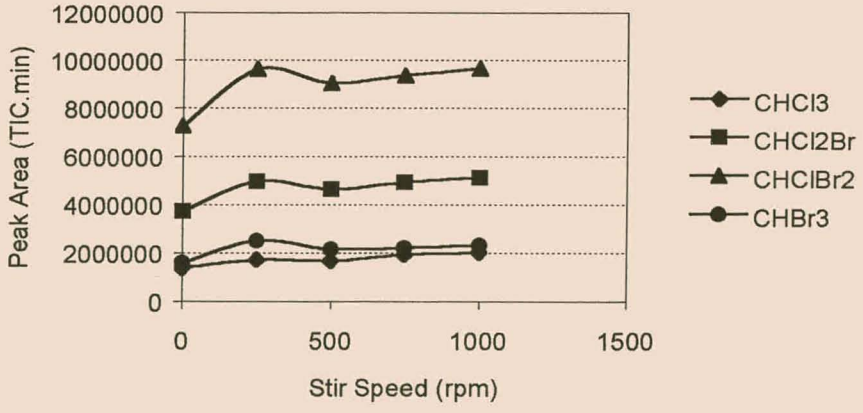

Figure 8.5(b): Stir speed effect: Salt saturation

Remarks:

- From Figure 8.5 (a) and (b) it was evident that stir speed only played a significant role in the salt saturated solution. A plateau peak area was reached after approximately 250 rpm stir speed.

- According to Eisert *et.al.* the amount of analyte adsorbed onto the fibre could, in some instances, be increased with a factor of 5 compared to that of the unstirred sample.

8.5.3 Ionic Strength Optimisation

Since the addition of salt to the aqueous medium increased the partitioning coefficients for the extraction of polar organic compounds onto the polymeric fibre coating (Zhang, 1994), it was important to verify this potentially positive effect for the analysis of THMs.

8.5.3.1 Objective

This study was devoted to investigate the effect of an increase in ionic strength of the aqueous matrix on the partitioning of polar organic compounds into the polymer coating. The effect of NaCl saturation on a standard THM mixture was investigated.

8.5.3.2 Procedure

General Experimental Conditions

THM stock solution	:	Standard THM mixture (5.3.7)
Sample Volume	:	20 mL
Instrumentation	:	SPME unit equipped with 100µm PDMS fibre
	:	Fisons GC/MS

SPME Experimental Conditions

Sample volume	:	20 mL
Adsorption time	:	20 min

Adsorption temp	:	20°C
Stir speed	:	750 rpm
Salt	:	See Table 7
Desorption temperature	:	200°C
Desorption time	:	10 min
Cryo trapping	:	2 min

Each sample was allowed an equilibration time of 5 minutes before extraction of the volatiles by means of the SPME procedure. The response was expressed in terms of peak area for the relevant THM species.

Table 8.10: Ionic Strength Distribution for NaCl

NaCl g/20mL	Ionic strength (M)
0	0
0.8	0.68
1.6	1.37
2.4	2.05
3.2	2.74
4.0	3.42
4.8	4.11
5.6	4.79
6.4	5.48
7.4	6.16

8.5.3.3 Results and Discussion

The peak areas for the THMs are summarised in Table 8.11(a) and (b).

Table 8.11: Ionic strength investigation (NaCl)

Ionic strength (M)	Peak area (TIC.min) $CHCl_3$	Peak area (TIC.min) $CHCl_2Br$	Peak area (TIC.min) $CHClBr_2$	Peak area (TIC.min) $CHBr_3$
0	599098	1502225	2124819	603631
0.68	617118	1793517	2198763	512405
1.37	647339	1641806	2260940	567250
2.05	661162	1910388	2412464	597810
2.74	807808	2359087	2829969	629419
3.42	850961	2753418	3289259	898712
4.11	977812	2702092	3983441	943056
4.79	1213940	3128084	4383321	1144919
5.48	2123490	5987545	8306934	2034940
6.16	2869019	7670173	11297012	2673227

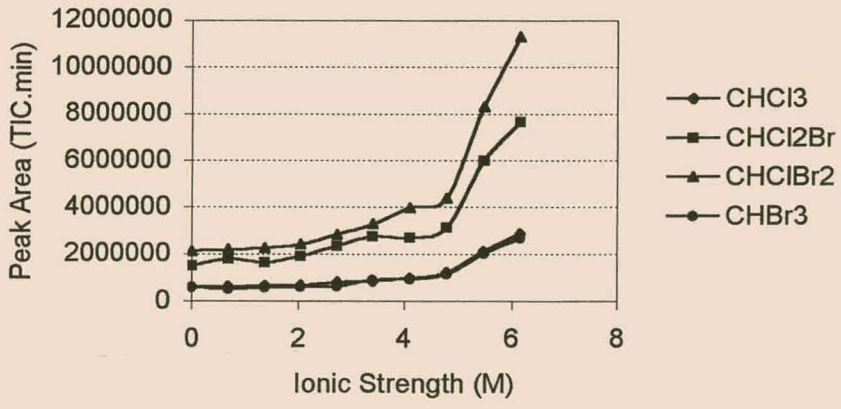

Figure 8.6: Ionic strength Effects (NaCl)

Remarks:

- From the above results, as well as Figure 8.6, it was concluded that an increase in ionic strength had a profound effect on the extraction efficiency of the analytes.

- These results corresponded well with results from in literature (Supelco Inc., 1996).

- It was obvious that the molecular mass of the THMs is not such an important factor, but the symmetry (charge distribution) well.

- Saturation of a synthetic sample with NaCl resulted in marked increased peak areas for all 4 THM species, which led to a significant improvement in sensitivity. This, however, could not be implemented for the following reason. Since salt had to be added to the sample bottle before the chlorination process was initiated, participation of ions in the chlorination process was inevitable. Bromide impurities (in the pro analisi sodium chloride) reacted with OCl^- species present in the chlorinated water by means of the following:

  $$OCl^- + Br^- \Leftrightarrow OBr^- + Cl^-$$

  Since OCl^- ion reacted with organic compounds to produce chlorinated disinfection by-products, OBr^- ion reacts in a similar fashion with the production of brominated by-products. A higher purity grade NaCl could solve the problem. That would however be very costly.

- The observation above is of substantial significance in water treatment by conventional coagulation and flocculation. It is crucial that the coagulation agents (e.g. $FeCl_3$) must be free of bromide. Otherwise additional brominated byproducts e.g. brominated THMs will be formed during chlorination.

8.5.4 Adsorption time

Although the literature (Eisert, 1996) suggests relatively short equilibrium times for both headspace and immersion analysis of THMs, the complex nature of treated water samples could alter this drastically.

8.5.4.1 Objective

Equilibrium times for optimal extraction of THMs was examined for both headspace and immersion analysis. This was determined for two scenarios, namely no salt added and saturation with salt.

8.5.4.2 Procedure

General Experimental Conditions

THM stock solution	:	Standard THM mixture (5.3.7)
Sample volume	:	20 mL
Instrumentation	:	SPME unit equipped with 100 μm PDMS fibre
	:	Fisons GC/MS

SPME Experimental Conditions

Sample volume	:	20 mL
Adsorption time	:	See Table 10
Adsorption temp	:	20°C
Stir speed	:	250 rpm
Salt	:	See Table 10
Desorption temperature	:	200°C
Desorption time	:	10 min
Cryo trapping	:	2 min

Table 8.13: Adsorption Times

Adsorption Time (min)			
Headspace / No Salt	Headspace / Salt	Immersion / No Salt	Immersion / Salt
1	2	1.5	1
5	5	5	5
10	10	10	10
20	20	20	20
30	30	30	30
60	60	60	60
120	120	120	120

An equilibrium period of 5 minutes was allowed before analysis.

8.5.4.3 Results and Discussion

As predicted by the orthogonal array, the solutions saturated with NaCl resulted in peak areas magnitudes larger compared to solutions containing no salt. Faster equilibrium times were, however, obtained with the solutions containing no salt (10 min) than with those saturated by NaCl (20 min.). (See Tables 8.14(a) and (b) and Figures 8.7(a)-(d))

Table 8.14(a): Adsorption time investigation (Headspace analysis)

Time (min)	NaCl (g/20mL)	Peak area $CHCl_3$	Peak area $CHCl_2Br$	Peak area $CHClBr_2$	Peak area $CHBr_3$
1	0	727815	1777272	2713525	698027
5	0	926878	1897688	3038886	820853
10	0	878764	2041770	3147118	868562
20	0	811606	2146075	3153464	856836
30	0	755351	1948136	2964547	672148
60	0	520853	1607284	1493201	481864
120	0	410764	1297199	2441651	757342
2	7.4	1613261	6126942	10515911	2325511
5	7.4	858515	4047687	8628343	1976086
10	7.4	1875988	6739982	12073703	2634376
20	7.4	2740821	8620979	13732065	2918339
30	7.4	2895580	8900957	14201940	3100177
60	7.4	3151498	9482490	15995435	3919599
120	7.4	2504861	7276714	11828333	2758533

Table 8.14(b): Adsorption time investigation (Immersion analysis)

Time (min)	NaCl (g/20mL)	Peak area $CHCl_3$	Peak area $CHCl_2Br$	Peak area $CHClBr_2$	Peak area $CHBr_3$
1.5	0	457306		1804487	324272
5	0	451446	1072061	2053980	368967
10	0	477594	1069713	2034405	416151
20	0	389936	1077833	2019551	396564
30	0	358293	938441	1899706	402926
60	0	305027	1045146	2132422	396492
120	0	337965	1347323	2197018	458125
1	7.4	433775	898695	1438751	309678
5	7.4	1280921	3151671	5126555	881357
10	7.4	1791286	4501743	7620768	1353555
20	7.4	1906734	5085256	6829855	1688427
30	7.4	2925110	6905725	10686708	2159851
60	7.4	1861927	7344346	11711824	2636722
120	7.4	1737750	6875287	11090034	2415140

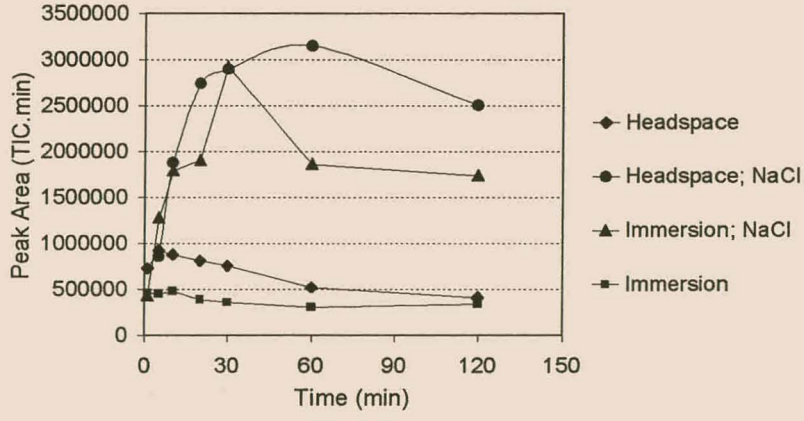

Figure 8.7(a): Peak areas for $CHCl_3$

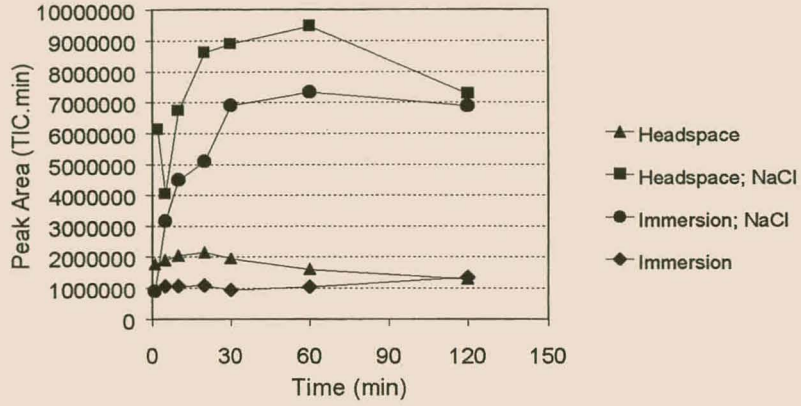

Figure 8.7(b): Peak areas for $CHCl_2Br$

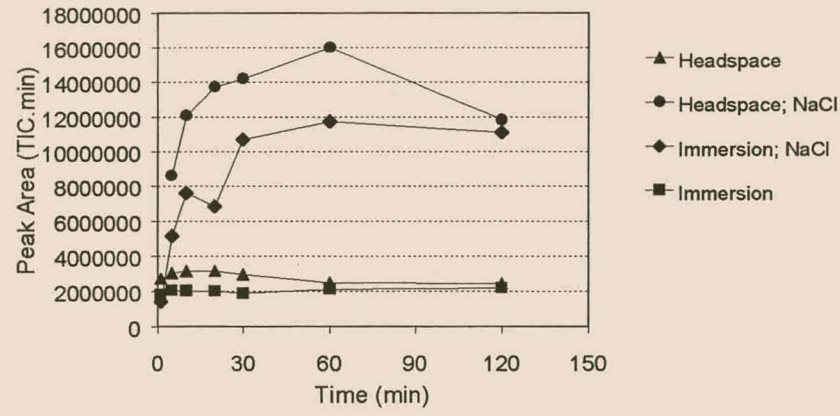

Figure 8.7(c): Peak areas for $CHClBr_2$

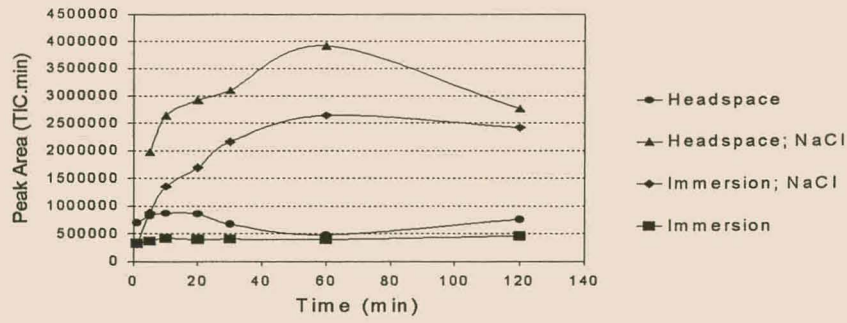

Figure 8.7(d): Peak areas for $CHBr_3$

Remarks:

From the graphic results above (Figure 8.7 (a)-(d)) the following conclusions can be drawn:

- Without salt saturation equilibrium is reached within 10 minutes for both the headspace and aqueous matrices. The headspace extraction is however more efficient, resulting in a larger mass transfer from the sample to the fibre coating.

- The process of salt saturation introduces additional ions into solution. This results in a longer equilibrium time (±20 min). The mass transfer of analyte for both headspace and aqueous medium was however markedly improved.

- Although the obvious choice for fast and effective adsorption is headspace extraction with salt saturation, a practical problem - especially when a large number of samples must be analised – cause this method to be impractical. The problem of saturating the solution in a closed vial with salt, after the chlorination period, remains unsolved. Headspace analysis without salt saturation was therefore opted for.

8.5.5 Analyte Volume

From equation (1) and (2) (See 7.1.4), it was deduced that sample volumes exerted no significant effect on the extraction efficiency of the SPME procedure.

During preliminary investigations SPME extractions of THMs from 1 mL samples were done. Calibration curves – not reported here – became highly non-linear at low concentrations. This was ascribed to a too small sample volume. It was therefore necessary to increase the sample volume to 20 mL.

8.5.6 SPME Desorption Optimisation

8.5.6.1 Desorption Temperature

In Chapter 7 it was concluded that an increase in desorption temperature had no significant effect on the efficiency of $CHCl_3$ analysis. Since the 4 THM species showed similar tendencies in the orthogonal array investigation, the conclusion concerning the desorption temperature for $CHCl_3$ was extrapolated to the remaining THM species. A desorption temperature of 200°C was therefore selected for THM analysis.

8.5.6.2 Desorption Time

8.5.6.2.1 Objective

THMs were cryo focussed at the beginning of the GC column for a period of 2 minutes during each analysis. The effect of variation of desorption time on the desorption efficiency was investigated during this analysis.

8.5.6.2.2 Procedure

General Experimental Conditions

THM stock solution	:	Standard THM mixture (5.3.7)
Sample volume	:	20 mL
Instrumentation	:	SPME device equipped with 100 µm PDMS fibre
	:	Fisons GC/MS

SPME Experimental Conditions

Sample volume	:	20 mL
Adsorption time	:	10 min
Adsorption temperature	:	20°C
Stir speed	:	500 rpm
Salt	:	No Salt

Desorption temperature	:	200°C
Desorption time	:	2min, 4min, 6min, 8min, 10min, 12min
Cryo trapping	:	2 min

8.5.6.2.3 Results and Discussion

Table 8.15: Desorption time investigation

Tyd (min)	Peak area (TIC.min) $CHCl_3$	Peak area (TIC.min) $CHCl_2Br$	Peak area (TIC.min) $CHClBr_2$	Peak area (TIC.min) $CHBr_3$
12	566692	2100004	2199219	552569
10	664331	2248040	2611057	571765
8	537782	1546592	2611585	610403
6	581271	1506657	2081566	535241
4	571101	2391899	2178634	592651
2	575703	1633422	2369078	525789

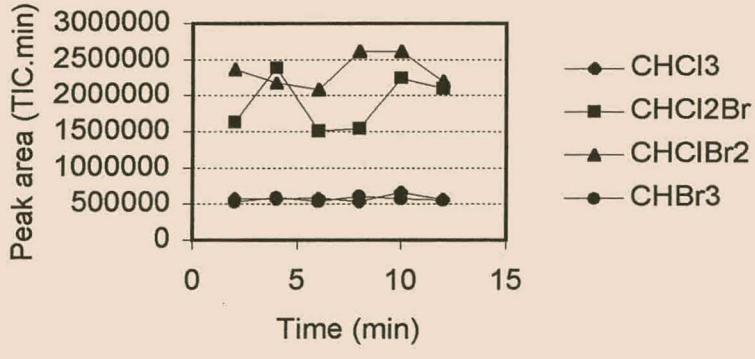

Figure 8.8: Desorption time investigation

Remarks:

- From the results above it can be deduced that desorption time has no significant influence on the efficiency of the desorption process. The observed variation in peak areas was attributed to normal experimental variation.

- A desorption time of 2 minutes was therefore regarded as sufficient during analysis of THMs.

- Longer desorption times would result in a faster degradation of the fibre of the SPME device.

8.5.7 Reproducibility

Reproducibility of the analytical method for the determination of THMs in drinking water was determined for various experimental conditions.

8.5.7.1 Ionic strength variation

8.5.7.1.1 Objective

Treated water from the Wynberg water treatment plant was used during this investigation to determine whether reproducible results could be obtained when THM analyses were performed for different salts for ionic strength adjustment. Two salts, i.e. NaCl and Na_2SO_4, were investigated. The latter one was chosen due to the absence of Br^- impurities (See 8.5.3.3).

8.5.7.1.2 Procedure

General Experimental Conditions

Ionic Strength Scenario 1

Sample volume	:	20 mL
Buffer	:	0.5 mL
Adsorption time	:	20 min
Adsorption temperature	:	20°C
Salt	:	No salt

Ionic Strength Scenario 2

Sample volume	:	20 mL
Buffer	:	0.5 mL

Adsorption time	:	20 min
Adsorption temperature	:	20°C
Salt	:	7.4 g NaCl

Ionic Strength Scenario 3

Sample volume	:	20 mL
Buffer	:	0.5 mL
Adsorption time	:	20 min
Adsorption temperature	:	20°C
Salt	:	5.6 g Na_2SO_4 (Elvers, 1993, p.357)

SPME Desorption

Desorption temperature	:	200°C
Desorption time	:	2 min
Cryo trapping	:	2 min

8.5.7.1.3 Results and Discussion

Table 8.16 contains the results generated from the above investigation.

Table 8.16: Reproducibility Results for NaCl and Na_2SO_4 for ionic strength adjustment

	Salt content	CH_2Cl_2	THM			
			$CHCl_3$	$CHCl_2Br$	$CHClBr_2$	$CHBr_3$
Peak area (TIC.min) Wynberg	No salt	1451052	359793	151839	71178	0
	NaCl	5291586	1537756	767959	367642	0
	Na_2SO_4	2786122	796355	587603	147459	0
Peak area (TIC.min) Std	No salt	1282738	466768	1328112	2046602	545499
	NaCl	5196063	2303922	7061533	10618148	2591571
	Na_2SO_4	2202819	965354	4169488	4186444	1188940
Conc. (µg/L) Wynberg	No salt		51.106	20.213	7.686	0.000
	NaCl		49.155	21.358	8.500	0.000
	Na_2SO_4		48.917	22.285	6.962	0.000

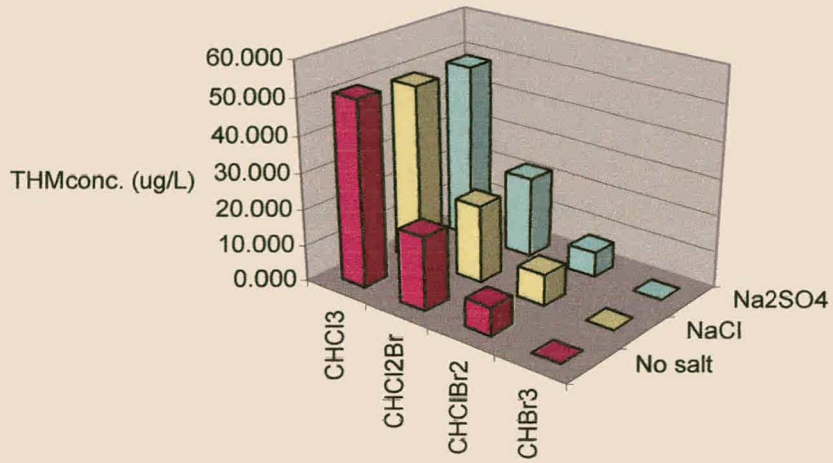

Figure 8.9: Reproducibility Results for NaCl and Na_2SO_4 for ionic strength adjustment

Remarks:

- From Figure 8.9 excellent reproducibility between the three scenarios was evident.
- Apart from the positive effect of increased sensitivity, which is evident from the increased peak areas, (See Table 8.16), no negative effect with respect of reproducibility by introduction of these salts could be detected. It would therefore be possible to analise chlorinated water samples by means of this method without the addition of NaCl or Na_2SO_4 to induce peak area enhancement.
- The concentration range for THMs in treated water samples is well within the detection limits of the analytical method. This would therefore resolve the problem of introducing NaCl with bromide contamination into the closed vial after the chlorination period (See 8.5.3.3 and 8.5.4.3).

8.5.8 Chlorination reproducibility

8.5.8.1 Objective

The objective of this study was to determine whether the chlorination process employed for the treatment of the water samples produced reproducible results.

8.5.8.2 Procedure

Raw water from the Wineberg catchment area was used to investigate the reproducibility of the chlorination process. The experiment was executed for five degrees of freedom.

General Experimental Conditions:

Raw Water	:	Wineberg catchment area
TOC content	:	7.80 mg/L
Nessler test	:	negative
Cl_2 concentration required	:	23.40 mg/L (See equation 2 (5.1.3.3))
Cl_2 water concentration	:	678.57mg/L (Determined by means of DPD titration)
Volume of Cl_2 water	:	0.924 mL (See equation 3 (5.1.3.3))
Sample volume	:	20 mL
Borate buffer	:	0.5 mL
Salt	:	0 g
Chlorination Period	:	3 days

SPME Experimental Conditions:

Adsorption time	:	20 min
Adsorption temperature	:	20°C
Agitation	:	Magnetically stirred (500 rpm)
Extraction matrix	:	headspace
Spike (CH_2Cl_2)	:	40 µL
Desorption temperature	:	200°C
Desorption time	:	2 min
Cryo trapping	:	2 min

The chlorination process was executed in accordance with the standardised methods given in Chapter 5 (5.1.3.3). The chlorination time was reduced to 3 days due to practical considerations.

8.5.8.3 Results and Discussion

Reproducibility results are summarised in Table 8.17 below.

Table 8.17: Reproducibility Results for the Chlorination Process

	Sample	CH_2Cl_2	$CHCl_3$	$CHCl_2Br$	$CHClBr_2$	$CHBr_3$
Peak area (TIC.min)	1	1150653	3019487	1034001	353480	0
	2	974952	2737915	929783	369805	0
	3	1312273	3387740	1251218	378553	0
	4	776194	2043558	694550	260966	0
	5	974419	2517788	849545	339294	0
	6	976223	2319371	867588	334612	0
	std (ave)	1081501	460993	1083168	2199369	512680
Conc. (µg/L)	1		461.7	179.4	224.3	0
	2		494.1	190.4	238.1	0
	3		454.2	190.4	238.0	0
	4		463.2	178.7	223.4	0
	5		454.6	174.1	217.6	0
	6		418.0	177.5	221.8	0
	std (ave)		75	200	250	30
STD Dev.			24.36	6.96	8.69	0

Remarks:

- The standard deviation values calculated for THM concentration determination indicated acceptable reproducibility for the chlorination process.

8.6 PROTOCOL FOR THM ANALYSIS

The protocol for THM analysis that resulted from this investigation is:

1. Pre-analysis Check List

Free active chlorine

Test distilled and deionised water for the presence of free active chlorine by means of the DPD titration method. (See 2 below)

THMs

Test distilled, deionised and raw water to be used in analysis for the presence of THMs by means of SPME and GC/MS analysis.

2. Cl_2 water Preparation

Fill an amber glass bottle with distilled water and bubble Cl_2 (g) through it for a few seconds. Use the DPD-titration method (Merck) for the determination of free active chlorine:

Reagents (See Addendum A for preparation):

Ammonium iron (II) sulfate solution

DPD reagent solution

Phosphate buffer solution

Calculation:

1 mL ammonium iron (II) sulfate solution $\cong$ 0.1 mg free active chlorine

$$\text{mg/L free active chlorine} = \frac{a \times 0.1 \times 1000}{b} \qquad (1)$$

a = mL of ammonium iron (II) sulfate solution consumed

b = mL of test water used

Incorporate the dilution factor in the b factor in equation (1).

Procedure:

Introduce 100 mL of test water into an Erlenmeyer flask of 150 mL capacity and add 5 mL DPD reagent solution and 5 mL phosphate buffer solution. Insert a magnetic stirrer rod with Teflon coating, and titrate the solution in a magnetic stirrer with ammonium iron (II) sulfate solution until the solution becomes colourless or an unchanging faint pink. Use a microburette with injection tube and nozzle, to introduce the ammonium iron (II) sulfate solution directly under the surface of the liquid. If the consumption is above 3 mL, start with a smaller volume of water which has been made up to 100 mL with double-distilled water. Because the Cl_2 water prepared by means of the above method has a high free active chlorine concentration, the following dilution should result in a consumption of less than 3 mL of ammonium iron (II) sulfate solution:

300µL Cl_2 water diluted to 100 mL with double distilled water.

Carry out determination in triplicate.

3. Chlorination Process

Reagents (See Addendum B for preparation):

Nessler's reagent

Borate buffer

Cl_2 water

Calculations:

$$Cl_2(mg/L) = 3 \times TOC(mg/L) + 7.6 \times NH_3\text{-}N(mg/L) \quad (2)$$

$$C_1V_1 = C_2V_2 \quad (3)$$

C_1: Cl_2 (mg/L) from titration of the stock solution

V_1: to be calculated

C_2: answer of equation (1)

V_2: 20.5mL

Procedure:

Test each raw and treated water sample with Nessler's reagent for the presence of ammonium salts by adding a few drops of reagent to the test water. An orange-brown precipitate will form to give a positive test. The amount of ammonium salts can be determined quantitatively by means of a method described by Merck (p.7-12). If the test is negative, equation (2) simplifies to

Cl_2(mg/L) = 3 x TOC (mg/L)

Introduce 20 mL treated water in an amber glass bottle equipped with a hole cap, teflon septum and a magnetic stir bar. Add 0.5 mL borate buffer to adjust the pH to 9.2. Calculate by means of equation (1) and (2) the volume of Cl_2 water necessary to disinfect the water samples.

Place sample bottles in a thermoregulated water bath at 25°C on a non-electric magnetic stirrer for a period of 7 days to allow for the process of THM formation.

4. SPME Adsorption Process

Reagents (See Addendum C for preparation):

30% Ascorbic acid solution

Methylene chloride solution

Calculations:

Volume of Ascorbic Acid (mL) = 1.2 x Cl_2 (mg/L) + 1.1 (4)

Cl_2 (mg/L): value calculated from equation (2)

Procedure:

Remove sample bottles from the water bath. Use equation (4) to calculate the volume of 30% ascorbic acid solution necessary to react with any remaining free active Cl_2 in solution. Add the calculated volume of ascorbic acid by means of a micro syringe. Then add, by means of a micro syringe through the septum, 40µL of CH_2Cl_2 solution as internal STD to each sample bottle. Place the amber glass sample bottle on a magnetic stirrer. Allow for an equilibration time of 10 minutes on the magnetic stirrer before continuing with the extraction of THMs.

Use the red hub (100μm PDMS) fibre for the SPME analysis. Insert the septum-piercing needle through the teflon septum and push the plunger down to expose the PDMS fibre to the headspace of the bottle. Adsorption conditions are as follows:

Adsorption time = 20min
Adsorption = headspace
Adsorption temp = 20°C
Stir Speed = 500 rpm

5. SPME Desorption Process and GC/MS Analysis

Retract the plunger to withdraw the PDMS fibre into the septum-piercing needle. Remove SPME unit from the sample bottle. Use CO_2 (dry) to cryo trap the volatiles at the beginning of the column. Insert the SPME into the injector of the GC/MS. See GC temperature program and MS program below. Push the plunger down to expose the fibre to the high temperature of the injector block for desorption of VOCs. Desorption conditions:

Desorption temp = 200°C
Desorption time = 2min
Cryo trapping = 2min

GC temperature program: Temp 1=45°C
Duration=4 min
Rate=9°C/min
Temp2=120°C
Duration=3 min

MS scan program: Mass range = 50-255

Peaks are integrated electronically.

THM Concentration Determination

Reagents (See Addendum D for preparation):

Standard THM solution: Chloroform
Bromodichloromethane
Dibromochloromethane
Bromoform

Methylene chloride

Calculations:

$$\text{THM conc.}\,(\mu\text{g/L}) = \frac{\text{Peak Area (sample)}}{\text{Peak Area (std)}} \times \frac{\text{Peak Area}\,(CH_2Cl_2\text{/std})}{\text{Peak Area}\,(CH_2Cl_2\text{/sample})} \times \text{THM conc. (std)} \qquad (5)$$

THM conc. ($CHCl_3$) = 75 µg/L
THM conc. ($CHCl_3$) = 200 µg/L
THM conc. ($CHCl_3$) = 250 µg/L
THM conc. ($CHCl_3$) = 30 µg/L

Procedure

For the determination of the concentration of each THM species, it is necessary to perform a standard THM analysis as well. 20 mL of a standard THM mixture are therefore introduced into an amber glass sample bottle together with 40µL methylene chloride (internal standard) as well as 0.5 mL borate buffer. Analysis for THMs in this standard mixture is according to procedure (4) and (5) in the protocol.

Chromatograms of both the unknown sample and the standard are integrated electronically. The resulting peak areas, together with the concentration of the standard THM under investigation, are subsequently substituted into equation (5) for the calculation of the unknown concentration.

ADDENDUM A

Ammonium iron (II) sulfate solution:

Dissolve 1.106g ammonium iron (II) sulfate GR in freshly boiled and cooled deionised water. Add 2mL 1 mol/L sulfuric acid, and make up to 1000 mL with the above-mentioned water.

DPD reagent solution:

Dissolve 0.11 g N,N-Diethyl-1,4-phenylenediammonium sulfate GR in deionised water with 2 mL 1mol/L sulfuric acid and 2.5 mL 0.02mol/L Titriplex III solution, and make up to 100 mL. Store the solution protected from light in a brown bottle. It is unuseable if a discolouration develops.

Phosphate buffer solution:

Dissolve 46 g Potassium dihydrogen phosphate GR and 24 g tri-Sodium phosphate 12-hydrate (LAB) in 1000 mL deionised water.

Sulfuric acid 1mol/L:

Make the contents of one ampoule of 0.5mol/L Sulfuric acid Titrisol concentrated solution for preparation of 1 litre of 1 N solution up to 500 mL with deionised water.

Titriplex III solution 0.02mol/L:

Make 200 mL 0.1mol/L Titriplex III metal (pM) indicator up to 1000 mL with deionised water.

ADDENDUM B

Nessler's reagent (Basset, 1979):

Dissolve 35 g of Potassium iodide in 100 mL of water, and add 4% Mercuric chloride solution, with stirring or shaking, until a slight red precipitate remains (about 325 mL are required). Then introduce, with stirring, a solution of 120 g of Sodium hydroxide in 250 mL of water, and make up to 1 litre with distilled water. Add a little more Mercuric chloride solution until there is a permanent turbidity. Allow the mixture to stand for one day and decant from sediment. Keep the solution stoppered in a dark-coloured bottle.

Borate buffer (Greenberg, 1992):

Dissolve 30.9 g anhydrous Boric acid (H_3BO_3) and 10.8 g Sodium hydroxide (NaOH) in 1 litre organic-free water. Refrigerate and prepare fresh weekly.

ADDENDUM C

30% Ascorbic acid

The solubility of ascorbic acid in water is recorded as being approximately 30% ($^m/_v$). To ensure no contamination of the treated water sample, ascorbic acid (Merck, pro analysi) was used. Add 30 g ascorbic acid to 70 mL distilled water.

Methylene chloride

Prepare a 50mg/L methylene chloride solution by diluting .0367mL mL of methylene chloride to 1 litre with distilled water.

ADDENDUM D

Environmental standard solutions (Supelco) are used for the preparation of standard solutions of THMs. Each ampoule contains 1 mL 5000 µg/mL of the specific THM in methanol. A dilution of one ampoule to 100 mL with distilled water would therefore result in a 50 mg/L THM solution.

Chloroform

Dilute one environmental standard $CHCl_3$ ampoule with distilled water to 100 mL in a volumetric flask.

Bromodichloromethane

Dilute one environmental standard $CHCl_2Br$ ampoule with distilled water to 100 mL in a volumetric flask.

Dibromochloromethane

Dilute one environmental standard $CHClBr_2$ ampoule with distilled water to 100 mL in a volumetric flask.

Bromoform

Dilute one environmental standard $CHBr_3$ ampoule with distilled water to 100 mL in a volumetric flask.

Standard THM mixture

From the above THM solutions the following amounts are used for a 1 litre dilution mixture:

$CHCl_3$: 1.5 mL 50 mg/L solution

$CHCl_2Br$: 4 mL 50 mg/L solution

$CHClBr_2$: 5 mL 50 mg/L solution

$CHBr_3$: 0.6 mL 50 mg/L solution

Methylene chloride

See Addendum C.

REFERENCES

Atkins P.W. (1978) Physical Chemistry, p.216, Oxford University Press

Casey T.J., Chua K.H. (1997) Aspects of THM formation in drinking water. *Journal of Water SRT – Aqua* **46** No.1 pp.31-39

Basset J., Denney R.C., Jeffery G.H., Mendham J. (Editors) (1979) Vogel's Text-Book of Quantitative Inorganic Analysis: Theory and Practice; 4th Edition; Longmans, Green and Co.

Eisert R., Levsen K. (1996) Solid-phase microextraction coupled to gas chromatography: a new method for analysis of organics in water. *Journal of Chromatography A* 733 p.143-157

Elvers B., Hawkins S., Russey W., Schulz G. (1993) Ullmann's Encyclopedia of Industrial Chemistry **A24** p. 319

Greenberg A.E., Clesceri L.S., Eaton A.D. (Editors) (1992) Standard Methods for the Examination of Water and Wastewater 18th Edition

Handbook of Chemistry and Physics, 49th Edition 1968-1969 The Chemical Rubber Company

Merck E. The Testing of Water, *Darmstadt*

Supelco Inc. (1996) Note 95

Van Steenderen R.A., Theron S.J., Engelbrecht A.C. (1988) An investigation into the occurrence and concentration of trihalomethanes and their precursors in South African drinking waters. *Report No. 194/1/89 WRC. Contract Report No. 670/9232/5*

Zhang Z. Yang M.J., Pawliszyn J. (1994) Solid-Phase Microextraction: A Solvent-Free Alternative for Sampling Preparation. *Analytical Chemistry* 66 No. 10 p.884A-853A

CHAPTER 9

Conclusions and Recommendations

9.1 CONCLUSIONS

I. In this investigation it was established that the specific design (Figure 9.1) of a falling film photocatalytic reactor, as developed at the Department of Chemistry, University of Stellenbosch, was capable of destroying NOM in raw water (6.1.3).

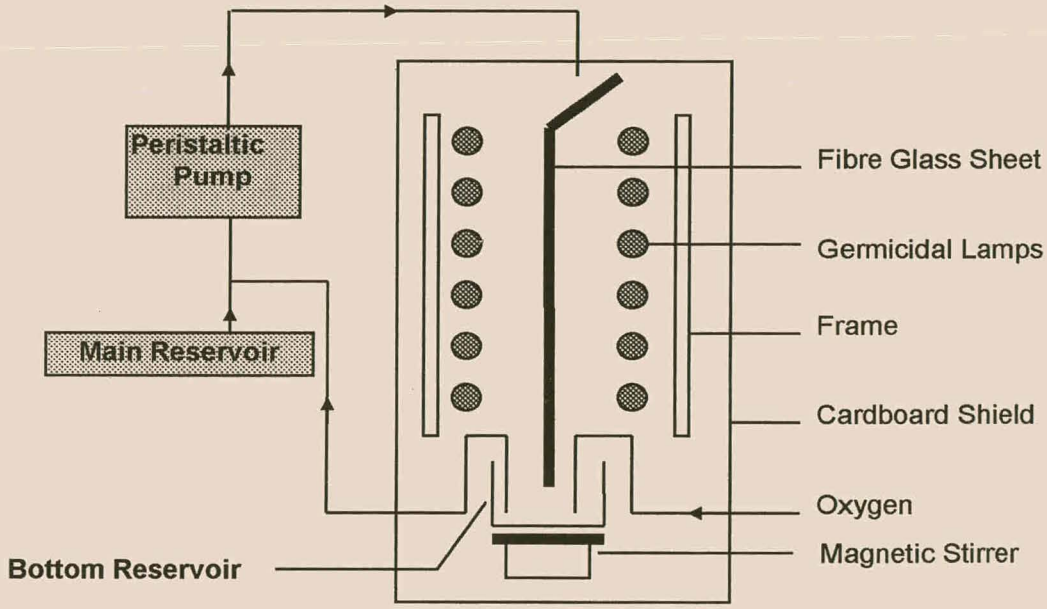

Figure 9.1: A Novel Falling Film Reactor

Although the photocatalytic reactor is capable of destroying NOM, the complete destruction of NOM in raw water could not be achieved. The scaling up of the reactor (Figure 9.2) (3.2.5), together with further optimisation of the factors specified could, nonetheless, improve the photocatalytic oxidation capabilities of the reactor further and should therefore be investigated.

Two limiting factors to consider is, however, firstly the **capacity** of the reactor (expressed in terms of volume of product water per unit time) and secondly the **cost-effectiveness** of the product water (expressed in terms of volume of product water per unit cost). These factors can essentially be considered the determining factors when assessing the feasibility of a newly

developed process and must therefore receive serious attention during the process of optimisation and scaling up.

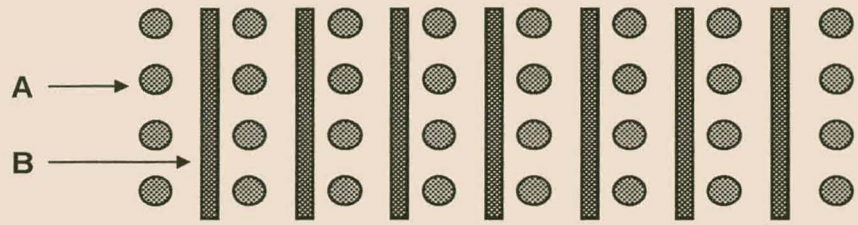

Figure 9.2: Diagram of horizontally scaled-up scenario (A: lamps; B: sheets)

II. The design of the experimental reactor assisted the optimisation of the destruction of NOM in raw water by allowing various modes of operation of the reactor e.g. immobilised bed, combination of immobilised bed and slurry mode, recirculation and single pass, to be investigated.

Optimisation of the immobilised bed-slurry mode of operation with recirculation using statistical methods indicated that both the catalyst loading (TiO_2 concentration) and the NOM content, was pH dependent. Response surfaces generated from statistical data (6.4.1.3.3), indicated optimal experimental conditions for the destruction of NOM in raw water (Figure 6.6).

The removal of the suspended catalyst as employed in the slurry mode is always difficult to implement due to the fineness of the catalyst. Optimisation of the immobilised bed reactor with single pass (flow-through) mode was therefore carried out. It was shown that this type of reactor and mode of operation could destroy NOM in raw water (6.4.2.3). From the reduction in NOM content with increasing number of single passes (Figure 6.7 and 6.8), it is evident that the extent to which the NOM content is reduced would depend on the number of sheets set up in series in a scaled-up version of the experimental reactor.

III. In this investigation it was also proved that the reduction of NOM could be monitored to various degrees of success by three analytical methods i.e. UV absorbance (at 254 nm), TOC content and THMFP.

When only colour removal was considered, UV absorbance (at 254 nm) was sufficient. It was proved however that when colour was removed, the TOC and THMFP could still be high, indicating the presence of organic compounds that do not contribute to the colour of the water. It

is therefore recommended that the latter two methods must be used to obtain a realistic characterisation of the organic content of the photocatalytically treated water.

It was observed that, when employing the TOC and THMFP methods, there was an initial increase in these values with photocatalytic oxidation. This was ascribed to the initial reduction in size of the larger NOM molecules (6.3.3) to form smaller, more reactive molecules. These smaller molecules react more readily with chlorine to form THMs and will also be oxidised with greater ease during the determination of the total organic carbon content.

IV. The procedure for determining THMFP, however is quite complicated and could yield non-reproducible results if not optimised. By a statistical optimisation of the procedure an analytical protocol was developed. This method can reveal important information regarding the NOM present in treated water and should be considered a vital step in any investigation of NOM removal from natural water (8.6).

9.2 RECOMMENDATIONS

Further investigations to improve the NOM reduction capabilities of the experimental reactor are advisable, before a larger scale reactor is attempted. The following aspects should be considered:

- Matrices other than glass fibre sheet e.g. FAC sheets must be investigated for NOM removal. Preliminary work has indicated an enormous reduction in the time required for the complete removal of e.g. the model pollutant 4-cholophenol (de Villiers, 1999) when employing FAC sheets, compared to the time required for complete removal of 4-cholophenol on a fibre glass sheet with TiO_2. The extremely large surface area available for adsorption of organic compounds onto the FAC sheets is responsible for this phenomenon. This immediately suggests that NOM can be removed from the raw water, also at an improved rate, by means of adsorption onto the surface of the FAC sheet, followed by photocatalytic oxidation.

- The reactor lends itself to scaling-up in more than one direction (3.2.5). This should be investigated thoroughly, e.g. series combinations of reactors (Figure 9.2) should be investigated to improve the effectiveness of NOM removal for the single pass mode.

- The pH dependence characteristics of the NOM concentration and the TiO_2 loading (6.4.1.3.3), should be manipulated to improve the destruction of NOM. The lowering of pH together with an increase of TiO_2 loading, as the water progresses through a series combination of sheets in the reactor, should be investigated.

- It must be investigated whether the photocatalytic treatment of NOM laden water should be preceded by conventional water treatment processes of coagulation and flocculation, or the sirofloc process. The catalytic process should then only be used for the final removal of the fulvic acids and other organic pollutants that are not removed by the flocculation process. This might, however, not prove to be the most cost-effective method. The principal advantage of the coupling of existing methods with photocatalysis, is that remaining contaminants, such as microcystins (de Villiers, 1999), which current water purification processes are unable to remove, will now also be removed from the water.

- It should be investigated whether radiation of NOM laden water with normal fluorescent lamps produces $^1\Delta_g$ oxygen that can destroy other organic pollutants.

- It must be investigated whether polarograms of coloured water with added ionic species e.g. Zn^{2+}, Pb^{2+} and Cu^{2+} could be used to characterize these waters.

- It must be investigated whether addition of some organic species to coloured water could not induce fluorescence in NOM and whether the fluorescence spectra could then be employed for the characterisation of these waters.

REFERENCES

De Villiers D. (1999) Design and Evaluation of Photocatalytic Reactors for Water Purification. *PhD Thesis in preparation, University of Stellenbosch*